

# The Nambu–Jona-Lasinio model of quantum chromodynamics

S. P. Klevansky

*Institut für Theoretische Physik, 6900 Heidelberg, Federal Republic of Germany*

The Nambu–Jona-Lasinio model is reviewed in its flavor SU(2) and SU(3) versions applied to quarks. The dynamical generation of quark masses is demonstrated as a feature of chiral symmetry breaking. One finds that the associated meson spectra, as well as the meson static properties, can be well described. Current-algebra results, which arise as a consequence of symmetry considerations, automatically hold for this model and are explicitly demonstrated to do so. These include the Goldberger-Treiman and Gell-Mann–Oakes–Renner relations. Effects of finite temperature, finite chemical potential, and strong Maxwell and chromoelectromagnetic fields on the dynamically generated quark mass and the meson spectra are discussed. The alternative procedure of bosonization to obtain an effective Lagrange density in mesonic degrees of freedom, using the derivative expansion, is also presented. The current status in relating the results of this model to that of chiral perturbation theory is critically examined.

## CONTENTS

I. Introduction	649	VII. Bosonization	688
II. The Nambu–Jona-Lasinio Model	652	A. Ginzburg-Landau description for quarks	689
A. Symmetries	652	B. Path-integral formulation in flavor SU(2) and the derivative expansion	691
B. The Bogoliubov-Valatin approach	654	C. Developments in flavor U(3)	695
C. The self-energy in Hartree and Hartree-Fock approximations	656	D. Correspondence with chiral perturbation theory	695
1. The two-flavor model	656	VIII. Concluding Remarks	698
2. The three-flavor model	656	Acknowledgments	698
D. Fierz transformations	658	Appendix A: The Six-Fermion Interaction	699
III. Regularization Schemes	659	Appendix B: Crossing Matrices for the Fierz Transformation	700
A. The three-momentum noncovariant cutoff scheme	660	Appendix C: The Total Energy	701
B. Covariant regularization schemes	661	Appendix D: The Thermodynamic Potential	701
1. The four-momentum covariant cutoff scheme	661	Appendix E: The Polarization Propagator at Finite Temperature	703
2. Regularization in proper time	661	Appendix F: Eigenvalues of the Field-Strength Tensor and Evaluation of Traces	704
3. The Pauli-Villars Scheme	661	Appendix G: The Polarization Propagator, Including a U(1) Field	705
C. Parameter choice	662	References	707
IV. Meson Masses and Regularization-Independent Relationships	663		
A. The two-flavor model	663		
1. The pion and sigma modes	663		
2. Goldstone modes in the chiral limit	665		
3. The pion-decay constant	665		
4. The Goldberger-Treiman, Gell-Mann–Oakes–Renner relations and the $\sigma$ - $\pi$ mass relation	666		
B. The three-flavor model	667		
1. Effective SU(3) Lagrangian and pion and kaon modes	667		
2. Goldstone bosons in the chiral limit	668		
3. $\eta$ and $\eta'$ mesons	669		
4. Vector-meson modes	671		
5. General discussion and outlook	672		
V. Effects of External Parameters I: Temperature and Chemical Potential	672		
A. Finite chemical potential	673		
B. Finite temperature	676		
1. The gap equation and thermodynamic potential	676		
2. Mesonic excitations	678		
VI. Effects of External Parameters II: Maxwell and Color Fields	679		
A. Maxwell fields	680		
1. Gap equation	680		
2. Meson modes	683		
3. Polarizabilities	685		
4. Electromagnetic form factor of the pion	685		
B. Chromoelectromagnetic fields	686		

In completing one discovery, we never fail to get an imperfect knowledge of others of which we could have no idea before, so that we cannot solve one doubt without creating several new ones.

Joseph Priestley (1786)

## I. INTRODUCTION

For some time now quantum chromodynamics has been accepted as the theory of strong interactions. The usefulness of this gauge theory is particularly seen in the kinematic range of large momentum transfer, where scattering processes are calculated with much success. This is due to the fact that, at short distances, the theory exhibits the phenomenon of *asymptotic freedom*. That is, the quark-gluon coupling strength becomes small; thus the wealth of perturbative techniques that have been developed for the study of quantum electrodynamics may be confidently extended to describe QCD processes in this so-called weak-coupling regime.

In contrast, away from large momentum transfer, or equivalently at larger distances, QCD is not so well understood, and existing calculational techniques produce

only rough numbers. Here the problem lies in the fact that the strong-coupling constant becomes large, and a perturbative approach cannot be justified. One now finds oneself in a strange predicament. One actually has at one's disposal a definite Lagrangian in which all the dynamics of the system are contained, but one is not easily able to extract useful information from it for most physical processes of interest, such as the properties of hadrons and their interactions, or the behavior of hadronic matter at high density. Several methods of approaching QCD have therefore been developed. The only one of these that attempts to actually solve the equations of motion of the theory *per se* is that of lattice gauge theory (see, e.g., Kogut, 1980 and Rebbi, 1986 for an overview, and Christ, 1991 and Kogut *et al.*, 1991 for some current results). This method carries with it problems of its own: one requires computer power in gigaflops in order to make reasonable calculations within acceptable time periods. There are also problems that arise in including fermions on a discretized lattice, so that approximations are necessary, even in these calculations.

One is thus strongly motivated to look for a simpler model Lagrange density that displays one or more of the essential features of QCD, but that is mathematically tractable. We would then be able to explore the consequences of the features that we have isolated as relevant. Such an approach is a common one to both nuclear and solid-state physics: in nuclear physics, for example, the many excited states available to a nuclear system via the continuum may be averaged out to provide an optical-model potential. In doing this, the  $N$ -body problem is reduced to a one-body problem for the purpose of calculating reaction rates. Basic to this approach is the recognition that many-body systems are only exactly soluble in exceptional or oversimplified situations. Thus it is sensible to attempt to isolate the relevant physics for a process and to study this either by making an approximation to the exact theory, or, as is commonly done for a theory as intractable as QCD, by creating models that serve to accentuate the main features of the theory.

The candidate model that we shall discuss in this review is the Nambu–Jona-Lasinio (NJL) model. In its original form, this model was constructed as a pre-QCD theory of nucleons that interact via an effective two-body interaction. This today is reinterpreted as a theory with quark degrees of freedom. Of primary importance is the fact that the Lagrange density of this model is constructed such that the symmetries of QCD that are also observed in nature are part and parcel of it. One of the most important of these is chiral symmetry, which is essential to the understanding of the lightest hadrons. QCD is distinguished not only by its many symmetries but also by the breaking of these symmetries. The NJL model is particularly useful for observing how these things happen. In particular, the dynamic generation of fermion masses brought about by the breaking of chiral symmetry is one of the features of the NJL model. The special role of the Goldstone modes (for two quark

flavors, these are the pions; for three quark flavors, the “pion octet”) can also be explicitly traced. Furthermore, there are the well-known results of current algebra, such as the Goldberger-Treiman and Gell-Mann–Oakes–Renner relations that hold for QCD. These must also hold for the NJL model, since they are a consequence of symmetry properties only. In the NJL model, they can be derived explicitly. The actual mechanism whereby chiral symmetry breaking (CSB) occurs in the NJL model follows closely the microscopic theory of superconductivity that was put forward by Bardeen, Cooper, and Schrieffer (1956). In the NJL model, one argues that the interaction between quarks and antiquarks, which arises from some complicated processes of gluon exchange, can be attractive, and leads to a quark-antiquark pair condensation in the vacuum, should the interaction exceed a critical strength. Other effects, such as gluon condensation, which do not play a direct role in chiral symmetry breaking, are not considered.

The NJL model of course has shortcomings as well. The interaction between quarks is assumed to be pointlike in character, with the result that it is not a renormalizable field theory. Hence, to define the NJL model completely as an *effective* model, a regularization scheme must be specified to deal with the improper integrals that occur. A regularization scheme specifies a length scale for the theory, which can be expressed as a cutoff on the quark momenta. One may regard the cutoff as an approximate, if crude, implementation of the property of asymptotic freedom of QCD: by suppressing the interaction between quarks for large spacelike momentum transfer, one simulates the behavior of the running coupling constant of QCD (Hatsuda and Kunihiro, 1985a; Bernard, Jaffe, and Meissner, 1988).

A second shortcoming of the NJL model, physical rather than mathematical, is that the local interaction does not confine quarks. For many questions, however, the issue of confinement may not be important. For example, the interaction of hadrons below the threshold for producing free quarks may not depend on the details of how the confinement is produced.

One of the purposes of this review is to provide a self-contained exposition of chiral symmetry breaking and its consequences, as it comes about in the NJL model. Because of its mathematical simplicity, the NJL model provides a good pedagogical framework for this discussion. The review will also investigate the properties of low-lying mesonic states that arise in the model, with particular attention to the influence of external conditions such as density, temperature, and electromagnetic and color fields. These questions are of interest in understanding the processes that occur in heavy-ion collisions, where high temperatures and densities are attained. Of course such collisions present a highly complicated scenario, as one expects that a locally deconfined phase, a plasma, would occur, which at some later stage would hadronize on cooling. The exact mechanism whereby this occurs is not yet understood quantitatively, but it involves the con-

cept of confinement, which is not a feature of the NJL model. Nevertheless, the interplay of chiral symmetry with temperature and density should be understood as a first step toward understanding these processes, and this is the reason for our interest.

Most of the literature that has accumulated in the last few years is restricted to rather brief communications with each new author introducing different notations and preferences in treating the field theory. Correspondingly, authors have also chosen a variety of different regularization schemes and parameter sets to regulate this model. It is thus a concomitant purpose of this review to present a unified approach to the literature, rather than simply providing a collection of results, in the hope of clarifying and demystifying the subject and making the task of the reader easier.

There is another range of models that claim a relationship to QCD for which an explicit Lagrangian can be given in terms of mesonic and/or fermionic degrees of freedom. They include the Skyrme model, in which the fermionic degrees of freedom appear as topological solitons (Skyrme, 1961, 1962), and variations thereof, which gained popularity in the early 1980s since it was shown that in the limit of a large number of colors  $N_c$ , quantum chromodynamics behaves as a theory of bosons ('t Hooft, 1974). Other models that specifically investigate this feature of chiral symmetry breaking and its consequences introduce phenomenological boson fields and couple these directly to the fermionic degrees of freedom (see, for example, Lee, 1981 and Pokorski, 1989 for detailed discussions). A connection between the NJL model and the boson models, in fact, exists and may be established by employing path-integral techniques to the NJL model to derive a so-called bosonized form of the NJL Lagrangian. This is a topic that we shall also discuss.

In this review, we do not follow the historical development of the model, since, as with all research, this proceeds along a winding path. We sketch this briefly here. This list of references gives an overview, but is not comprehensive. The NJL model with up and down quarks was used in its bosonized form as early as 1974 (Eguchi and Sugawara, 1974). This SU(2) version was then refined by Kikkawa (1976), Eguchi (1976), and Chakrabarti and Hu (1976). Kikkawa (1976) also introduced the U(3) version, i.e., with strange quarks as well as the up and down quarks. The model received a resurgence of interest in the 1980s, primarily in the SU(2) and U(3) versions. Work originating from Eastern Europe is based mainly on the bosonization technique (Ebert and Volkov, 1983; Volkov 1984, 1986; Ebert, 1985), within which the meson spectra, polarizabilities, and charge radii have been evaluated. In a series of papers, Kruglov (1984, 1988, 1989a, 1989b, 1989c) has used the NJL model to study, among other things, renormalization, Ward identities, and an instanton-induced effective interaction. The bosonized form of the model has also been studied by Ebert and Reinhardt (1986), Ruiz Arriola *et al.* (1989), Th. Meissner *et al.* (1988, 1990), Jaminon *et al.*

(1989), Hosaka (1990), Schüren, Ruiz Arriola, and K. Goeke (1991), and Ruiz Arriola (1991), the latter two papers of which deal with the connection of the NJL model to chiral perturbation theory as seen from the effective bosonized Lagrangian.

On the other hand, the use of the NJL model as expressed in terms of the fermionic degrees of freedom, in which it was originally constructed, has found favor with many authors. Hatsuda and Kunihiro (1984, 1985b, 1987a, 1987b) discuss the SU(2) NJL model at finite temperatures. The reader is also referred to Kunihiro (1987, 1989a, 1989b, 1991) for further studies on finite temperature.

The formulation of the NJL model in flavor SU(3) was first introduced by Kunihiro and Hatsuda (1988) and Bernard, Jaffe, and Meissner (1988), who constructed a suitable U(3) version and then removed the unwanted axial U(1) symmetry by including a term of the form suggested by 't Hooft (1976a, 1976b). The latter set of authors discuss the strangeness content of the nucleon within the model, a topic which has also been investigated by Hatsuda (1988) and Kunihiro (1988). There has been a series of articles initiated by Bernard, discussing the original SU(2) NJL model as applied to quarks (Bernard, 1986, 1987); finite-density and finite-temperature properties in either SU(2) or SU(3) (Bernard *et al.*, 1987a, 1987b; Bernard and Meissner, 1988a); electromagnetic form factors and charge radii (Bernard and Meissner, 1988b; Bernard and Vautherin, 1989; see also Blin *et al.*, 1988); and the vector-meson spectrum in SU(2) (Bernard and Meissner, 1988c; see also Blin *et al.*, 1990). The same topics have also been recently studied by Takizawa *et al.* (1989, 1991), Klimt *et al.* (1990), Lutz and Weise (1990), and Vogl *et al.* (1990). The results of the last three groups are reviewed by Vogl and Weise (1991). A time-dependent Hartree-Fock formalism embedded in a density-matrix approach has been studied by da Providência *et al.* (1987), while the inclusion of Maxwell and chromoelectromagnetic fields is discussed by Klevansky and Lemmer (1989), Klevansky *et al.* (1991), Bernard and Vautherin (1989), and Sukanuma and Tatsumi (1990, 1991). The reader is also referred to Rosenstein *et al.* (1991), who mention the NJL model in their review on dynamical symmetry breaking in four-fermion-interaction models. In a completely different context, Bardeen *et al.* (1990), Clark *et al.* (1990), and Pham (1990) have included the NJL mechanism in versions of the standard model, thereby relating the mass of the Higgs scalars to that of the top quark.

In this review, we study the NJL model in its standard context of modeling QCD, and we take the route designated by the set of authors mentioned in the preceding paragraph; i.e., we deal with the NJL model in its original fermionic form, choosing for each section to discuss one or more primary references that are representative of the topic in question. Bosonization is discussed thereafter. In more detail, the organization of this paper is as follows. In Sec. II, we introduce the Nambu–Jona-

Lasinio model, in its SU(2) and SU(3) versions, from symmetry considerations of QCD. We follow the Bogoliubov-Valatin approach, as this method allows for an explicit display of the particle-antiparticle pairing in the vacuum. We move on to the Green's-function approach for calculating the self-energy, which is more readily generalizable to include the effects of external parameters. The Fierz transformation is also discussed.

We devote Sec. III to a description of regularization schemes, dealing with the three-dimensional noncovariant cutoff, the covariant four-dimensional cutoff, regularization in proper time, and the Pauli-Villars scheme.

In Sec. IV, the polarization propagator is introduced in both the SU(2) and SU(3) flavor models and the meson spectrum is calculated.

The effect of introducing external parameters such as finite chemical potential and temperature is discussed, somewhat lengthily, in Sec. V.

Applied Maxwell and chromoelectromagnetic fields are discussed in Sec. VI.

In Sec. VII, bosonization of the NJL Lagrangian is discussed as an alternative method for analyzing its properties, and the connection with chiral perturbation theory is elucidated.

In Sec. VIII, we conclude by drawing a critical balance of the weaknesses and strengths of this method.

Finally, a word on notation. In this review we have consistently followed the notational conventions given in Itzykson and Zuber (1980), for example. In particular, we use the Minkowski space metric  $g^{\mu\nu} = \{1, -1, -1, -1\}$ , while  $\gamma_5 = i\gamma^0\gamma^1\gamma^2\gamma^3$ , where  $\gamma^\mu$  are the standard Dirac spinors.

## II. THE NAMBU–JONA-LASINIO MODEL

### A. Symmetries

The Lagrangian of quantum chromodynamics is given as

$$\mathcal{L}_{\text{QCD}} = -\frac{1}{4}\mathcal{F}_{\mu\nu}^a\mathcal{F}_{\mu\nu}^a + \bar{\psi}(i\mathcal{D} - M)\psi, \quad (2.1)$$

where the field-strength tensor  $\mathcal{F}_{\mu\nu}^a$  is

$$\mathcal{F}_{\mu\nu}^a = \partial_\mu A_\nu^a - \partial_\nu A_\mu^a + gf_{abc}A_\mu^b A_\nu^c \quad (2.2)$$

and the covariant derivative is  $(D_\mu)_{cc'} = \delta_{cc'}\partial_\mu - ig\frac{1}{2}(\lambda^a)_{cc'}A_\mu^a$ . As will be standard notation throughout this work, greek indices  $\mu, \nu = 0 \dots 3$  refer to Lorentz vector labels; the labels  $a, b, c = 1 \dots 8$  have the dimension of the adjoint representation of SU(3); and  $c, c' = 1 \dots 3$  in context are color labels dimensioned by the fundamental representation of SU(3). The strong-coupling constant is given as  $g$ , and  $f_{abc}$  are the structure constants of SU(3). Flavor indices, which will be denoted as  $f, f'$  have been suppressed to simplify the notation.

In Eq. (2.1),  $M$  is a color-independent mass matrix in flavor space and is phenomenological. Whatever its ori-

gin,  $M$  can be brought to diagonal form through flavor-mixing transformations, so that the fermion mass contribution to  $\mathcal{L}_{\text{QCD}}$  may be written as

$$\mathcal{L}_{\text{mass}} = -\sum_{c=1}^3 \sum_{f=1}^6 m_f \bar{\psi}^{fc} \psi^{fc}. \quad (2.3)$$

The  $m_f$  are not observables if QCD implies quark confinement, but can be determined in terms of observable hadronic masses through current algebra. These are the so-called current quark masses as opposed to the notion of constituent quark masses used in phenomenological quark models of hadronic structure.

Intermediate-energy hadronic physics in the non-strange sector, which runs over the MeV–GeV energy range, should be well described by the dynamics of the lowest-mass quarks,  $u$  and  $d$ . Then  $\mathcal{L}_{\text{QCD}}$  can be written as

$$\mathcal{L}_{\text{QCD}} = \mathcal{L}_{\text{chiral}} - (m_u \bar{u}u + m_d \bar{d}d) + \mathcal{L}_{\text{scbt}}, \quad (2.4)$$

where  $\mathcal{L}_{\text{scbt}}$  refers to the Lagrangian associated with the heavier flavors  $s, c, b, t$  and the chiral part is given by

$$\mathcal{L}_{\text{chiral}} = -\frac{1}{4}\mathcal{F}_{\mu\nu}^a\mathcal{F}_{\mu\nu}^a + \bar{\psi}i\mathcal{D}\psi, \quad \psi = \begin{pmatrix} u \\ d \end{pmatrix}. \quad (2.5)$$

The bilinear form occurring in Eq. (2.5) is invariant under the transformation  $U\psi \rightarrow \psi$ , where  $U$  can be, for example, the  $2 \times 2$  unitary matrix in flavor space, the Dirac matrix  $\gamma_5$  in spinor space, or some combination of flavor and spinor matrices. The pure unitary transformations  $U_V(1)$  and  $SU_V(2)$  are the well-known symmetries that correspond to baryon and isospin conservation, respectively. They are listed, together with their transformation properties and realization in nature, in Table I. Transformations that include  $\gamma_5$ , the  $SU_A(2)$  and the  $U_A(1)$ , are the so-called chiral or axial symmetries, and their properties are also listed in Table I. Axial transformations alter the parity that is associated with a state. Therefore a direct manifestation of  $SU_A(2)$  in nature would require that each isospin multiplet be accompanied by a mirror multiplet that has opposite parity. Since no such multiplets are observed in nature, we conclude that  $SU_A(2)$  should not be directly realized by QCD. Likewise, since one does not observe opposite parity partners to all the hadrons, one must conclude that  $U_A(1)$  should also not be realized directly by QCD. It is believed that the  $SU_A(2)$  symmetry is manifested in the Goldstone mode<sup>1</sup> via chiral symmetry breaking and that the accompanying pseudoscalar  $I=1$  massless bosons are to be associated with the pions. This thesis is supported by the experimentally observed low mass of the pion. In comparison with the nucleon mass, one has

<sup>1</sup>The Goldstone theorem (Goldstone, 1961; Goldstone *et al.*, 1962) states that the spontaneous breaking of a continuous global symmetry implies the existence of associated massless spinless particles.

TABLE I. Symmetries, their transformation properties, associated conserved currents, and manifestation in nature are given for the case of two flavors.

Symmetry	Transformation	Current	Name	Manifestation
$SU_V(2)$	$\psi \rightarrow e^{-i\tau \cdot \omega/2} \psi$	$J_\mu^k = \bar{\psi} \gamma_\mu \tau^k \psi$	isospin	approx. conserved
$U_V(1)$	$\psi \rightarrow e^{-i\alpha} \psi$	$j_\mu = \bar{\psi} \gamma_\mu \psi$	baryonic	always conserved
$SU_A(2)$	$\psi \rightarrow e^{-i\tau \cdot \theta \gamma_5/2} \psi$	$J_{5\mu}^k = \bar{\psi} \gamma_\mu \gamma_5 \tau^k \psi$	chiral	CSB; Goldstone mode
$U_A(1)$	$\psi \rightarrow e^{-i\beta \gamma_5} \psi$	$j_{5\mu} = \bar{\psi} \gamma_\mu \gamma_5 \psi$	axial	$U_A(1)$ “puzzle”

$m_\pi/m_N=0.15$ . On the other hand, if  $U_A(1)$  were to be realized in the same fashion by QCD, it would require the existence of an  $I=0$  pseudoscalar meson having roughly the same mass as the pion. No such candidate was observed, and thus arose the  $U_A(1)$  puzzle: where is the Goldstone boson? The problem was resolved by 't Hooft (1976a, 1976b), who showed that, due to instanton effects, the  $U_A(1)$  symmetry should not result in physical manifestations. We do not deal with this complexity further here, but rather focus our attention on the spontaneous breaking of the  $SU_A(2)$  symmetry. Color  $SU(3)$  symmetry, which is exact, will not play a role in our further considerations.

The generalization to flavor  $SU(3)$  symmetry is straightforward. One replaces the isospin Pauli matrices  $\tau^k, k=1..3$ , of Table I by the flavor matrices  $\lambda^a, a=1..8$ ; the spinor  $\psi$  in Eq. (2.5) is enlarged in flavor space,  $\psi=[u, d, s]$ ; and, in Eq. (2.4), the mass perturbation Lagrangian becomes  $\mathcal{L}_{\text{mass}}=m_u \bar{u}u + m_d \bar{d}d + m_s \bar{s}s$ . Clearly  $\mathcal{L}_{\text{scbt}} \rightarrow \mathcal{L}_{\text{cbl}}$ . Thus the overall continuous symmetries of QCD on display are

$$\mathcal{G}=SU_V(3) \otimes SU_A(3) \otimes U_V(1) \otimes U_A(1), \quad (2.6)$$

with the well-known realization of  $SU_V(3)$  in the nucleon octet (eightfold way), and  $SU_A(3)$  broken to give the Goldstone modes of the “ $\pi$ ” octet. The  $U_A(1)$  puzzle is, as before, resolved by instanton effects. The continuous symmetries given in Eq. (2.6) are often quoted in the equivalent decomposition  $[SU(3) \otimes U(1)]_L \otimes [SU(3) \otimes U(1)]_R$ , where  $L$  and  $R$  refer to the chiral forms left and right, respectively, and  $\psi_{L,R} = \frac{1}{2}(1 \mp \gamma_5)\psi$  transforms as  $\psi_{L,R} \rightarrow \exp(-i\omega_{L,R}^a \lambda^a/2 - i\delta_{L,R})\psi_{L,R}$ .

At this point, we comment that there is no known dynamical reason why  $SU_A(2)$  or  $SU_A(3)$  should be realized in the Goldstone mode. It is convincing, however, in view of the low masses of the pseudoscalar bosons.

One now wishes to construct a model Lagrangian that is simpler to work with than that of QCD, yet which contains the same symmetry structure of QCD. One is naturally led to the pre-QCD model of Nambu and Jona-Lasinio (1961a), who considered nucleons interacting via a two-body interaction that was constructed to have  $SU_V(2) \otimes SU_A(2) \otimes U_V(1) \otimes U_A(1)$  symmetry in its original form, and later excluded the  $U_A(1)$  symmetry (Nambu and Jona-Lasinio, 1961b), in accordance with experimental observation. Since at their time quarks were not

known, Nambu and Jona-Lasinio used nucleons, i.e., protons, neutrons, and their antiparticles, as the “elementary” building blocks. In their model, the nucleon-antinucleon interaction channel is attractive and, in analogy to the effective electron-electron interaction in a superconductor, is responsible for the formation of Cooper-like pairs that consist of a nucleon and antinucleon. Nambu and Jona-Lasinio also identified the pseudoscalar Goldstone bosons occurring in the theory with pions. To translate this picture over to QCD, one notes that an effective interaction between quarks could arise from some complicated processes involving gluon exchange, just as the effective electron-electron interaction in BCS theory arises, not from the Coulomb interaction between electrons, but rather from the electron-phonon interaction.

One reinterprets the NJL model as a quark Lagrangian, for which it is well suited. A possible candidate for  $\mathcal{L}_{\text{chiral}}$  that has  $SU_V(2) \otimes SU_A(2) \otimes U_V(1)$  symmetry is

$$\mathcal{L}_{\text{chiral}}^{(1)} = \bar{\psi} i \not{\partial} \psi + G[(\bar{\psi} \psi)^2 + (\bar{\psi} i \gamma_5 \tau \psi)^2]. \quad (2.7)$$

The invariance of Eq. (2.7) under  $SU_A(2)$  symmetry can be confirmed by noting that

$$\begin{aligned} (\bar{\psi} \psi) &\rightarrow (\bar{\psi} \psi) \cos \theta - (\bar{\psi} i \gamma_5 \tau \cdot \hat{\theta}) \sin \theta, \\ (\bar{\psi} i \gamma_5 \tau_i \psi) &\rightarrow (\bar{\psi} i \gamma_5 \tau_i \psi) + (\bar{\psi} \psi) \hat{\theta}_i \sin \theta \\ &\quad - (\bar{\psi} i \gamma_5 \tau \cdot \hat{\theta} \psi) \hat{\theta}_i (1 - \cos \theta), \end{aligned} \quad (2.8)$$

under the transformation  $\psi \rightarrow \exp(-i\tau \cdot \theta \gamma_5/2)\psi$ , as listed in Table I. The angles  $\hat{\theta}_i$  are  $\hat{\theta} = \theta_i/|\hat{\theta}|$ . For a Lagrangian invariant under  $SU_V(3) \otimes SU_A(3) \otimes U_V(1)$ ,  $\mathcal{L}_{\text{chiral}}$  takes the form (Bernard, Jaffe, and Meissner, 1988)

$$\begin{aligned} \mathcal{L}_{\text{chiral}}^{(2)} &= \bar{\psi} i \not{\partial} \psi + G \sum_{a=0}^8 [(\bar{\psi} \lambda^a \psi)^2 + (\bar{\psi} i \gamma_5 \lambda^a \psi)^2] \\ &\quad - K [\det \bar{\psi} (1 + \gamma_5) \psi + \det \bar{\psi} (1 - \gamma_5) \psi], \end{aligned} \quad (2.9)$$

with  $\lambda^0 = \sqrt{2/3}I$ . Here the determinant is in flavor space, and  $G$  and  $K$  are coupling constants. One notes that the four-fermion symmetric term of Eq. (2.9) is invariant under  $U(3)$ , while the determinantal term, constructed along the suggestion of 't Hooft (1976), is required to remove the  $U_A(1)$  symmetry that would otherwise be present. It is apparent that Eqs. (2.7) and (2.9) have formally the same structure if one rewrites (2.7) as the sum of two terms,

$$\mathcal{L}_{\text{chiral}}^{(1)} = \mathcal{L}_{\text{sym}}^{(1)} + \mathcal{L}_{\text{det}}^{(1)}, \quad (2.10)$$

where

$$\mathcal{L}_{\text{sym}}^{(1)} = \frac{1}{2} G \sum_{i=0}^3 [(\bar{\psi} \tau^i \psi)^2 + (\bar{\psi} i \gamma_5 \tau^i \psi)^2] \quad (2.11)$$

and

$$\begin{aligned} \mathcal{L}_{\text{det}}^{(1)} &= \frac{1}{2} G [(\bar{\psi} \psi)^2 + (\bar{\psi} i \gamma_5 \tau \psi)^2 - (\bar{\psi} i \gamma_5 \psi)^2 - (\bar{\psi} \tau \psi)^2] \\ &= G [\det \bar{\psi} (1 + \gamma_5) \psi + \det \bar{\psi} (1 - \gamma_5) \psi]. \end{aligned} \quad (2.12)$$

Thus for two quark flavors, a more general structure could be obtained—here the coupling strengths of the symmetric and determinantal terms are set equal so that (2.11) and (2.12) can be combined to give Eq. (2.7). The structure of the determinantal term for the two-flavor model is two-body in nature; i.e., it contains four-fermion-interaction vertices, while for three quark flavors, the determinantal term is three-body in character, or contains six-fermion-interaction vertices. However, since calculations will be performed in the mean-field

approximation, the three-flavor NJL model will in principle be no more difficult to treat than the two-flavor one. In this case, the six-fermion term can be reduced to an effective four-fermion vertex, which can then be handled in the usual way. While there is little technical difference in the handling of the two- and three-flavor models, the six-fermion-interaction vertex brings new physics with it. As we shall see, the flavor-mixing nature of this interaction leads to the mixing of the pure pseudoscalar modes  $\eta_0$  and  $\eta_8$  to form the physical  $\eta$  and  $\eta'$  mesons. Details will be given in Secs. II.C.2 and IV.B.3. For illustrative purposes, we shall deal as far as possible with the SU(2) version of  $\mathcal{L}_{\text{chiral}}$ .

For the sake of completeness, we remark that the chosen form of the three-flavor version of  $\mathcal{L}_{\text{chiral}}$  given in Eq. (2.9) is sufficient for satisfying the symmetry requirements set by QCD, but it is by no means unique. The most general form for the four-fermion-interaction term that includes other bilinear constructions of the vector and axial-vector currents in SU(3),  $j_\mu^k = \bar{\psi} \gamma_\mu \lambda^k \psi$  and  $J_{5\mu}^k = \bar{\psi} \gamma_\mu \gamma_5 \lambda^k \psi$ , that are also invariant under  $\text{SU}_V(3) \otimes \text{SU}_A(3) \otimes \text{U}_V(1) \otimes \text{U}_A(1)$  is (Klimt *et al.*, 1990)

$$\begin{aligned} \mathcal{L}^{(4)} &= C_1 [(\bar{\psi} \delta^C \lambda_0 \gamma_\mu \psi)^2 + (\bar{\psi} \delta^C \lambda_0 \gamma_\mu \gamma_5 \psi)^2] + C_2 [(\bar{\psi} \delta^C \lambda_i \gamma_\mu \psi)^2 + (\bar{\psi} \delta^C \lambda_i \gamma_\mu \gamma_5 \psi)^2] \\ &+ C_3 [(\bar{\psi} \lambda_j^C \lambda_0 \gamma_\mu \psi)^2 + (\bar{\psi} \lambda_j^C \lambda_0 \gamma_\mu \gamma_5 \psi)^2] + C_4 [(\bar{\psi} \lambda_j^C \lambda_i \gamma_\mu \psi)^2 + (\bar{\psi} \lambda_j^C \lambda_i \gamma_\mu \gamma_5 \psi)^2] \\ &+ C_5 [(\bar{\psi} \delta^C \lambda_0 \gamma_\mu \psi)^2 - (\bar{\psi} \delta^C \lambda_0 \gamma_\mu \gamma_5 \psi)^2] + C_6 [(\bar{\psi} \lambda_j^C \lambda_0 \gamma_\mu \psi)^2 - (\bar{\psi} \lambda_j^C \lambda_0 \gamma_\mu \gamma_5 \psi)^2]. \end{aligned} \quad (2.13)$$

Here  $\lambda_j^C$  are the Gell-Mann matrices in color space,  $\delta^C$  is the unit matrix in color space, and the  $C_1 \dots C_6$  are nonindependent coupling strengths. Constructing a Fierz-invariant Lagrange density from Eq. (2.13) leads one to the commonly used combination

$$\begin{aligned} \mathcal{L}^{(4)} &= \frac{1}{2} G_1 \sum_{i=0}^8 [(\bar{\psi} \lambda^i \psi)^2 + (\bar{\psi} \lambda^i i \gamma_5 \psi)^2] - \frac{1}{2} G_2 \sum_{i=0}^8 [(\bar{\psi} \lambda^i \gamma_\mu \psi)^2 + (\bar{\psi} \lambda^i \gamma_\mu \gamma_5 \psi)^2] \\ &- \frac{1}{2} G_3 [(\bar{\psi} \lambda^0 \gamma_\mu \psi)^2 + (\bar{\psi} \lambda^0 \gamma_\mu \gamma_5 \psi)^2] - \frac{1}{2} G_4 [(\bar{\psi} \lambda^0 \gamma_\mu \psi)^2 - (\bar{\psi} \lambda^0 \gamma_\mu \gamma_5 \psi)^2] + \mathcal{L}_4^{\text{color octet}}, \end{aligned} \quad (2.14)$$

where  $G_1, \dots, G_4$  are independent coupling constants that may be expressed in terms of the constants  $C_1, \dots, C_6$ . The term  $\mathcal{L}_4^{\text{color octet}}$  contains bilinears that include the color Gell-Mann matrices. For details regarding Fierz transformations, we refer the reader to Sec. II.D. It has been shown (Bernard, Jaffe, and Meissner, 1988) that the introduction of other such bilinear terms as occur in (2.14) leads to results that are qualitatively similar to those obtained by using Eq. (2.9). For simplicity, we shall use as far as possible the representation (2.7) or (2.9) as our model chiral Lagrangian.

The NJL model, with Lagrangian as specified by Eq. (2.4) with  $\mathcal{L}_{\text{chiral}}$  given by (2.7) in the two-flavor version or the appropriate generalization to three-flavors, has shortcomings that are a consequence of the use of an effective contact interaction. This interaction is not confining; so it should only be applied to properties for which confinement is not expected to be essential. It also renders the model nonrenormalizable. This is a serious problem, which again reminds one that this is to be treat-

ed as an effective theory. In applications, it is standard practice to introduce one cutoff parameter to regulate the theory, that is, to use one characteristic length scale for the interaction. A careful procedure must therefore be employed in regulating the different divergent quantities that occur, since it is essential that the consequences of the symmetries (such as the existence of the Goldstone mode) continue to hold. That this can be enforced in a nonrenormalizable theory that is regulated by one parameter only is not clear, since the different integrals to be regulated may diverge with different strengths. We comment on this at appropriate states and devote Sec. III to the discussion of the various regularization schemes that are commonly used.

## B. The Bogoliubov-Valatin approach

In this section we shall explicitly examine the structure of the ground state in the mean-field approximation. Let

us consider the chirally symmetric two-flavor NJL Lagrangian, given as

$$\mathcal{L}_{\text{NJL}} = \bar{\psi} i \not{\partial} \psi + G [(\bar{\psi} \psi)^2 + (\bar{\psi} i \gamma_5 \tau \psi)^2] . \quad (2.15)$$

For simplicity, the perturbative mass term of the Lagrangian has been set equal to zero. The Hamiltonian density corresponding to this Lagrangian is

$$\mathcal{H}_{\text{NJL}} = -i \bar{\psi} \boldsymbol{\gamma} \cdot \nabla \psi - G [(\bar{\psi} \psi)^2 + (\bar{\psi} i \gamma_5 \tau \psi)^2] , \quad (2.16)$$

and the Fourier expansion of the field operators at  $t=0$ ,

$$\begin{aligned} \psi(\mathbf{x}, 0) = \sum_s \int \frac{d^3 p}{(2\pi)^3} [b(\mathbf{p}, s) u(\mathbf{p}, s) e^{i\mathbf{p} \cdot \mathbf{x}} \\ + d^\dagger(\mathbf{p}, s) v(\mathbf{p}, s) e^{-i\mathbf{p} \cdot \mathbf{x}}] , \end{aligned} \quad (2.17)$$

defines the annihilation operators  $b(\mathbf{p}, s)$  and  $d(\mathbf{p}, s)$  of particle and antiparticle of momentum  $\mathbf{p}$  and helicity  $s$  that destroy the normal or unpaired vacuum  $|0\rangle$ , i.e.,  $b(\mathbf{p}, s)|0\rangle = d(\mathbf{p}, s)|0\rangle = 0$ . We work in unit volume unless otherwise stated. The spinors  $u(\mathbf{p}, s)$  and  $v(\mathbf{p}, s)$  are helicity eigenstates satisfying  $\not{p} u(\mathbf{p}, s) = \not{p} v(\mathbf{p}, s) = 0$ , and are normalized such that  $u^\dagger(\mathbf{p}, s) u(\mathbf{p}, s) = v^\dagger(\mathbf{p}, s) v(\mathbf{p}, s) = 1$ .

One now introduces a BCS-like variational ground state

$$|\text{vac}\rangle = \prod_{\mathbf{p}, s=\pm 1} [\cos\theta(p) + s \sin\theta(p) b^\dagger(\mathbf{p}, s) d^\dagger(-\mathbf{p}, s)] |0\rangle \quad (2.18)$$

that contains pairs of zero total momentum and zero total helicity. This trial ground state differs from the traditional BCS theory in that the pairing is between a particle and its antiparticle, and not between pairs of like particles. The operators that annihilate this vacuum are given by the Bogoliubov-Valatin transformation as

$$\begin{aligned} B(\mathbf{p}, s) &= \cos\theta(p) b(\mathbf{p}, s) + s \sin\theta(p) d^\dagger(-\mathbf{p}, s) , \\ D(\mathbf{p}, s) &= \cos\theta(p) d(\mathbf{p}, s) - s \sin\theta(p) b^\dagger(-\mathbf{p}, s) . \end{aligned} \quad (2.19)$$

It is now possible to evaluate the expectation value of  $\mathcal{H}_{\text{NJL}}$  with respect to the vacuum (2.18). This becomes a simple (if tedious) task, if one expresses (2.17) in terms of the quasiparticle operators  $B(\mathbf{p}, s)$  and  $D(\mathbf{p}, s)$  as

$$\begin{aligned} \psi(\mathbf{x}, 0) = \sum_s \int \frac{d^3 p}{(2\pi)^3} [B(\mathbf{p}, s) M_1(\mathbf{p}, s) e^{i\mathbf{p} \cdot \mathbf{x}} \\ + D^\dagger(\mathbf{p}, s) M_2(\mathbf{p}, s) e^{-i\mathbf{p} \cdot \mathbf{x}}] , \end{aligned} \quad (2.20)$$

with

$$\begin{aligned} M_1(\mathbf{p}, s) &= [\cos\theta(p) + \gamma^0 \sin\theta(p)] u(\mathbf{p}, s) \\ M_2(\mathbf{p}, s) &= [\cos\theta(p) - \gamma^0 \sin\theta(p)] u(\mathbf{p}, s) \end{aligned} \quad (2.21)$$

and makes use of the spinor relation  $\gamma_0 s v(-\mathbf{p}, s) = u(\mathbf{p}, s)$  and the helicity sum

$$\sum_s u(\mathbf{p}, s) u^\dagger(\mathbf{p}, s) = \frac{1}{2} (1 - \boldsymbol{\gamma} \cdot \hat{\mathbf{p}} \gamma^0) .$$

One finds

$$\begin{aligned} W[\phi] &= -2N_c N_f \int \frac{d^3 p}{(2\pi)^3} p \cos\phi(p) \\ &\quad - 4G(N_c N_f)^2 \left[ \int \frac{d^3 p}{(2\pi)^3} \sin\phi(p) \right]^2 \end{aligned} \quad (2.22)$$

for the total energy in the Hartree approximation, up to an unimportant constant. Here  $N_c$  is the number of colors and  $N_f$  the number of flavors of the system. The angle  $\phi(p) = 2\theta(p)$ . The form of  $\phi(p)$  that minimizes Eq. (2.22) is obtained from  $\delta W / \delta \phi(p) = 0$ , or

$$p \tan\phi(p) = 4GN_c N_f \int \frac{d^3 q}{(4\pi)^3} \sin\phi(q) . \quad (2.23)$$

This is the so-called gap or self-consistency equation. In this model it takes on a specifically simple form, which is due to the four-fermion contact interaction. We note that the right-hand side of this equation is independent of momentum and is, in fact, just a constant. Calling this constant  $m^*$ , we have

$$\tan\phi(p) = \frac{m^*}{p} \quad \text{and} \quad \sin\phi(p) = \frac{m^*}{(p^2 + m^{*2})^{1/2}} , \quad (2.24)$$

which may be inserted back into (2.23) to yield the more familiar version of the NJL gap equation,

$$m^* = 4GN_c N_f \int \frac{d^3 p}{(2\pi)^3} \frac{m^*}{E_p} . \quad (2.25)$$

In performing the calculations in this section, we have implied that the ultraviolet divergences that arise from the contact interaction are to be regulated by cutting off the three momenta  $\mathbf{p}^2$  at  $\Lambda^2$ . Doing this, one recovers the condition of Nambu and Jona-Lasinio (1961a),

$$\frac{\pi^2}{GN_c N_f \Lambda^2} = \left[ \left( 1 + \frac{m^{*2}}{\Lambda^2} \right)^{1/2} - \frac{m^{*2}}{\Lambda^2} \sinh^{-1} \frac{\Lambda}{m^*} \right] , \quad (2.26)$$

which has a solution for values of the coupling strength that exceed a critical value  $G_c$ , where  $G_c \Lambda^2 = \pi^2 / N_c N_f$ .

The Bogoliubov-Valatin approach developed here serves to highlight the physics of the situation: simply stated, this is that the ground state that minimizes the total energy does not have the symmetry of the underlying Lagrangian. An ansatz for its form, Eq. (2.18) explicitly displays the Cooper-pair-like structure of particles and antiparticles that is responsible for the breaking of chiral symmetry. It also introduces the gap equation as the condition that minimizes the total energy.

This approach has, however, several disadvantages. In particular, the concept of quasiparticle transformations is difficult to generalize to include the effects of external parameters, such as finite temperature, density, and the presence of external fields. It is therefore useful to turn to the equivalent, but more tractable, approach of many-body theory via Green's functions.

### C. The self-energy in Hartree and Hartree-Fock approximations

#### 1. The two-flavor model

In this section we continue to work with the two-flavor NJL model, as defined by Eq. (2.15). The Hartree and Fock terms that form the mean-field approximation to the self-energy cannot easily be drawn for a contact interaction. We therefore illustrate the self-energy graphically by temporarily giving the interaction a finite range (see Fig. 1).

Using the appropriate Feynman rules for a four-fermion interaction, the self-energy associated with the scalar vertex  $(\bar{\psi}\psi)^2$  is given as

$$\begin{aligned}\Sigma^s &= \Sigma_{\text{Hartree}}^s + \Sigma_{\text{Fock}}^s \\ &= 2G[\text{Tr}S(x, x) - iS(x, x)],\end{aligned}\quad (2.27)$$

where  $\text{Tr}$  denotes a color, flavor, and spinor trace, while that associated with the pseudoscalar vertex  $(\bar{\psi}i\gamma_5\tau\psi)^2$  is

$$\begin{aligned}\Sigma^{\text{ps}} &= \Sigma_{\text{Hartree}}^{\text{ps}} + \Sigma_{\text{Fock}}^{\text{ps}} \\ &= 2G(i\gamma_5\tau)\text{Tr}iS(x, x)i\gamma_5\tau \\ &\quad - 2G(i\gamma_5\tau)iS(x, x)(i\gamma_5\tau),\end{aligned}\quad (2.28)$$

in terms of the time-ordered single-particle fermion Green's function  $S(x, x')$  that is defined as  $iS(x, x') = \langle T\psi(x)\bar{\psi}(x') \rangle$ . In general, this propagator satisfies the equation of motion

$$[i\partial_x - \Sigma]S(x, x') = \delta^{(4)}(x - x'), \quad (2.29)$$

where  $\Sigma(x, x')$  is the total self-energy, due in this case to both the scalar and pseudoscalar interaction vertices,  $\Sigma = \Sigma^s + \Sigma^{\text{ps}}$ . For a contact interaction, the mean-field calculation of  $\Sigma(x, x')$  is independent of both  $x$  and  $x'$ , as can be seen from Eqs. (2.27) and (2.28), so that one may immediately identify the constant  $\Sigma$  as the mass of the particles of the system,  $\Sigma = m^*$ . Then Eq. (2.29) has the well-known solution in momentum space,

$$S(p) = \frac{\not{p} + m^*}{p^2 - m^{*2}}. \quad (2.30)$$

The Fourier transform of this may be inserted into both Eqs. (2.27) and (2.28). One must now perform the traces. One notes that integrals that are odd in  $p$  do not contribute, and one may rearrange the remaining terms in the self-energy to give the form

$$\Sigma = m^* = m_0 + 2iG[N_c N_f + \tfrac{1}{2}] \int \frac{d^4 p}{(2\pi)^4} \text{tr} S(p). \quad (2.31)$$

Equation (2.31) becomes the gap equation (2.25), which was derived in Sec. II.B via the Bogoliubov-Valatin transformation, upon neglecting the exchange contribution (the factor one-half in the square brackets) and setting  $m_0 = 0$ . Here we have taken the liberty of including the perturbative current quark mass  $m_u = m_d = m_0$  in the

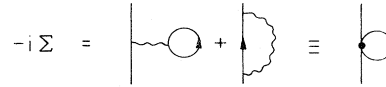


FIG. 1. Hartree and Fock contributions to the self-energy for a particular interaction vertex.

formalism, and the symbol  $\text{tr}$  refers to the trace over spinor indices only.

Another comment is in order. The Hartree-Fock calculation of (2.31) is seen to contain terms of order  $GN_c$  and  $G$ . As has been emphasized by Blin, Hiller, and Schaden (1988), to the extent that the NJL model is to be regarded as an effective theory of interacting quarks that follows from QCD in the large  $N_c$  limit ('t Hooft, 1976a, 1976b) where  $GN_c \sim O(1)$ , one should properly regard the Hartree approximation as the first term in an expansion of  $N_c^{-1}$ . From this point of view, it is consistent to ignore the Fock contribution to Eq. (2.31), which is seen to be of order  $N_c^{-1}$ , since higher-order diagrams that are also of this order, but which lie outside the scope of Hartree-Fock, are not included.

#### 2. The three-flavor model

We now consider the effective SU(3) Lagrangian, introduced in Sec. II.A,

$$\begin{aligned}\mathcal{L}_{\text{NJL}} &= \bar{\psi}i\partial\psi + G \sum_{a=0}^8 [(\bar{\psi}\lambda^a\psi)^2 + (\bar{\psi}i\gamma_5\lambda^a\psi)^2] \\ &\quad - K[\det\bar{\psi}(1+\gamma_5)\psi + \det\bar{\psi}(1-\gamma_5)\psi] + \mathcal{L}_{\text{mass}} \\ &= \bar{\psi}i\partial\psi + \mathcal{L}^{(4)} + \mathcal{L}^{(6)} + \mathcal{L}_{\text{mass}}\end{aligned}\quad (2.32)$$

with  $\mathcal{L}_{\text{mass}} = m_u\bar{u}u + m_d\bar{d}d + m_s\bar{s}s$ . Because of the experience gained in Sec. II.C.1, we need only consider the self-energy associated with the four-fermion-interaction term  $\Sigma^{(4)}$  in the Hartree approximation. Directly translating the Feynman diagram for this (only the scalar interaction vertex contributes!), one finds

$$\Sigma_f^{(4)} = 2iGN_c \sum_a (\lambda^a)_{ff} \sum_g \int \frac{d^4 p}{(2\pi)^4} (\lambda^a)_{gg} \text{tr} S^g(p) \quad (2.33)$$

with flavor indices  $f$  and  $g$  explicitly displayed. It has already been assumed here that  $S$  is diagonal in flavor. One can evaluate  $\Sigma$  for each of the flavors at hand to find the result

$$\Sigma_f^{(4)} = 4iGN_c \int \frac{d^4 p}{(2\pi)^4} \text{tr} S^f. \quad (2.34)$$

This shows that the specific form of the two-body interaction considered relates the self-energy of a quark of a given flavor to the propagator of that flavor only. We comment that, for this interaction, the Hartree and Hartree-Fock approximations are identical, since the exchange contributions from the scalar and pseudoscalar



terms exactly cancel.

An alternative approach for calculating the Hartree-Fock approximation to the self-energy is to Wick-contract all possible pairs of creation and destruction field operators in the Lagrangian, so that only two remain “alive” as operators. One aims at obtaining the form

$$\mathcal{L} = -\bar{\psi}\Sigma\psi, \quad (2.35)$$

from which we can directly identify the self-energy. We apply this technique to calculate the self-energy  $\Sigma^{(6)}$  that arises from the six-fermion interaction. Details of this calculation are relegated to Appendix A. There it is shown that

$$\mathcal{L}^{(6)} \rightarrow \bar{\psi}^i K \{2N_c^2 + 3N_c + 1\} (\text{tr} S^j)(\text{tr} S^k) \psi^i, \quad i \neq j \neq k, \quad (2.36)$$

on performing the Wick contractions. Therefore one may identify

$$\Sigma_i^{(6)} = -K \{2N_c^2 + 3N_c + 1\} (\text{tr} S^j)(\text{tr} S^k), \quad i \neq j \neq k, \quad (2.37)$$

for a quark of flavor  $i$ , indicating that flavor mixing originates from the  $U_A(1)$  breaking contribution to the Lagrangian in the Hartree-Fock approximation. The total self-energy for the Lagrangian (2.32) for a particular quark flavor is then

$$m_i^* = m_i + 4iGN_c \text{tr} S^i - K \{2N_c^2 + 3N_c + 1\} (\text{tr} S^j)(\text{tr} S^k), \quad i \neq j \neq k, \quad (2.38)$$

as was originally derived by Bernard, Jaffe, and Meissner

$$\begin{aligned} \frac{1}{2}\mathcal{L}^{(6) \rightarrow (4)} = & \frac{N_c + 1}{12} K \{2(i \text{tr} S^s + 2i \text{tr} S^u)(\bar{\psi}\lambda^0\psi)^2 - 3i \text{tr} S^s[(\bar{\psi}\lambda^1\psi)^2 + (\bar{\psi}\lambda^2\psi)^2] \\ & - 3i \text{tr} S^s(\bar{\psi}\lambda^3\psi)^2 - 3i \text{tr} S^u[(\bar{\psi}\lambda^4\psi)^2 + (\bar{\psi}\lambda^5\psi)^2] \\ & - 3i \text{tr} S^u[(\bar{\psi}\lambda^6\psi)^2 + (\bar{\psi}\lambda^7\psi)^2] + (i \text{tr} S^s - 4i \text{tr} S^u)(\bar{\psi}\lambda^8\psi)^2 \\ & + \sqrt{2}(i \text{tr} S^s - i \text{tr} S^u)(\bar{\psi}\lambda^0\psi)(\bar{\psi}\lambda^8\psi) + \sqrt{2}(i \text{tr} S^s - i \text{tr} S^u)(\bar{\psi}\lambda^8\psi)(\bar{\psi}\lambda^0\psi) + (\lambda \rightarrow \gamma_5 \lambda)\}. \end{aligned} \quad (2.40)$$

A full discussion of the meson properties will be given in Sec. IV. However, we may note here that in addition to having terms that are proportional to

$$(\bar{\psi}\lambda^i\psi)^2 \quad \text{and} \quad (\bar{\psi}\gamma_5\lambda^i\psi)^2, \quad (2.41)$$

which occur in the standard  $U(3)$  four-fermion term, one also has such *mixed* terms as

$$(\bar{\psi}\lambda^0\gamma_5\psi)(\bar{\psi}\lambda^8\gamma_5\psi), \quad (\bar{\psi}\lambda^8\gamma_5\psi)(\bar{\psi}\lambda^0\gamma_5\psi), \quad (2.42)$$

and their scalar counterparts. Since the meson modes that are supported are identified by the quantum numbers associated with the four-fermion products, we see immediately that the pseudoscalar mesons associated



FIG. 2. Six-fermion vertex, reduced in the mean-field approximation to an effective four-fermion vertex.

(1988). Assuming that  $KN_c^2 \sim O(1)$ , the consistent  $1/N_c$  expansion requires

$$\Sigma_i = m_i^* = m_i + 4iGN_c \text{tr} S^i - 2KN_c^2 (\text{tr} S^j)(\text{tr} S^k), \quad i \neq j \neq k, \quad (2.39)$$

as the lowest-order term. As before, in Eqs. (2.38) and (2.39),  $m_i$  refer to the current quark masses of flavor  $i$ .

Equations (2.37) and (2.39) indicate the fact that in the mean-field approximation, flavor mixing originates from the  $U_A(1)$  breaking contribution to the Lagrangian. The  $U_A(1)$  term also has the physical consequence that the degeneracy of the  $\eta$  and  $\eta'$  mesons is lifted. This may be seen directly if we write the six-fermion Lagrange density as an effective four-fermion interaction. Such an effective four-fermion term is useful in general for constructing a systematic procedure for analyzing Feynman diagrams making up the self-energy and for identifying the meson modes that are supported. One way of going about this is to Wick-contract out one quark and one antiquark field operator from the six-fermion form, so that the six-fermion interaction is left in the form of an effective four-fermion interaction, to which the standard Feynman rules may be applied. This is indicated schematically in Fig. 2. The actual calculation is performed in Appendix A. One finds

with the  $\lambda^0$  and  $\lambda^8$  terms, i.e., the  $\eta_0$  and  $\eta_8$  mesons, will be mixed because of the effect of Eq. (2.42). This will then give rise to the physical  $\eta$  and  $\eta'$ .

Finally, we remark that the self-energy corresponding to the Hartree and Fock terms can be derived directly from Eq. (2.40) by applying the Feynman rules. The direct contribution is

$$\Sigma_{\text{Hartree}}^i = -2N_c(N_c + 1)K \text{tr} S^j \text{tr} S^k \quad \text{with } i \neq j \neq k, \quad (2.43)$$

whereas the exchange term gives

$$\Sigma_{\text{Fock}}^i = -(N_c + 1)K \text{tr} S^j \text{tr} S^k, \quad i \neq j \neq k. \quad (2.44)$$

The sum of these two terms gives, as expected, the result (2.37). It indicates, however, that for the six-fermion interaction, in addition to working in the Hartree approximation, one should, strictly speaking, also drop terms that are not of order  $O(1)$  in  $KN_c^2$ , in order to construct a consistent expansion in  $1/N_c$ .

#### D. Fierz transformations

In this section, we look at the Fierz transformation applied to the NJL model. The Fierz transformation is a purely technical device that is used to examine the effect of a rearrangement of fermion field operators that occur in quartic products at the same space-time point. In effect, with the four-fermion-interaction Lagrangians given in Eqs. (2.15) and (2.32), one asks the question as to how the direct and exchange terms are related to one another. This technique is mentioned frequently in the literature pertaining to the NJL model and is useful in several ways. Here we list some interesting features that arise from Fierz-transforming the NJL interaction Lagrangian, and we discuss them in more detail in what follows.

(i) A simple local color current-current interaction leads directly to the four-fermion term of the SU(3) Lagrangian given in Eq. (2.32).

(ii) The self-energy arising as the direct contribution of the Fierz-transformed Lagrangian is equivalent to the exchange contribution that would arise from the original Lagrange density. This occurs simply as a consequence of the definition of the Fierz transform. It is on occasion simpler to know the Fierz-transformed Lagrangian in order to obtain the exchange contribution to the self-energy. We shall use this approach to construct the self-energy in the flavor SU(2) model, when we work with finite temperature and chemical potential in Sec. V. We therefore derive the Fierz-transformed Lagrange density here for this case.

(iii) If we work with a Lagrange density that is invariant under Fierz transformations, the self-energy in the Hartree-Fock approximation can be constructed as twice the direct or Hartree contribution arising from this Lagrange density. This follows as a consequence of point (ii) above.

In what follows, we define what is meant by the Fierz transformation, but we present most of the technical detail in Appendix B.

Let us denote the interaction vertex tensor in spinor, flavor, and color space as  $\Gamma_{ab}^k$ , with  $a = (\alpha, f, c)$  combin-

ing indices in these three spaces. The superscript  $k$  spans the space of matrices in the three spaces given. Then a general four-fermion-interaction term can be written as

$$\bar{\psi}_a(4)\Gamma_{ab}^k\psi_b(2)\bar{\psi}_c(3)\Gamma_{cd}^k\psi_d(1), \quad (2.45)$$

and the Fierz transformation asks what the relation of this interaction is to the term

$$\bar{\psi}_a(4)\Gamma_{ab}^k\psi_b(1)\bar{\psi}_c(3)\Gamma_{cd}^k\psi_d(2) \quad (2.46)$$

in which particles 1 and 2 have been exchanged. Denoting  $\mathcal{F}$  as the operator that performs the Fierz transformation, one can easily construct (2.46) from (2.45) by permuting the field operators to exchange 1 and 2 and relabeling the indices  $b \leftrightarrow d$ :

$$\begin{aligned} \mathcal{F}[\bar{\psi}_a(4)\Gamma_{ab}^k\psi_b(2)\bar{\psi}_c(3)\Gamma_{cd}^k\psi_d(1)] \\ = -\bar{\psi}_a(4)\psi_d(1)\bar{\psi}_c(3)\psi_b(2)\Gamma_{ab}^k\Gamma_{cd}^k \\ = -\bar{\psi}_a(4)\psi_b(1)\bar{\psi}_c(3)\psi_d(2)\Gamma_{ad}^k\Gamma_{cb}^k. \end{aligned} \quad (2.47)$$

The requirement that (2.47) reproduce (2.46) implies that one requires a knowledge of the transformation  $\Gamma_{ad}^k\Gamma_{cb}^k \rightarrow \Gamma_{ab}^k\Gamma_{cd}^k$ , which can be formulated as

$$\sum_k \Gamma_{cb}^k \Gamma_{da}^k = \sum_{km} c_{mk} \Gamma_{ca}^m \Gamma_{db}^m, \quad (2.48)$$

where  $c_{mk}$  is the crossing matrix that satisfies  $\sum_{mk} c_{mk} c_{km} = 1$ . In Dirac space, the crossing matrix is well known and can be found in standard texts such as Itzykson and Zuber (1980). A summary of this is given in Appendix B, where we also calculate the SU(3) and SU(2) crossing matrices for color, flavor, and isospin. The final results are summarized as

$$\begin{pmatrix} 1 & 1 \\ \tau & \tau \end{pmatrix}_{fg';gf'} = \begin{pmatrix} \frac{1}{2} & \frac{1}{2} \\ \frac{3}{2} & \frac{1}{2} \end{pmatrix} \begin{pmatrix} 1 & 1 \\ \tau & \tau \end{pmatrix}_{ff';gg'} \quad (2.49)$$

for SU(2), while

$$\begin{pmatrix} \lambda^0 & \lambda^0 \\ \lambda^i & \lambda^i \end{pmatrix}_{fg';gf'} = \begin{pmatrix} \frac{1}{3} & \frac{1}{3} \\ \frac{8}{3} & -\frac{1}{3} \end{pmatrix} \begin{pmatrix} \lambda^0 & \lambda^0 \\ \lambda^i & \lambda^i \end{pmatrix}_{ff';gg'} \quad (2.50)$$

for SU(3).

We are now in a position to apply the Fierz transform. Let us examine some examples. First we consider the four-fermion-interaction term of Eq. (2.32). Replacing  $\Gamma$  in (2.47) first by  $\lambda \otimes 1 \otimes 1^c$  and then by  $\lambda \otimes (i\gamma_5) \otimes 1^c$  in flavor, Dirac and color space, one has

$$\mathcal{F} \left[ \sum_{i=0}^8 [(\bar{\psi}\lambda^i\psi)^2 + (\bar{\psi}\lambda^i i\gamma_5\psi)^2] \right] = -(\bar{\psi}_\alpha^{fc}\psi_\beta^{f'c'}\bar{\psi}_\alpha^{gd}\psi_\beta^{g'd'}) \sum_{i=0}^8 (\lambda^i)_{fg'}(\lambda^i)_{gf'} [1_{\alpha\beta'}1_{\alpha'\beta} + (i\gamma_5)_{\alpha\beta'}(i\gamma_5)_{\alpha'\beta}] 1_{cd}^c 1_{dc'}^c. \quad (2.51)$$

We now make use of Eqs. (2.50) and (B1) to arrive at the result

$$\mathcal{F} \left[ \sum_{i=0}^8 [(\bar{\psi}\lambda^i\psi)^2 + (\bar{\psi}\lambda^i i\gamma_5\psi)^2] \right] = -\frac{1}{2}[(\bar{\psi}\gamma^\mu\lambda^c\psi)^2 - (\bar{\psi}\gamma^\mu\gamma^5\lambda^c\psi)^2]. \quad (2.52)$$

A Fierz transformation applied to the right-hand side would of course give the original Lagrange density back again. What we notice is that the U(3)-invariant four-fermion-interaction Lagrangian is equivalent to a local color-color interaction that has the spinor structure of vector minus axial vector.

It is also of interest to examine the Fierz transform of the SU(2) interaction Lagrangian, Eq. (2.15). This follows from combining

$$\mathcal{F}(\bar{\psi}\psi)^2 = -(\bar{\psi}_\alpha^{f_c}\psi_\beta^{f'_c}\bar{\psi}_\alpha^{g_d}\psi_\beta^{g'_d})[(1)_{f_g'}(1)_{g_f'}]1_{\alpha\beta'}1_{\alpha'\beta}1_{cd'}^c1_{dc'}^c \quad (2.53)$$

and

$$\mathcal{F}(\bar{\psi}i\gamma_5\tau\psi)^2 = -(\bar{\psi}_\alpha^{f_c}\psi_\beta^{f'_c}\bar{\psi}_\alpha^{g_d}\psi_\beta^{g'_d})[(\tau^i)_{f_g'}(\tau^i)_{g_f'}](i\gamma_5)_{\alpha\beta'}(i\gamma_5)_{\alpha'\beta}1_{cd'}^c1_{dc'}^c. \quad (2.54)$$

Using Eqs. (2.49) and (B1), one finds that

$$\begin{aligned} \mathcal{F}[(\bar{\psi}\psi)^2 + (\bar{\psi}i\gamma_5\tau\psi)^2] &= \frac{1}{8N_c} [2(\bar{\psi}\psi)^2 + 2(\bar{\psi}i\gamma_5\tau\psi)^2 - 2(\bar{\psi}\tau\psi)^2 - 2(\bar{\psi}i\gamma_5\psi)^2 - 4(\bar{\psi}\gamma^\mu\psi)^2 - 4(\bar{\psi}i\gamma^\mu\gamma_5\psi)^2 \\ &\quad + (\bar{\psi}\sigma^{\mu\nu}\psi)^2 - (\bar{\psi}\sigma^{\mu\nu}\tau\psi)^2], \end{aligned} \quad (2.55)$$

where color octet contributions have been neglected. One sees, by comparing (2.52) and (2.55), the relative simplicity of the Fierz transformation of an interaction Lagrangian that maintains flavor U( $N$ ) symmetry. Equation (2.55) will prove useful to us when we work at finite temperature and chemical potential, as we shall simply be able to read off the exchange contributions to the self-energy from this result. We discuss this feature of the Fierz transform in the following example.

Let us consider, for the sake of being definite, the two-body interaction contribution to  $\mathcal{L}_{\text{chiral}}$  of Eq. (2.32),

$$\mathcal{L}_I = G \sum_{i=0}^8 [(\bar{\psi}\lambda^i\psi)^2 + (\bar{\psi}i\gamma_5\lambda^i\psi)^2], \quad (2.56)$$

for which the Fierz-transformed Lagrangian has been given in Eq. (2.52). One has three ways of writing an interaction Lagrangian that will give us the same value for the self-energy. We may consider either of the cases

- (a)  $\mathcal{L}_I$ ,
- (b)  $\mathcal{F}(\mathcal{L}_I)$ ,
- (c)  $\frac{1}{2}[\mathcal{L}_I + \mathcal{F}(\mathcal{L}_I)]$ ,

the last of which is by construction Fierz invariant.

The self-energy that is obtained from (a),

$$\Sigma = 2Gi\lambda^i \int \frac{d^4p}{(2\pi)^4} \text{Tr} S\lambda^i, \quad (2.58)$$

arises solely from the Hartree term, since the exchange term gives zero, whereas that calculated from (b), although numerically identical, arises purely from the Fock term, since in that case, the Hartree term vanishes. Consequently a consistent calculation of the self-energy from (c) must include *both* Hartree and Fock terms, since they are identical. This simply amounts to an overall readjustment of the coupling constant by a factor of 2, if one calculates the Hartree term only. Technically, one is of course now including the Fock contribution, as one must do.

The Fierz-transformed Lagrangian has a further use in

that it allows an immediate identification of the quantum numbers of the associated collective modes that are mesonic in character, since it displays the nature of the interaction vertices explicitly. As can be seen from Eq. (2.55), the Fierz transform of the form of the particular Lagrangian that we have chosen indicates, among other things, the vector-meson modes that can possibly be accessed. In practice, however, the strength associated with the Fierz-transformed interaction is generally insufficiently attractive in the vector and axial-vector channels (Nambu and Jona-Lasinio, 1961b; Eguchi and Sugawara, 1974), so that an additional term with a further independent coupling strength is required to generate the associated modes, as is given, for example, by the term accompanying the strength  $G_2$  in the generalized form of the NJL four-fermion interaction in Eq. (2.14). The interested reader is referred to Takizawa *et al.* (1989,1991), Blin *et al.* (1990), and Klimt *et al.* (1990) for further details. Here, we shall concern ourselves primarily with the pseudoscalar modes and their behavior.

In conclusion of this section, we comment that a Fierz transformation of the six-fermion interaction can also be defined as that transformation that leaves this interaction invariant under all possible permutations of the quark spinors  $\psi$  occurring in it. The reader is referred to Klimt *et al.* (1990) for explicit details.

### III. REGULARIZATION SCHEMES

As has already been mentioned, the contact interaction renders the NJL model nonrenormalizable. One therefore requires a procedure for regulating divergent quantities. Strictly speaking, in a nonrenormalizable theory, an infinite number of counterterms must be included in the Lagrangian, or equivalently, a new regulator should be introduced for each quantity that is calculated (see, for example, Itzykson and Zuber, 1980). On the other hand, a useful theory cannot afford an infinite number of parameters, and one's physical sense suggests that the in-

teraction should have a single length scale associated with it. Even making this simplification, there are several possible schemes that can be introduced and implemented in several different ways. Which, therefore, is the “right” one? The answer to this question is that *all* are: a nonrenormalizable model *per se* is not unique; it depends on the form of regularization chosen. That is, the regularization scheme determines the model, and not vice versa. One must therefore look to physical and not just mathematical content. Regularization should be undertaken in such a manner that physically expected properties of the model and symmetry considerations are maintained. For the NJL model, there are two obvious physical criteria that should be fulfilled: (a) from Sec. II.B, it is clear that the minimization of the total energy should give rise to the gap equation, and (b) symmetry requirements impose the existence of a zero mode or Goldstone boson. We shall not check these conditions stringently here. In fact, as was done in the original article of Nambu and Jona-Lasinio (1961a), we shall, on occasion, simply ignore the fact that we are dealing with divergent integrals and proceed to manipulate them as if they were convergent, showing thereby that the expected physical result is obtained. This is an acceptable procedure only if one assumes that the cutoff involved is much larger than all relevant momenta. The serious reader should, however, be warned about handling the ambiguities associated with improper integrals. The problem lies in the fact that the stage at which the regularization procedure is applied is crucial to the final result, since the normal calculational procedures of, for example, shifting variables and integration by parts are no longer legal mathematical manipulations. This will be demonstrated in an explicit example, when such a calculation arises in Sec. IV.A.2. In this section, however, we shall simply introduce the various regularization schemes, by applying them to the gap equation, and we shall provide a list of the standard parameters that are used for each procedure.

In the literature, the NJL model has been presented with many schemes: the noncovariant and physically intuitive three-momentum cutoff, and a host of covariant schemes that include the four-momentum cutoff in Euclidean space, the regularization in proper time, and the Pauli-Villars method. These latter three all have the attractive feature of being Lorentz invariant. For the sake

of being definite, we consider the SU(2) flavor model as given by Eq. (2.15), but include a small average current quark mass  $m_0$ , and we shall express the gap equation in all four schemes. One finds that the model, in any scheme, requires two parameters, the coupling strength  $G$  and a cutoff  $\Lambda$ , say. Traditionally, these are fixed by setting the quark condensate density per flavor at its empirical value,  $\langle \bar{u}u \rangle = \langle \bar{d}d \rangle = -(250 \text{ MeV})^3$  (see, for example, Reinders *et al.*, 1985), and the pion-decay constant to the measured value  $f_\pi = 93 \text{ MeV}$ . This will be given in Sec. III.C.

#### A. The three-momentum noncovariant cutoff scheme

In this case, the procedure is straightforward—a cutoff on  $\mathbf{p}^2 < \Lambda^2$  is imposed on all integrals after carrying out the  $p_0$  integration. The self-consistency condition (2.31) neglecting exchange then reads

$$m^* = m_0 + 4GN_c N_f m^* \int^\Lambda \frac{d^3p}{(2\pi)^3} \frac{1}{E_p}, \quad (3.1)$$

with  $E_p^2 = p^2 + m^{*2}$ ; since the integral occurring on the right-hand side of Eq. (3.1) has the simple analytic form

$$\int^\Lambda \frac{d^3p}{(2\pi)^3} \frac{1}{E_p} = \frac{1}{4\pi^2} \left[ \Lambda \sqrt{m^{*2} + \Lambda^2} - m^{*2} \sinh^{-1} \frac{\Lambda}{m^*} \right], \quad (3.2)$$

one may recover the result already given in Eq. (2.26). An evaluation of the total energy-momentum tensor is given in Appendix C. One finds

$$\begin{aligned} \frac{\langle T^{00} \rangle}{N_c N_f} = & -2 \int^\Lambda \frac{d^3p}{(2\pi)^3} \frac{\mathbf{p}^2}{E_p} \\ & - 4m^{*2} G N_c N_f \left[ \int^\Lambda \frac{d^3p}{(2\pi)^3} \frac{1}{E_p} \right]^2, \end{aligned} \quad (3.3)$$

a result which may be compared with Eq. (2.22). If one treats  $m^*$  as a parameter, one can verify that the minimization of this equation leads to the gap equation in the Hartree approximation. Alternatively, a calculation of the change in energy density between the condensed and normal phases, for  $m^*/\Lambda \ll 1$ , can be calculated to be

$$\begin{aligned} \langle \delta T^{00} \rangle = & \langle T^{00} \rangle_{\text{condensed}} - \langle T^{00} \rangle_{\text{normal}} \\ \simeq & -\frac{\Lambda^4}{8\pi^2} \frac{m^{*2}}{\Lambda^2} \left[ 1 - \frac{\pi^2}{G N_c N_f \Lambda^2} \right] \end{aligned} \quad (3.4)$$

and, as expected, is always seen to be negative when the gap equation is satisfied, indicating that the condensed phase is the energetically favored state. A typical value for the condensation energy is given in Sec. III.C, where the parameters associated with this regularization scheme are also discussed. The results, in comparison with the other regularization schemes, are presented in Table II.

TABLE II. Values of  $G_{\text{HF}}, G, \Lambda, m^*$ , and the condensation energy for  $N_c N_f = 6$  in the regularization schemes (a) three-momentum cutoff, (b) four-momentum cutoff, (c) proper time, and (d) Pauli-Villars.

Scheme	$m^*$ (MeV)	$\Lambda$ (MeV)	$G_{\text{HF}} \Lambda^2$	$G \Lambda^2$	$\langle -\delta T^{00} \rangle$ (MeV) <sup>4</sup>
(a)	313	653	1.98	2.14	143
(b)	238	1015	3.63	3.93	125
(c)	200	1086	3.49	3.78	115
(d)	241	859	2.62	2.84	126

## B. Covariant regularization schemes

### 1. The four-momentum covariant cutoff scheme

The four-momentum regulator restricts the Euclidean four-momentum

$$p_E^2 = \mathbf{p}^2 + p_4^2 < \Lambda^2, \quad (3.5)$$

where  $p_0 = ip_4$ . Performing a Wick rotation in the integral occurring in the gap equation (2.31), and again neglecting exchange, one has

$$m^* = m_0 + \frac{1}{2\pi^2} GN_c N_f m^* F_2(m^*, \Lambda), \quad (3.6)$$

where

$$F_2(m^*, \Lambda) = -i(4\pi)^2 \int^\Lambda \frac{d^4 p}{(2\pi)^4} \frac{1}{p_E^2 + m^{*2}}. \quad (3.7)$$

Evaluated explicitly, this is

$$F_2(m^*, \Lambda) = \Lambda^2 - m^{*2} \log \left[ 1 + \frac{\Lambda^2}{m^{*2}} \right]. \quad (3.8)$$

Once again, the parameters associated with solving Eq. (3.6) in this regularization scheme are discussed in Sec. III.C and are listed in Table II.

### 2. Regularization in proper time

A general description of the covariant regularization schemes can be obtained if one makes use of the real-space version of the single-particle Green's function. For a free particle of mass  $m^*$  this is

$$S(x, x') = -\frac{1}{(4\pi)^2} (i\partial_x + m^*) \times \int_{-\infty}^0 \frac{d\tau}{\tau^2} \exp[im^{*2}\tau + i(x - x')^2/4\tau] \quad (3.9)$$

in the Schwinger proper-time form (Schwinger, 1951). The gap equation in real space is, from Eq. (2.31), again neglecting exchange,

$$m^* = m_0 + 2iGN_c N_f \text{tr} S(x, x), \quad (3.10)$$

and the insertion of Eq. (3.9) brings it into the form

$$m^* = m_0 - \frac{i}{2\pi^2} N_c N_f m^* \int_{-\infty}^0 \frac{d\tau}{\tau^2} e^{im^{*2}\tau}. \quad (3.11)$$

It is useful to deform the integral on  $\tau$  into the upper-left-quarter plane indicated in Fig. 3. Then only the section from  $\tau = i\infty$  to  $\tau = 0$  contributes. Making the change of variable  $\tau = is$ , one can write

$$m^* = m_0 + \frac{1}{2\pi^2} GN_c N_f m^* \int_0^\infty \frac{ds}{s^2} e^{-m^{*2}s}. \quad (3.12)$$

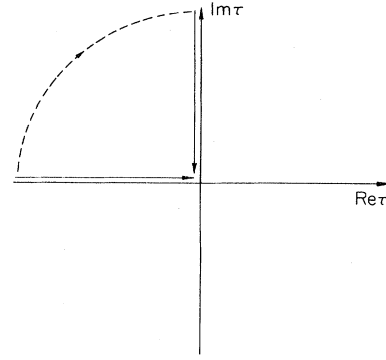


FIG 3. Deformation of the integration path into the imaginary  $\tau$  plane.

It is at this point that one wishes to regulate the divergent integral

$$F_2 = \int_0^\infty \frac{ds}{s^2} e^{-m^{*2}s}. \quad (3.13)$$

Indeed, subtracting off suitable counterterms,

$$F_2(m^{*2}, \Lambda^2) = \int_0^\infty \frac{ds}{s^2} e^{-sm^{*2}} [1 - (1 + s\Lambda^2)e^{-s\Lambda^2}] \frac{ds}{s^2} \quad (3.14)$$

leads to Eq. (3.8) obtained in the four-dimensional Euclidean regularization scheme, when evaluated explicitly. Proper-time regularization, however, involves simply the introduction of a lower limit cutoff on the integral (3.13). One then has

$$F_2(m^{*2}\eta) = \int_\eta^\infty \frac{ds}{s^2} e^{-m^{*2}s} = \frac{1}{\eta} E_2(m^{*2}\eta). \quad (3.15)$$

Once again, the choice of parameters and solution of the gap equation in this scheme will be discussed in Sec. III. C.

### 3. The Pauli-Villars scheme

The method of Pauli and Villars (1949) is an attractive one, because it preserves gauge invariance. Here, one introduces an arbitrary number of regulating masses  $M_a$  and constants  $C_a$  and chooses these in such a way that the constructs that one wishes to regulate become finite. For the function  $F_2$  of Eq. (3.13), which must be regulated in order to calculate the dynamically generated mass from the self-consistency condition, one introduces the constants  $C_a$  and masses  $M_a$ , such that

$$F_2(m^{*2}) = \lim_{\rho \rightarrow 0} \sum_{a=0}^\infty C_a \frac{1}{\rho} E_2[M_a^2 \rho], \quad (3.16)$$

with  $C_0 = 1$  and  $M_0 = m^*$ . The remaining  $M_a$  and  $C_a$  are to be determined. Noting that, for small arguments,

$$E_n(z) = \frac{(-z)^{n-1}}{(n-1)!} [-\ln z + \psi(n)] - \sum_{\substack{m=0 \\ m \neq n-1}}^{\infty} \frac{(-z)^m}{(m-n+1)m!}, \quad (3.17)$$

One can construct  $F_2$  as

$$F_2 = \lim_{\rho \rightarrow 0} \left[ \sum_a C_a M_a^2 \log M_a^2 \rho - \psi(2) \sum_a C_a M_a^2 + \frac{1}{\rho} \sum_a C_a + O(\rho) \right]. \quad (3.18)$$

In order that this quantity converge in the limit  $\rho \rightarrow 0$ , one must impose the conditions

$$\sum_a C_a = 0 \quad \text{and} \quad \sum_a C_a M_a^2 = 0. \quad (3.19)$$

Then the regularized form of  $F_2$  is

$$F_2(m^*) = \sum_a C_a M_a^2 \log M_a^2 / m^{*2}. \quad (3.20)$$

As is standard practice (see, for example, Itzykson and Zuber, 1980), we introduce only one regulator,  $\Lambda$ . This can be done by setting

$$M_a^2 = m^{*2} + \alpha_a \Lambda^2, \quad (3.21)$$

where  $\alpha_0 = 0$  and  $C_0 = 1$ . Now Eq. (3.19) can be written as conditions on the  $\alpha_a$ . Minimally, the label  $a$  must run from 0 to 2, and the conditions read

$$\begin{aligned} C_1 + C_2 &= -1, \\ \alpha_1 C_1 + \alpha_2 C_2 &= 0. \end{aligned} \quad (3.22)$$

The solution of these equations is not unique. We make the standard choice (Itzykson and Zuber, 1980)  $C_1 = 1$ ,  $C_2 = -2$ , for which correspondingly  $\alpha_1 = 2$  and  $\alpha_2 = 1$ . Armed with these values, one may now explicitly solve the resultant gap equation for specific choices of the parameters  $G$  and  $\Lambda$ . Results are given in the following section and are summarized in Table II.

### C. Parameter choice

The Nambu–Jona-Lasinio model, with any of the foregoing regularization schemes, has two parameters, the coupling strength  $G$  and a cutoff parameter which we have denoted as  $\Lambda$ , except in the proper-time scheme, where the cutoff  $\eta$  has been introduced. (We ignore for the moment the small average current quark mass  $m_0$ , which is used later to fit the pion mass.) One has, however, two physical quantities—the pion-decay constant  $f_\pi$  and the quark condensate density—that are known, the former experimentally from measurements of the decay  $\pi^- \rightarrow \mu^- + \nu_\mu$ , while the latter is deduced from sum rules (Reinders *et al.*, 1985). These parameters can also be calculated in the framework of the NJL model. The quark

condensate density is, in fact, the order parameter of the phase transition associated with the restoration of chiral symmetry. One defines the scalar density as

$$n_s = \frac{1}{2} \langle [\bar{\psi}(x), \psi(x)] \rangle = -i \text{Tr} S(x, x), \quad (3.23)$$

so that the quark condensate density per flavor is

$$\langle \bar{u}u \rangle = \langle \bar{d}d \rangle = n_s / N_f = -\frac{3}{4\pi^2} m^* F_2 \quad (3.24)$$

for the covariant schemes in the two-flavor model, while the noncovariant calculation gives

$$\langle \bar{u}u \rangle = \langle \bar{d}d \rangle = -6m^* \int^\Lambda \frac{d^3p}{(2\pi)^3} \frac{1}{E_p}. \quad (3.25)$$

The pion-decay constant is calculated from the vacuum to one-pion axial-vector current matrix element. This will be discussed in detail in Sec. IV.A.3. For the various schemes, one finds

$$\begin{aligned} 3D \text{ cutoff (a)} \quad f_\pi^2 &= N_c m^{*2} \int^\Lambda \frac{d^3p}{(2\pi)^3} \frac{1}{E_p^3}, \\ 4D \text{ cutoff (b)} \quad f_\pi^2 &= \frac{N_c m^{*2}}{4\pi^2} \left[ \log \frac{(m^{*2} + \Lambda^2)}{m^{*2}} - \frac{\Lambda^2}{m^{*2} + \Lambda^2} \right], \end{aligned} \quad (3.26)$$

$$\text{Proper time (c)} \quad f_\pi^2 = \frac{N_c m^{*2}}{4\pi^2} E_1(m^{*2}\eta),$$

$$\text{Pauli-Villars (d)} \quad f_\pi^2 = -\frac{N_c m^{*2}}{4\pi^2} \sum_a C_a \log M_a^2 / m^{*2},$$

where the integral occurring in (a) for the three-momentum cutoff is given explicitly as

$$\int^\Lambda \frac{d^3p}{(2\pi)^3} \frac{1}{E_p^3} = -\frac{1}{2\pi^2} \left[ \frac{\Lambda}{\sqrt{m^{*2} + \Lambda^2}} - \sinh^{-1} \frac{\Lambda}{m^*} \right]. \quad (3.27)$$

We now take the experimental value of  $f_\pi$  to be 93 MeV, while the value of the quark condensate density is taken as  $\langle \bar{u}u \rangle = \langle \bar{d}d \rangle = -(250 \text{ MeV})^3$ . Building  $-\langle \bar{u}u \rangle^{1/3} / f_\pi$  from the relations (3.24) or (3.25) and (3.26), we solve for  $m^* / \Lambda$  or  $m^{*2} \eta$ , as the case may be. Thus  $m^*$  and  $\Lambda$  or  $\eta$  are determined. Finally, we use the gap equation from (3.1) or (3.6) to determine the coupling strength  $G$ . The current quark mass has been set to zero. The results are listed in Table II, with the value of  $G$  referring to the strength associated with the Hartree approximation given explicitly in these equations, while the value  $G_{\text{HF}}$  refers to the coupling strength in the Hartree-Fock approximation, in which the factor  $GN_c N_f$  in (3.1) or (3.6) is replaced by  $G[N_c N_f + \frac{1}{2}]$ . Where the proper-time scheme has been quoted, the value  $1/\sqrt{\eta}$  is given in lieu of  $\Lambda$ .

One notices the following features. In the three-

dimensional cutoff scheme, the value for  $m^*$  is attractive in that it is roughly one-third of the nucleon mass. The covariant schemes, on the other hand, are all characterized by a somewhat smaller value of the dynamically generated quark masses. The value of the cutoff in both covariant and noncovariant cases is comparable, bearing in mind that the covariant cutoff restricts the four-momentum. For small values of  $m^*/\Lambda$ , one may estimate

$$\Lambda_{\text{covariant}} \simeq \sqrt{2} \Lambda_{\text{noncovariant}}.$$

For the noncovariant cutoff  $\Lambda = 653$  MeV given in Table II part (a), this relation gives the covariant cutoffs as  $\Lambda = 923$  MeV, which lies within the numerical range covered by schemes (b)–(d).

In the limit  $m^*/\Lambda \ll 1$ , the value of the integral in Eq. (3.27) can be simplified with the aid of the gap equation, Eq. (3.1) for zero current quark mass, to yield the following approximation for the pion-decay constant from Eq. (3.26),

$$f_\pi^2 = \frac{N_c N_f \Lambda^2}{4\pi^2} \left[ 1 - \frac{\pi^2}{G N_c N_f \Lambda^2} \right] + O(m^{*2}/\Lambda^2), \quad (3.28)$$

using the three-momentum cutoff. Then the condensation energy, calculated from Eq. (3.5) for small  $m^*/\Lambda$ , can be expressed in the regularization free form

$$\langle \delta T^{00} \rangle = -\frac{1}{2} m^{*2} f_\pi^2. \quad (3.29)$$

The same result is obtained from other regularization schemes. It is seen from Table II that this value varies from 115 to 143 (MeV)<sup>4</sup> for the different schemes quoted, this variation arising solely from the different values of the dynamical mass that are generated. We note that the condensation energy is of the same order as the empirical MIT bag constant.

In closing this section, we restate our procedure on regularization. In all the schemes presented, we have chosen the minimal procedure of introducing a single cutoff parameter to regulate all quantities that are calculated. The NJL model, defined together with a regularization prescription, is regarded as an effective theory. We comment that some authors (Jaminon *et al.*, 1989), working with a bosonized effective NJL Lagrangian, discuss the inclusion of two cutoff parameters and show that the range of such possible cutoffs is enlarged within their procedure.

#### IV. MESON MASSES AND REGULARIZATION-INDEPENDENT RELATIONSHIPS

In this section, we wish to study the mesonic modes and their properties. In the two-flavor model, we examine the pseudoscalar isovector modes and the scalar isoscalar mode that correspond to the  $\pi$  and  $\sigma$  mesons, respectively. We shall derive explicit equations for the masses and coupling strengths of both of these modes

within the NJL model. Since we can also obtain an explicit equation for the pion-decay constant  $f_\pi$ , we shall also be able to establish the appropriate current-algebra results, viz., the Goldberger-Treiman and Gell-Mann–Oakes–Renner relations, in a way that does not depend on the regularization scheme that is chosen. We shall find, too, that the masses of the pseudoscalar and scalar mesons are related to one another by an equation that is also independent of the regularization scheme used.

For the three-flavor NJL model, we shall study the pseudoscalar-meson spectrum that consists of the  $\pi$ ,  $K$ ,  $\eta$ , and  $\eta'$  mesons. In so doing, we shall pay particular attention to the role of the six-fermion interaction in obtaining the mass splitting of the  $\eta$  and  $\eta'$ .

Before we embark on our task, we must address the problem of how we view a meson as a degree of freedom in the model. We tackle this question directly in the following section, where we first examine the pion mode.

#### A. The two-flavor model

##### 1. The pion and sigma modes

A minimal local interaction Lagrangian that would describe the coupling of a pion field  $\pi$  to nucleon fields  $\psi_N$  is given by

$$\mathcal{L}_{\pi NN} = i G_{\pi NN} \bar{\psi}_N(x) \gamma_5 \tau \cdot \pi \psi_N(x) \quad (4.1)$$

with the coupling strength  $G_{\pi NN}$  of the pions to the nucleons. This model can be taken over into the quark picture by regarding the fermion fields as quark fields,  $\psi_N \rightarrow \psi$ . The coupling strength on the quark level is then  $g_{\pi qq}$ , and one has

$$\mathcal{L}_{\pi NN} \rightarrow \mathcal{L}_{\pi qq} = i g_{\pi qq} \bar{\psi}(x) \gamma_5 \tau \cdot \pi \psi(x). \quad (4.2)$$

One may decompose

$$\tau \cdot \pi = \tau^{(+)} \pi^{(+)} + \tau^{(-)} \pi^{(-)} + \tau^{(3)} \pi^{(3)},$$

where the operators

$$\pi^{(\pm)} = \frac{1}{\sqrt{2}} (\pi_1 \mp i \pi_2) \quad (4.3)$$

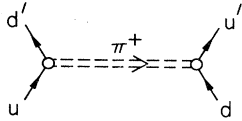
destroy a  $\pi^+$  or  $\pi^-$ , respectively. Correspondingly, the operators  $\tau^{(+)}$  and  $\tau^{(-)}$  are defined as

$$\tau^{(\pm)} = \frac{1}{\sqrt{2}} (\tau_1 \pm i \tau_2). \quad (4.4)$$

The scattering diagram of, for example,  $(ud) \rightarrow (d'u')$ , shown in Fig. 4, has the value

$$[\bar{d}' i \gamma_5 \tau^{(-)} u] [(i g_{\pi qq})^2] \frac{i}{k^2 - m_\pi^2} [\bar{u}' i \gamma_5 \tau^{(+)} d], \quad (4.5)$$

from which one may detach the legs to define an effective interaction

FIG. 4. Scattering diagram of  $(ud) \rightarrow (d'u')$ .

$$\begin{array}{c} \text{---} \\ \text{---} \\ \text{---} \\ \text{---} \end{array} \Rightarrow \begin{array}{c} \text{---} \\ \text{---} \\ \text{---} \\ \text{---} \end{array} = (i\gamma_5)\tau^{(-)} \frac{-ig_{\pi qq}^2}{k^2 - m_\pi^2} (i\gamma_5)\tau^{(+)} \quad (4.6)$$

for the exchange of a  $\pi^{(+)}$ . This formula holds true for all the other pion exchanges as well, with the appropriate  $\tau$  matrices inserted.

$$\begin{aligned} iU_{ij}(k^2) &= (i\gamma_5)T_i \left[ 2iG + 2iG \left[ \frac{1}{i} \Pi_{ps}(k^2) \right] 2iG + 2iG \left[ \frac{1}{i} \Pi_{ps}(k^2) \right] 2iG \left[ \frac{1}{i} \Pi_{ps} \right] 2iG + \dots \right] (i\gamma_5)T_j \\ &= (i\gamma_5)T_i \left[ \frac{2iG}{1 - 2G\Pi_{ps}(k^2)} \right] (i\gamma_5)T_j, \end{aligned} \quad (4.7)$$

where  $T_i$  selects the appropriate channel  $T_i = T_j = \tau_3$  for the  $\pi^0$  or  $T_i = \tau^{(\pm)}$ ,  $T_j = \tau^{(\mp)}$  for creating a  $\pi^+$  or  $\pi^-$ . The proper polarization insertion  $-i\Pi_{ps}$  is given as

$$\begin{aligned} \frac{1}{i} \Pi_{ps}(k^2) &= - \int \frac{d^4 p}{(2\pi)^4} \text{Tr} i\gamma_5 T_i iS(p + \tfrac{1}{2}k) i\gamma_5 T_j iS(p - \tfrac{1}{2}k) \\ & \quad (4.8) \end{aligned}$$

on translating the diagram in Fig. 6.

By comparing the result (4.7) with Eq. (4.6), one sees that one is required to solve

$$1 - 2G\Pi_{ps}(k^2) = 0 \quad (4.9)$$

in order to obtain the mass of the pseudoscalar mode, while the coupling constant  $g_{\pi qq}$  can be related to the residue at the pole of (4.7). To do this, one expands the expression in (4.7) about its pole at  $k^2 = m_\pi^2$  that is given when (4.9) is satisfied, to find

$$iU_{ij}(k^2) \simeq (i\gamma_5)T_i \frac{-i(\partial\Pi_{ps}/\partial k^2)^{-1}|_{k^2=m_\pi^2}}{k^2 - m_\pi^2} (i\gamma_5)T_j, \quad (4.10)$$

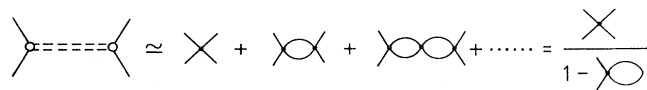


FIG. 5. Effective interaction in the random-phase approximation. Only the direct term is considered.

An effective interaction for the exchange of a pion can also be obtained from the NJL interaction Lagrangian. We consider, for the sake of being definite, the two-flavor version given in Eq. (2.15), but allow for the inclusion of a small current quark mass  $m_u = m_d = m_0$  that explicitly breaks the chiral symmetry of this Lagrangian. The second term of (2.15),  $(\bar{\psi}i\gamma^5\tau\psi)^2$ , is responsible for exciting the isovector pseudoscalar  $J^{PC}=0^{-+}$  mode to be identified as the pion. The effective interaction resulting from the exchange of a  $\pi$  meson can be expressed to leading order in  $N_c$  as an infinite sum of terms in the random-phase approximation (RPA) that is recognized to be a geometric progression. We consider the direct terms only in this sum and illustrate this diagrammatically in Fig. 5.

Calling the diagram on the left-hand side of Fig. 5,  $iU_{ij}(k^2)$ , one has

from which we may deduce that

$$g_{\pi qq}^2 = (\partial\Pi_{ps}/\partial k^2)^{-1}|_{k^2=m_\pi^2}. \quad (4.11)$$

We comment that Eq. (4.9) was first derived by Nambu and Jona-Lasinio (1961a, 1961b), who examined a Bethe-Salpeter equation for the vertex function in the ladder approximation. It is also clear that the scalar mode  $\sigma$  that is associated with the term  $(\bar{\psi}\psi)^2$  of the Lagrangian (2.15) can be handled in much the same way, with the zero of the function  $[1 - 2G\Pi_s(k^2)]$  defining the mass, and an analogous coupling strength  $g_{\sigma qq}$ ,

$$g_{\sigma qq}^2 = (\partial\Pi_s/\partial k^2)^{-1}|_{k^2=m_\sigma^2}, \quad (4.12)$$

relating this mode to its coupling to quark fields. Here the scalar proper polarization is given as

$$\frac{1}{i} \Pi_s(k^2) = - \int \frac{d^4 p}{(2\pi)^4} \text{Tr} iS(p + \tfrac{1}{2}k) iS(p - \tfrac{1}{2}k), \quad (4.13)$$

since the vertex of Fig. 6,  $i\gamma_5 T$ , is simply replaced by a 1 in both spinor and flavor space. Thus, in either the scalar or pseudoscalar case, the respective lowest-order term that contributes to the proper polarization must be calculated.

$$\frac{1}{i} \Pi_{ps}(k^2) = i\gamma_5 T \text{ (loop) } i\gamma_5 T$$

FIG. 6. Lowest-order contribution to the polarization propagator in the pseudoscalar channel.  $T$  selects the isospin channel;  $T_i = T_j = \tau_3$  for  $\pi^0$  or  $T_i = \tau^{(\pm)}$ ,  $T_j = \tau^{(\mp)}$  for the  $\pi^\pm$ .



## 2. Goldstone modes in the chiral limit

One can demonstrate explicitly that the pseudoscalar mode, in the absence of a current quark mass, has zero mass and can thus be identified as the Goldstone boson.

This is an exact result that is a consequence of Goldstone's theorem, and it is reflected in the calculation of the proper polarization in the RPA. Performing the trace on color, spinor, and flavor indices in Eq. (4.8), the proper polarization is

$$\frac{1}{i} \Pi_{\text{ps}}(k^2) = -4N_c N_f \int \frac{d^4 p}{(2\pi)^4} \frac{m^{*2} - p^2 + \frac{1}{4}k^2}{[(p + \frac{1}{2}k)^2 - m^{*2}][(p - \frac{1}{2}k)^2 - m^{*2}]} . \quad (4.14)$$

In order to bring this equation into a form from which one can easily extract  $m_\pi$ , and which is also equivalent to the self-consistency condition when  $m_0=0$ , one writes the denominator in terms of partial fractions,

$$\frac{1}{[(p + \frac{1}{2}k)^2 - m^{*2}][(p - \frac{1}{2}k)^2 - m^{*2}]} = \frac{1}{2(p^2 + \frac{1}{4}k^2 - m^{*2})} \left[ \frac{1}{[(p + \frac{1}{2}k)^2 - m^{*2}]} + \frac{1}{[(p - \frac{1}{2}k)^2 - m^{*2}]} \right] . \quad (4.15)$$

The numerator of (4.14) can be written as  $(m^2 - p^2 - \frac{1}{4}k^2) + \frac{1}{2}k^2$ , so that Eq. (4.14) takes the form

$$\begin{aligned} \frac{1}{i} \Pi_{\text{ps}}(k^2) = & 2N_c N_f \int \frac{d^4 p}{(2\pi)^4} \left[ \frac{1}{[(p + \frac{1}{2}k)^2 - m^{*2}]} + \frac{1}{[(p - \frac{1}{2}k)^2 - m^{*2}]} \right] \\ & - 4N_c N_f \frac{1}{2} k^2 \int \frac{d^4 p}{(2\pi)^4} \frac{1}{[(p + \frac{1}{2}k)^2 - m^{*2}][(p - \frac{1}{2}k)^2 - m^{*2}]} . \end{aligned} \quad (4.16)$$

The latter term of this equation is abbreviated as  $I(k^2)$ , i.e.,

$$I(k^2) = \int \frac{d^4 p}{(2\pi)^4} \frac{1}{[(p + \frac{1}{2}k)^2 - m^{*2}][(p - \frac{1}{2}k)^2 - m^{*2}]} . \quad (4.17)$$

Making appropriate shifts of variables in the first term of Eq. (4.16), one has

$$\frac{1}{i} \Pi_{\text{ps}}(k^2) = 4N_c N_f \int \frac{d^4 p}{(2\pi)^4} \frac{1}{p^2 - m^{*2}} - 2N_c N_f k^2 I(k^2) . \quad (4.18)$$

The same integral that occurs in Eq. (4.18) arises in the gap equation: evaluating Eq. (2.31) to leading order in  $N_c$ , one sees that it has the explicit form

$$m^* = m_0 + 8iGN_c N_f m^* \int \frac{d^4 p}{(2\pi)^4} \frac{1}{p^2 - m^{*2}} . \quad (4.19)$$

One may eliminate the integral in (4.18), using (4.19), to obtain

$$1 - 2G \Pi_{\text{ps}}(k^2) = \frac{m_0}{m^*} + 4iGN_c N_f k^2 I(k^2) , \quad (4.20)$$

from which one may deduce that the mass of the pseudoscalar mode is

$$m_\pi^2 = -\frac{m_0}{m^*} \frac{1}{4iGN_c N_f I(m_\pi^2)} . \quad (4.21)$$

It follows immediately that  $m_\pi^2$  vanishes in the chiral limit, i.e., when  $m_0=0$ . This can be expressed in an alternative fashion: one notes that in this limit, the relation (4.9) expressed in terms of (4.18) is exactly equivalent to the self-consistency condition (4.19).

We remark at this stage that the step from Eq. (4.16) to (4.18) assumes that one can *make* the shift of variable independently of the regularization scheme employed. Since the integrals diverge and must be regulated, this does not follow automatically. Here one has made the implicit assumption that a cutoff to be imposed would tend to infinity on going from (4.16) to (4.18), and one ignores any finite-size effects that would otherwise destroy the required end result, viz., that the Goldstone modes appear (see Nambu and Jona-Lasinio, 1961a). Alternatively, one can demand that the regularization procedure enforce this behavior. In the Pauli-Villars regularization procedure, this condition is automatically fulfilled by the conditions that regulate the gap equation. Since  $m_\pi^2=0$  must be a consequence of chiral symmetry breaking, we regard this necessarily as a result that is independent of regularization scheme.

## 3. The pion-decay constant

The pion-decay constant is calculated from the vacuum to one-pion axial-vector matrix element, which is indicated in Fig. 7.

Translating the diagram, one finds

$$ik_\mu f_\pi \delta^{ij} = - \int \frac{d^4 p}{(2\pi)^4} \text{Tr} \left[ i\gamma_\mu \gamma_5 \frac{\tau^i}{2} iS(p + \frac{1}{2}k) i g_{\pi qq} \gamma_5 \tau^j iS(p - \frac{1}{2}k) \right] , \quad (4.22)$$

having written  $\Gamma = ig_{\pi qq} \gamma_5 \tau^j$  in terms of the pion-to-quark-quark coupling strength  $g_{\pi qq}$ . The symbol Tr is, as before, reserved for the trace over color, flavor, and spinor labels. Using the relation  $\text{tr} \tau^i \tau^j = 2\delta^{ij}$  and performing the traces, one has

$$ik_\mu f_\pi = -N_c g_{\pi qq} \int \frac{d^4 p}{(2\pi)^4} \text{tr} [\gamma_\mu \gamma_5 S(p + \tfrac{1}{2}k) \gamma_5 S(p - \tfrac{1}{2}k)] , \quad (4.23)$$

and the trace over spinor labels yields

$$ik_\mu f_\pi = N_c g_{\pi qq} 4m^* k_\mu I(k^2) , \quad (4.24)$$

where  $I(k^2)$  is as defined in Eq. (4.17). We have already derived an equation for the pion-quark-quark coupling in (4.11). Together with Eq. (4.20), one finds the explicit form

$$g_{\pi qq}^{-2} = -4iGN_c I(0) \quad (4.25)$$

that has been taken at zero-momentum transfer. Squaring Eq. (4.24) and inserting (4.25) at  $k^2=0$ , one arrives at an explicit equation for the pion-decay constant that is independent of the regularization scheme used,

$$f_\pi^2 = -4iN_c m^{*2} I(0) . \quad (4.26)$$

In actual numerical calculations, of course, some scheme must be specified. The scheme-dependent equations for  $f_\pi$ , calculated from Eq. (4.26), are listed in Eq. (3.26).

#### 4. The Goldberger-Treiman, Gell-Mann–Oakes–Renner relations and the $\sigma$ - $\pi$ mass relation

From the previous section, we may combine Eqs. (4.25) and (4.26) to obtain the regularization-free result

$$f_\pi^2 g_{\pi qq}^2 = m^{*2} , \quad (4.27)$$

which is the quark level version of the Goldberger-Treiman relation (Goldberger and Treiman, 1958).

In practice, one is interested in the chiral limit  $m_0 \rightarrow 0$  only as a useful check that the regularization scheme is being consistently used. Otherwise, a small current quark mass  $m_0$  of the order of 5 MeV is required to fix the pion mass at the average value of 140 MeV. (A typical set of values sets  $m_u \simeq 4$  MeV,  $m_d \simeq 7$  MeV, and  $m_s \simeq 150$  MeV; see Gasser and Leutwyler, 1982 for a review.) With this, the last of the available parameters is fixed.

Yet a further regularization-scheme-independent result that also follows from current algebra can be simply

demonstrated. Combining Eq. (4.21) for the pion mass with (4.26) for  $f_\pi$ , one finds

$$m_\pi^2 f_\pi^2 = m_0 m^* (2G)^{-1} . \quad (4.28)$$

One notes, however, that the scalar density can be written in terms of  $m^*$ . This can be seen, for example, on comparing Eqs. (3.25) and (3.1) to get

$$m^* = -2GN_f \langle \bar{u}u \rangle + m_0 , \quad (4.29)$$

a result which is also independent of regularization scheme. Equation (4.29) can be used to eliminate  $m^*$  from Eq. (4.28), yielding the result

$$m_\pi^2 f_\pi^2 \simeq -m_0 \langle \bar{\psi}\psi \rangle , \quad (4.30)$$

which is the lowest-order approximation to the current-algebra result

$$f_\pi^2 m_\pi^2 = -\tfrac{1}{2}(m_u + m_d) \langle \bar{u}u + \bar{d}d \rangle , \quad (4.31)$$

derived by Gell-Mann, Oakes, and Renner (1968).

As mentioned earlier, the isoscalar scalar mode associated with the term  $(\bar{\psi}\psi)^2$  can be evaluated in the same fashion, with the proper polarization given in Eq. (4.13). Following the same steps that lead to (4.20), one arrives at the result

$$1 - 2G\Pi_s(k^2) = \frac{m_0}{m^*} + 4iGN_c N_f (k^2 - 4m^{*2}) I(k^2) , \quad (4.32)$$

so that the mass of the mode is given as

$$m_\sigma^2 = -\frac{m_0}{m^*} [4iGN_c N_f I(m_\sigma^2)]^{-1} + 4m^{*2} \quad (4.33)$$

and the coupling constant associated with this mode, from Eq. (4.12), is

$$g_{\sigma qq}^{-2} = -4iN_c I(m_\sigma^2) . \quad (4.34)$$

$I(k^2)$  is regarded as a smooth function that is slowly varying, so that we can assume that  $I(m_\sigma^2) \simeq I(0)$  and obtain the relation

$$m_\sigma^2 = 4m^{*2} + m_\pi^2 \quad (4.35)$$

that links the pion and sigma masses. This is also a result that is independent of the regularization scheme employed.

Let us now summarize the results obtained for the two-flavor model. With three parameters— $m_0$ ,  $G$ , and a regularization-scheme-dependent cutoff  $\Lambda$ —the pion-decay constant  $f_\pi$ , quark condensate density  $\langle \bar{\psi}\psi \rangle$ , and

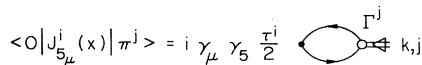


FIG. 7. Vacuum to one-pion and axial-vector current matrix element, as a Feynman diagram.  $\Gamma^j$  is the vertex function.

the pion mass can be fixed. The dynamically generated quark mass, the mass of the scalar-meson mode, and the couplings of these exchanged bosons to quark matter can be calculated. Further, results of current algebra such as the Goldberger-Treiman and Gell-Mann–Oakes–Renner relationships, which necessarily must hold as a consequence of the chiral symmetry of the model, can be explicitly demonstrated to do so within the model, independent of the regularization scheme that is chosen. Numerically, the inclusion of a small current quark mass shifts somewhat the parameters given in Table II. For the Pauli-Villars scheme, which will be implemented in Sec. VI, the parameters  $G\Lambda^2=2.87$ ,  $\Lambda=851$  MeV, and  $m_0=5.2$  MeV fix  $f_\pi=93$  MeV,  $\langle\bar{\psi}\psi\rangle=(-250 \text{ MeV})^3$  per quark flavor, and  $m_\pi=135$  MeV. The dynamically generated quark mass then falls at  $m^*=265$  MeV and the scalar mode at 546 MeV.

### B. The three-flavor model

In this section we examine the flavor dependence of the pseudoscalar-meson modes in flavor SU(3). We deal with the pion and kaon sector first, confirming once again that these are both Goldstone bosons. The  $\eta$  and  $\eta'$  mesons, whose masses are split due to the six-fermion interaction, are described separately. We also comment briefly on the vector-meson spectrum.

#### 1. Effective SU(3) Lagrangian and pion and kaon modes

SU(3) flavor versions of the NJL model have been investigated by Takizawa *et al.* (1989), Bernard, Jaffe, and Meissner (1988), Klimt *et al.* (1990), and Vogl *et al.* (1990). Here we use the form introduced by the first of these references, and which is given in Eq. (2.32), and we continue to work to  $O(1)$  in  $N_c$ . The pseudoscalar sector is now enlarged to form the nonet of pions, kaons, and  $\eta$  and  $\eta'$  mesons. Let us, however, examine the pion and kaon sector first, since their description involves a simple generalization of the ideas developed in Sec. IV. A. 1 for the SU(2) sector. We shall then examine the  $\eta$  and  $\eta'$ ,

which are mixtures of the pure singlet and octet states of SU(3), in a somewhat more sophisticated, if complex, procedure. The  $\pi^0$ ,  $\pi^\pm$ ,  $K^\pm$ ,  $K^0$ , and  $\bar{K}^0$  can be described by examining the generalized form of Eq. (4.8),

$$\frac{1}{i}[\Pi_{ps}(k^2)]_{ij} = -N_c \sum_{ff'} \int \frac{d^4p}{(2\pi)^4} \text{tr} \gamma_5(T_i)_{ff'} S^f(p + \tfrac{1}{2}k) \times \gamma_5(T_j)_{ff'} S^{f'}(p - \tfrac{1}{2}k), \quad (4.36)$$

where the flavor indices  $f$  and  $f'$  are explicitly included, and  $\text{tr}$  refers to the spinor trace only. Now  $T_i$  and  $T_j$  select the appropriate flavor channel,

$$T_i = \begin{cases} \lambda_3, & \pi^0 \\ \frac{1}{\sqrt{2}}(\lambda_1 \pm i\lambda_2), & \pi^\pm \\ \frac{1}{\sqrt{2}}(\lambda_6 \pm i\lambda_7), & K^0, \bar{K}^0 \\ \frac{1}{\sqrt{2}}(\lambda_4 \pm i\lambda_5), & K^\pm, \end{cases} \quad (4.37)$$

and one is required to solve the generalized form of the dispersion relation (4.9),

$$1 - 2K_i^{(+)}\Pi_{ps} = 0, \quad (4.38)$$

for each isospin channel  $i$  to obtain the masses of the modes for that channel. Once again, the coupling strength of each mode to a quark-quark vertex,  $g_{\pi qq}$  and  $g_{K qq}$ , is given by the residue at the pole of the effective interaction, evaluated at the mass of the respective mode. The coupling strengths  $K_i^{(+)}$  appropriate to each channel must now be determined.

Of key importance in writing Eq. (4.38) is the recognition that the three-flavor NJL Lagrangian (2.32) can be brought into a form similar to that of the two-flavor NJL Lagrangian (2.15) by writing the six-fermion-interaction term that occurs in (2.32) in an effective two-body form, as in Eq. (2.40). Combining (2.40) with the four-fermion-interaction term of (2.32), one may write an effective three-flavor NJL Lagrangian as

$$\begin{aligned} \mathcal{L}_{\text{NJL}} = & \bar{\psi} i \not{\partial} \psi + \sum_{i=0}^8 [K_i^{(-)}(\bar{\psi} \lambda^i \psi)^2 + K_i^{(+)}(\bar{\psi} i \gamma^5 \lambda^i \psi)^2] + [\tfrac{1}{2}K_m^{(-)}(\bar{\psi} \lambda^8 \psi)(\bar{\psi} \lambda^0 \psi) + \tfrac{1}{2}K_m^{(+)}(\bar{\psi} i \gamma^5 \lambda^8 \psi)(\bar{\psi} i \gamma^5 \lambda^0 \psi)] \\ & + [\tfrac{1}{2}K_m^{(-)}(\bar{\psi} \lambda^0 \psi)(\bar{\psi} \lambda^8 \psi) + \tfrac{1}{2}K_m^{(+)}(\bar{\psi} i \gamma^5 \lambda^0 \psi)(\bar{\psi} i \gamma^5 \lambda^8 \psi)] + \mathcal{L}_{\text{mass}}, \end{aligned} \quad (4.39)$$

where the flavor-dependent effective coupling constants  $K_i^{(\pm)}$  and  $K_m^{(\pm)}$  are given in terms of  $G$  and  $K$  as

$$\begin{aligned} K_0^{(\pm)} &= G \mp \tfrac{1}{3}N_c K(i \text{tr} S^s + 2i \text{tr} S^u), \\ K_1^{(\pm)} &= K_2^{(\pm)} = K_3^{(\pm)} = G \pm \tfrac{1}{2}N_c K i \text{tr} S^s, \\ K_4^{(\pm)} &= K_5^{(\pm)} = K_6^{(\pm)} = K_7^{(\pm)} = G \pm \tfrac{1}{2}N_c K i \text{tr} S^u, \\ K_8^{(\pm)} &= G \mp \tfrac{1}{6}N_c K(i \text{tr} S^s - 4i \text{tr} S^u), \end{aligned} \quad (4.40)$$

and the mixed-flavor terms have the coupling strengths

$$K_m^{(\pm)} = \mp \tfrac{1}{3}N_c K \sqrt{2}(i \text{tr} S^s - i \text{tr} S^u). \quad (4.41)$$

The origin of the relative sign difference that occurs in the scalar and pseudoscalar couplings can be traced back to Eq. (2.40), where the pseudoscalar term occurs with the opposite sign to its form in (4.39).

## 2. Goldstone bosons in the chiral limit

A check on the consistency of this formulation is the confirmation that the pseudoscalar mesons reemerge as Goldstone bosons in the limit of  $\mathcal{L}_{\text{mass}} \rightarrow 0$ . Since the  $\pi$  mesons are degenerate, and the  $K$  mesons also, it suffices to set up the dispersion relation for the  $\pi^0$  and  $K^0$ . We examine first the  $\pi^0$ . Then Eq. (4.36) requires that we select the meson channel  $T_i = T_j = \lambda_3$ . Since this matrix is diagonal, (4.36) becomes

$$\frac{1}{i} \Pi_{\text{ps}}^\pi(k^2) = -2N_c \int \frac{d^4 p}{(2\pi)^4} \text{tr} \gamma_5 S^u(p + \tfrac{1}{2}k) \gamma_5 S^u(p - \tfrac{1}{2}k), \quad (4.42)$$

denoting

$$[\Pi_{\text{ps}}(k^2)]_{33} = \Pi_{\text{ps}}^\pi(k^2).$$

We have also used the fact that since  $m_u = m_d$ , the propagators

$$S^u(p) = (\not{p} + m_u^*) / (p^2 - m_u^{*2})$$

and

$$S^d(p) = (\not{p} + m_d^*) / (p^2 - m_d^{*2})$$

are equal. Thus, formally, Eq. (4.42) differs from the two-flavor equation (4.8) only in the flavor trace given in that equation, and the manipulations of Eqs. (4.14) through (4.19) can be repeated to give the similar form

$$\frac{1}{i} \Pi_{\text{ps}}^\pi(k^2) = 8N_c \int \frac{d^4 p}{(2\pi)^4} \frac{1}{p^2 - m_u^{*2}} - 4N_c k^2 I_u(k^2), \quad (4.43)$$

with  $I_u(k^2)$  given by  $I(k^2)$  in Eq. (4.17) with  $m^* \rightarrow m_u^*$ . It is useful to express the first term of (4.43) in terms of the spinor trace of the propagator in  $x$  space,  $\text{tr} S^i(x, x) = \text{tr} S^i(0) = \text{tr} S^i$ , so that

$$\frac{1}{i} \Pi_{\text{ps}}^\pi(k^2) = 2N_c \frac{1}{m_u^*} \text{tr} S^u - 4N_c k^2 I_u(k^2). \quad (4.44)$$

We now introduce the gap equation, which, from Eq. (2.39), can be written as

$$\begin{aligned} m_u^* &= m_u + 4iGN_c \left[ 1 + \frac{N_c}{2} \frac{K}{G} i \text{tr} S^s \right] \text{tr} S^u \\ &= m_u + 4iN_c K_3^{(+)} \text{tr} S^u, \end{aligned} \quad (4.45)$$

for a quark of flavor  $u$ . Eliminating  $\text{tr} S^u$  from (4.44) by using (4.45), one finds that the dispersion relation can be obtained on solving Eq. (4.38), which takes the form

$$1 - 2K_3^{(+)} \Pi_{\text{ps}}^\pi(k^2) = \frac{m_u}{m_u^*} + 8iK_3^{(+)} N_c k^2 I_u(k^2) = 0 \quad (4.46)$$

here, and may be compared with Eq. (4.20). One sees that the two-flavor limit may easily be extracted on setting  $K$  in  $K_3^{(+)}$  to zero, and that the limit  $m_u = 0$  recovers

the Goldstone nature of the pion.

Treatment of the  $K$  mesons is more complicated, since the additional mass parameter  $m_s \neq m_u$ . This has, among other things, the consequence that the self-energy of the strange quark,

$$m_s^* = m_s + 4iGN_c \text{tr} S^s - 2KN_c^2 (\text{tr} S^u)^2 \quad (4.47)$$

from Eq. (2.39), cannot be factored as in (4.45) into a term that contains an effective coupling strength. The gap equations (4.45) and (4.47) warrant comment. Unlike the SU(2) case, the SU(3) self-energy equations for the masses  $m_u^* = m_d^*$  and  $m_s^*$  are coupled via the mass dependences of these flavors that occur in the traces of the Green's functions found in these equations. In practice, a numerical solution to these coupled equations (4.45) and (4.47) must be obtained before the meson modes can be evaluated.

The polarization propagator for the  $K^0$  can be constructed from Eq. (4.36) as

$$\begin{aligned} \frac{1}{i} \Pi_{\text{ps}}^{K^0}(k^2) &= -N_c \sum_{ff'} \int \frac{d^4 p}{(2\pi)^4} \text{tr} \gamma_5 (\lambda_6^-)_{ff'} \\ &\quad \times S^f(p + \tfrac{1}{2}k) \gamma_5 (\lambda_6^+)_{f'f} \\ &\quad \times S^{f'}(p - \tfrac{1}{2}k) \end{aligned} \quad (4.48)$$

which can be evaluated in flavor space, to give

$$\frac{1}{i} \Pi_{\text{ps}}^{K^0}(k^2) = -2N_c \int \frac{d^4 p}{(2\pi)^4} \text{tr} \gamma_5 S^s(p + \tfrac{1}{2}k) \gamma_5 S^d(p - \tfrac{1}{2}k). \quad (4.49)$$

In order to determine the dispersion relation for the  $K^0$ , one is required to find values of  $k^2$  for which

$$1 - 2K_6^{(+)} \Pi_{\text{ps}}^{K^0}(k^2) = 0. \quad (4.50)$$

The task now at hand is to calculate the polarization here for unequal masses. We show consistency by recovering the known result at  $k = 0$ , viz., that  $m_{K^0}^2 = 0$  is a solution of (4.50) for zero current quark mass, so that the  $K^0$  correctly emerges as a Goldstone mode. To do this, we perform the spinor trace on Eq. (4.49), leading to the result

$$\frac{1}{i} \Pi_{\text{ps}}^{K^0}(0) = -4N_c \int \frac{d^4 p}{(2\pi)^4} \frac{2(m_s^* m_d^* - p^2)}{(p^2 - m_s^{*2})(p^2 - m_d^{*2})}. \quad (4.51)$$

Then the identity

$$2(m_s^* m_d^* - p^2) = m_s^{*2} - p^2 + m_d^{*2} - p^2 - (m_s^* - m_d^*)^2$$

enables us to write

$$\begin{aligned} \frac{2(m_s^* m_d^* - p^2)}{(p^2 - m_s^{*2})(p^2 - m_d^{*2})} &= -\frac{1}{p^2 - m_s^{*2}} - \frac{1}{p^2 - m_d^{*2}} \\ &\quad - \frac{(m_s^* - m_d^*)^2}{(p^2 - m_s^{*2})(p^2 - m_d^{*2})}. \end{aligned} \quad (4.52)$$

We expand the last term of this equation in terms of partial fractions in the inverse of the difference of the two denominators, and, inserting the result into Eq. (4.51), we may write

$$\begin{aligned} \frac{1}{i} \Pi_{\text{ps}}^{K^0}(0) = & 4N_c \left[ 1 + \frac{m_s^* - m_d^*}{m_s^* + m_d^*} \right] \int \frac{d^4 p}{(2\pi)^4} \frac{1}{p^2 - m_s^{*2}} \\ & + 4N_c \left[ 1 - \frac{m_s^* - m_d^*}{m_s^* + m_s^*} \right] \int \frac{d^4 p}{(2\pi)^4} \frac{1}{p^2 - m_d^{*2}}, \end{aligned} \quad (4.53)$$

which may be simplified further as

$$\frac{1}{i} \Pi_{\text{ps}}^{K^0}(0) = \frac{2N_c}{m_s^* + m_d^*} (\text{tr} S^s + \text{tr} S^d) \quad (4.54)$$

with the introduction of the trace of the propagator in  $x$  space. One can build the sum  $m_s^* + m_d^*$  from Eqs. (4.45) and (4.47) to find

$$\begin{aligned} m_d^* + m_s^* &= m_d + m_s + (4iGN_c + 2iKN_c^2 i \text{tr} S^d)(\text{tr} S^s + \text{tr} S^d) \\ &= m_d + m_s + 4iN_c K_6^{(+)} (\text{tr} S^s + \text{tr} S^d) \end{aligned} \quad (4.55)$$

and eliminate the traces in (4.54), so that

$$1 - 2K_6^{(+)} \Pi_{\text{ps}}^{K^0}(0) = \frac{m_d + m_s}{m_d^* + m_s^*}. \quad (4.56)$$

This confirms that in the limit of zero current quark mass, the  $K^0$  is indeed a Goldstone particle.

In practical calculations of the mass of the  $\pi$  and  $K$  mesons that include small current quark masses, one solves Eqs. (4.46) and (4.50) numerically, having, of course, prior to this determined  $m_u^* = m_d^*$  and  $m_s^*$  from the set of coupled gap equations.

### 3. $\eta$ and $\eta'$ mesons

The calculations of the  $\eta$  and  $\eta'$  meson spectra remains to be addressed. Up to this point, we have easily been able to apply the results of the SU(2) calculation of the meson modes and their respective coupling strengths to the SU(3) calculation, since the form in which the pseudoscalar channels described by  $T$  in Eq. (4.37) appear in the Lagrangian (4.39) is directly analogous to the form in which these channels are coupled in the SU(2) Lagrangian (2.15). Consequently, the summation of bubbles in the construction of the effective interaction, as in Eq. (4.7) and Fig. 7, selected its specific isospin channel by choosing at each stage the same proper polarization part  $[\Pi_{\text{ps}}]_{ij}$ . In dealing now with the  $I=0$  channel that describes the  $\eta$  and  $\eta'$ , one notices that the SU(3) Lagrangian (4.39) contains not only terms proportional to  $\lambda_0 \otimes \lambda_0$  and  $\lambda_8 \otimes \lambda_8$ , but contains also the mixing terms  $\lambda_8 \otimes \lambda_0$  and  $\lambda_0 \otimes \lambda_8$ . One must thus examine the construction of the effective interaction more carefully. To this end, let us remove the external interaction vertices from Fig. 7 and construct first the bubble sum, which represents the full



FIG. 8. Schematic representation for the Bethe-Salpeter equation for the polarization propagator.

polarization propagator in the RPA and is denoted here as  $F_{ij}$ . Here the labels  $i$  and  $j$  refer to the nine flavor channels as selected by the basis given by extending  $T$  in (4.37) to include  $T_i = \lambda_0$  and  $\lambda_8$  also.  $F_{ij}$  satisfies the coupled set of equations

$$\frac{1}{i} F_{ij} = \frac{1}{i} \Pi_{ij} + \frac{1}{i} \Pi_{ik} 2iK_{kl} \frac{1}{i} F_{lj}, \quad (4.57)$$

or

$$F = \Pi + 2\Pi K F \quad (4.58)$$

in a matrix notation. This relation is represented schematically in Fig. 8.

Since we shall deal hereafter only with the pseudoscalar modes, we shall suppress the subscript ps in writing  $\Pi$ . The coupling constants in SU(3) are the pseudoscalar coupling strengths and are diagonal,

$$K_{kl} = K_k^{(+)} \delta_{kl}, \quad (4.59)$$

except for the mixed couplings

$$K_{08} = K_{80} = \frac{1}{2} K_m^{(+)}. \quad (4.60)$$

Likewise, the proper polarization insertions  $\Pi_{ij}$  are diagonal,

$$\Pi_{ij} = \Pi_i \delta_{ij}, \quad (4.61)$$

except for the off-diagonal elements

$$\Pi_{08} = \Pi_{80}. \quad (4.62)$$

The diagonal nature of (4.59) and (4.61) in the  $I=1$  and  $I=\frac{1}{2}$  channels corresponding to the  $\pi$  and  $K$  mesons enables us to solve (4.57) for  $F$  and recover our previous results. For example, choosing  $i=j=3$ , one has, from solving (4.57),

$$\begin{aligned} F_{33} &= \frac{\Pi_{33}}{1 - 2K_{33} \Pi_{33}} \\ &= \frac{\Pi_{\text{ps}}^\pi}{1 - 2K_3^{(+)} \Pi_{\text{ps}}^\pi}, \end{aligned} \quad (4.63)$$

and the poles of this propagator recover the masses of the  $\pi$ . In general, however, one can consider the full matrix  $F$ , which, from (4.57), is

$$F = (1 - 2\Pi K)^{-1} \Pi. \quad (4.64)$$

Now the effective interaction is given in terms of  $F$ , via Fig. 9, as

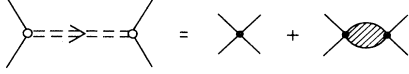


FIG. 9. Effective interaction in terms of the full polarization propagator.

$$iU = (i\gamma_5)T_i 2iK_{ij}(i\gamma_5)T_j + (i\gamma_5)T_i 2iK_{il} \frac{1}{i} F_{lk} 2iK_{kj} i\gamma_5 T_j$$

$$= (i\gamma_5)T_i i(2K + 2KF2K)_{ij} i\gamma_5 T_j, \quad (4.65)$$

using matrix notation. It is useful to define  $M_{ij} = [2K + 2KF2K]_{ij}$ , so that

$$1 - 2\Pi K = \begin{bmatrix} 1 - (2\Pi_{00}K_{00} + 2K_{80}\Pi_{80}) & -2(\Pi_{00}K_{08} + 2K_{88}\Pi_{08}) \\ -(2K_{00}\Pi_{80} + 2K_{80}\Pi_{88}) & 1 - (2K_{08}\Pi_{80} + 2K_{88}\Pi_{88}) \end{bmatrix}, \quad (4.68)$$

so that  $M$  can be written as

$$M = \frac{1}{D} \begin{bmatrix} A & B \\ B & C \end{bmatrix}, \quad (4.69)$$

where

$$A = 2K_{00}[1 - 2\Pi_{88}K_{88}] + (2K_{08})^2\Pi_{88},$$

$$B = 2K_{00} + \Pi_{08}(2K_{00}2K_{88} - (2K_{08})^2), \quad (4.70)$$

$$C = 2K_{88}[1 - 2\Pi_{00}K_{00}] + (2K_{08})^2\Pi_{00},$$

and  $D$  denotes the determinant of the matrix in Eq. (4.68).

The effective interaction in the  $I=0$  channel is then

$$U^{I=0} = i\gamma_5 [M_{00}\lambda_0 \otimes \lambda_0 + M_{08}\lambda_0 \otimes \lambda_8 + M_{80}\lambda_8 \otimes \lambda_0 + M_{88}\lambda_8 \otimes \lambda_8] i\gamma_5. \quad (4.71)$$

As before, the poles of the effective interaction or polarization propagator yield the dispersion relations for the mesons. In this case these are the poles of  $M$  in Eq. (4.67) that are determined by solving

$$D = \det[1 - 2\Pi K] = 0, \quad (4.72)$$

which is the generalized form of Eq. (4.38). One identifies  $m_\eta$  with the smaller, and  $m_{\eta'}$  with the larger, root. The coupling strengths, and in this case the mixing angles, can be obtained by expanding the effective interaction in the vicinity of the mass of the mode and examining the residues. Let us do this explicitly for the  $\eta$ .

We may expand  $U^{I=0}$  about  $m_\eta$ . Then one has

$$U = (i\gamma_5)T_i [M_{ij}] i\gamma_5 T_j; \quad (4.66)$$

employing the solution (4.64), one finds that

$$M = 2K [1 + [1 - 2\Pi K]^{-1} 2\Pi K]$$

$$= 2K [1 - 2\Pi K]^{-1}, \quad (4.67)$$

with due regard to the required order of the matrix multiplications. In dealing with the  $I=0$  channel, it suffices to investigate the  $2 \times 2$  submatrix  $M_{ij}$ , where  $i$  and  $j$  take the values 0 or 8. This reflects the fact that  $T_i$  and  $T_j$  refer to either  $\lambda_0$  or  $\lambda_8$  in determining the mixing of the singlet and octet states to form the  $\eta$  and  $\eta'$ . One has

$$U^{I=0} \simeq i\gamma_5 \frac{M_{00}}{(d/dk^2)\log D} \bigg|_{k^2 \rightarrow m_\eta^2}$$

$$\times \frac{1}{k^2 - m_\eta^2} \left[ \lambda_0 \otimes \lambda_0 + a_\eta \lambda_0 \otimes \lambda_8 + a_\eta \lambda_0 \otimes \lambda_0 + \frac{M_{88}}{M_{00}} \lambda_8 \otimes \lambda_8 \right], \quad (4.73)$$

where the quantity in square brackets is to be evaluated at  $k^2 = m_\eta^2$ , and

$$a_\eta = \frac{M_{08}}{M_{00}} \bigg|_{k^2 \rightarrow m_\eta^2}.$$

To do this, one notes that

$$\det M = \det(2K) \det(1 - 2\Pi K)^{-1} = \det(2K)/D \quad (4.74)$$

from the definition (4.67). However,  $\det M = (AC - B^2)/D^2$  from Eq. (4.69). Thus

$$AC - B^2 = \det(2K)D. \quad (4.75)$$

It follows therefore that at a root of  $D$ , one has  $AC = B^2$ , or that  $M_{88}/M_{00} = C/A = B^2/A^2 = a_\eta^2$ , so that one may factor  $U^{I=0}$ . One has

$$U^{I=0} = i\gamma_5 \frac{g_{\eta qq}^2}{k^2 - m_\eta^2} (-\sin\theta_\eta \lambda_0 + \cos\theta_\eta \lambda_8)$$

$$\otimes (-\sin\theta_\eta \lambda_0 + \cos\theta_\eta \lambda_8), \quad (4.76)$$

where

$$\frac{g_{\eta qq}^2}{1 + a_\eta^2} = \frac{M_{00}}{(d/dk^2)\log D(k^2)} \bigg|_{k^2 \rightarrow m_\eta^2} \quad (4.77)$$

and  $\tan\theta_\eta = -1/a_\eta$  through the identification

$$\lambda_0 + a_\eta \lambda_8 = (1 + a_\eta^2)^{1/2} (-\sin\theta_\eta \lambda_0 + \cos\theta_\eta \lambda_8).$$

The strength  $\cos\theta_\eta$  represents the mixing of the  $\eta$  and  $\eta'$ , although  $\theta_\eta$  cannot be regarded as a mixing angle in the sense that it occurs in the quark model (Bernard, Jaffe, and Meissner, 1988). Solutions of the Bethe-Salpeter equation are not eigenstates of an energy-independent Hermitian Hamiltonian, with the consequence that the matrix of couplings of the  $\eta$  and  $\eta'$  to  $\eta^0$  and  $\eta^8$  is not orthogonal.

Results from the different authors who have dealt with flavor SU(3) (Bernard, Jaffe, and Meissner, 1988; Takizawa *et al.*, 1989; Klimt *et al.*, 1990) differ somewhat, due to the differences in the level of approximation made in  $1/N_c$  and to the slight differences in the choice of the SU(3) Lagrangian employed. For the pseudoscalar-meson spectrum, which has been developed here theoretically, we quote the results calculated by Klimt *et al.* (1990) and display the spectrum in Fig. 10. One sees in Fig. 10(a) that in the limit of exact chiral symmetry where  $m_u = m_d = m_s = 0$  and  $K = 0$ , the pseudoscalar nonet ( $\pi, K, \bar{K}, \eta, \eta'$ ) appear as Goldstone modes.

The inclusion of the 't Hooft interaction removes the  $U_A(1)$  symmetry explicitly, leaving the  $SU(3) \otimes SU(3)$  intact and shifting the  $\eta'$  mass away from zero [Fig. 10(b)]. Finally, the introduction of the nonzero current quark masses,  $m_u = m_d \approx 5$  MeV and  $m_s \approx 130$  MeV, breaks the chiral symmetry, so that the pseudoscalar mesons have the masses given in Fig. 10(c). Here we quote the remaining parameters used as  $G\Lambda^2 \sim 5$ ,  $\Lambda \sim 1$  GeV, and  $K\Lambda^5 \sim 70$  for this calculation, which have been taken from Klimt *et al.* (1990) and notationally adjusted so that the gap equations solved by these authors are coincident with Eqs. (4.45) and (4.47).

Meson masses, decay constants, and meson-quark coupling strengths are listed in Table III for the extended pa-

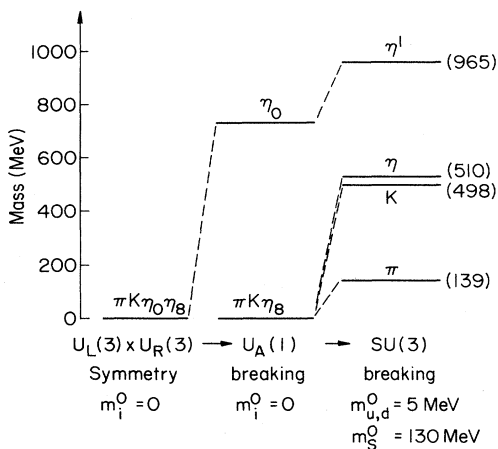


FIG. 10. Pseudoscalar-meson spectrum in the SU(3) flavor model (after Klimt *et al.*, 1990). The parameters used are described in the text.

TABLE III. Pseudoscalar-meson properties. Empirical values are given in brackets [after Klimt *et al.* (1990)].

	$\pi$	$K$	$\eta$	$\eta'$
Mass $m$ (MeV)	139 (139)	498 (495)	509 (548)	969 (958)
Decay constant $f$ (MeV)	93.3 (93.3)	96.3 (114)	93.4	93.3
Meson-quark couplings $g_{mQ}$	3.87	4.04	3.77	2.68

rameter set, used by Klimt *et al.* (1990), that is necessary to describe the vector-meson sector. This is given in the following section.

In general, the value of the mixing angle  $\theta_\eta$  obtained by Bernard, Jaffe, and Meissner (1988), Takizawa *et al.* (1989), and Klimt *et al.* (1990) varies between  $\theta = -6.9^\circ$  and  $\theta = -13.9^\circ$ . Experimentally (Gilman and Kauffman, 1987), data from the decays  $\eta(\eta') \rightarrow \gamma\gamma$ ,  $\psi \rightarrow \eta(\eta')\gamma$ ,  $\psi \rightarrow$  pseudoscalar + vector and  $\pi^- p$  scattering indicate that  $\theta_\eta \approx -20^\circ$ , while tensor meson-decay data suggest that  $\theta_\eta \approx -10^\circ$ . On the other hand, the semiempirical value obtained from the quadratic Gell-Mann–Okubo mass formula is  $\theta_\eta = -10^\circ$ , while that from the linear Gell-Mann–Okubo formula is  $\theta_\eta = -23^\circ$ . Thus this issue is not completely settled.

Values of the ratio  $f_K/f_\pi$  calculated by the various groups of authors lie between 1.02 and 1.08, and these underestimate the empirical value  $f_K/f_\pi = 1.21 - 1.28$ .

#### 4. Vector-meson modes

The interested reader is further referred to Takizawa *et al.* (1989, 1991), Klimt *et al.* (1990), and Vogl and Weise (1991) for the calculation of the vector-meson modes, for which it is necessary to include an additional term [ $G_2 \neq 0$  from Eq. (2.14)] in the NJL Lagrangian studied in order to achieve a sufficiently attractive force in the vector and axial-vector channels, and also to Blin *et al.* (1990), who study resonances in the mesonic strength functions in an alternative approach.

In the following, we briefly report the results of Klimt *et al.* (1990), without presenting detailed theoretical calculations. Using the Lagrangian given by Eq. (2.14), with the extended parameter set  $m_u = m_d = 5.5$  MeV,  $m_s = 131.5$  MeV,  $\Lambda = 0.9$  GeV,  $G_1\Lambda^2 = 3.97$ ,  $G_2\Lambda^2 = 2.63$ ,  $G_3 = G_4 = 0$ , and  $K\Lambda^5 = 70.6$ , these authors obtain a best fit to both the pseudoscalar- and vector-meson sectors, with the former as listed in Table III. With these parameters, the pion-decay constant is fixed at its empirical value,  $f_\pi = 93.3$  MeV, while the value of  $f_K = 96.3$  MeV. The condensates are measured as  $\langle \bar{u}u \rangle = \langle \bar{d}d \rangle = -(247.8 \text{ MeV})^3$  and  $\langle \bar{s}s \rangle = -(258.3 \text{ MeV})^3$ , and the dynamically generated quark masses lie at  $m_u = m_d = 363.9$  MeV and  $m_s = 522.2$  MeV.

In the chiral limit, when  $m_u = m_d = m_s = 0$ , the vector-meson modes  $\rho$ ,  $K^*$ ,  $\omega_0$ , and  $\omega_8$  form a degenerate

TABLE IV. Vector-meson modes and decay constants [after Klimt *et al.* (1990)]. Empirical values (Dumbrajs *et al.*, 1983) are listed in brackets.

	$\rho$	$\omega$	$K^*$	$\phi$
Mass $m$ (MeV)	77.2 (770)	785 (783)	892 (992)	1047 (1020)
Decay constant $f$ (MeV)	7.0 (5.3)	24.0 (15.2)	17.0	25.0 (13.4)

set with a common mass  $m_V \simeq 770$  MeV. When the current quark masses are turned up to their actual values, the  $\omega_0 - \omega_8$  singlet-octet pair turns into the  $\omega$  and  $\phi$ , such that the  $\phi$  is an almost pure  $\bar{s}s$  state, while the  $\omega$  remains almost degenerate with the  $\rho$ . It is necessary to include a further tensor piece in the interaction with yet another coupling strength, in order to describe the mass splitting of the  $\rho$  and  $\omega$ . The numerical values for these masses, together with the meson-decay constants, are listed in Table IV.

The results of current algebra that are specific to the vector-meson sector, such as the Weinberg formula (Weinberg, 1967) and the KSFR relation (Kawarabayashi and Suzuki, 1966; Riazuddin and Fayyazuddin, 1966), can also be shown to hold; this is discussed by Ebert and Reinhardt (1986).

## 5. General discussion and outlook

In conclusion of this section, we review what we have accomplished in the flavor SU(3) NJL model. Let us restrict ourselves to the pseudoscalar sector, which has been presented in detail in this section. The SU(3) model, as given by Eq. (2.32), contains two coupling strengths, one regulator, and three current quark masses. With these parameters, one wishes to describe the meson nonet ( $\pi, K, \eta, \eta'$ ), the pion- and kaon-decay constants, and the three quark condensate densities. We may choose the parameters ( $m_u, m_d$ ) to fit the pion mass and fix  $G$  and  $\Lambda$  by setting  $f_\pi$  and the light quark condensates to their respective empirical values. The remaining parameters ( $m_s, K$ ) are fixed by styling a best fit to the remaining observables, with  $m_s$  fixing the mass of the kaons in the strange sector, and  $K$ , as discussed, serving to split the masses of the  $\eta$  and  $\eta'$ . All quantities turn out to have reasonable values. In addition, the current-algebra relations, the Goldberg-Treiman and Gell-Mann–Oakes–Renner relationships, are obtained “free of charge,” as a consequence of the built-in chiral symmetry.<sup>2</sup>

<sup>2</sup>One of course also obtains an additional scalar-meson spectrum, but since the physical identification of these modes is unclear, we do not deal with these further here.

Our good description of the pseudoscalar mesonic sector comes, however, as almost no surprise, since we have constructed it to be so from symmetry principles, and we have enough parameters to reproduce the meson nonet,  $f_\pi$ , and the light quark condensate, depositing our uncertainties primarily in  $f_K$  and  $\langle \bar{s}s \rangle$ . Wherein, therefore, lies the relevance of the model? Its value lies perhaps not so much in its predictive power up to this point, but, as will be investigated, rather in the (qualitative) insights it gives into various aspects of hadronic relativistic many-body physics, particularly in studying the response of a quark system to external parameters such as temperature, finite chemical potential, strong fields, and the equation of state of quark matter—in short, in investigating properties of quark matter. This model also has relevance in determining further static properties of quarks, such as form factors and charge radii, which will be dealt with in Sec. VI. Another problem of interest that can be studied within the NJL model relates to the  $\Sigma_{\pi N}$  term that is measured in  $\pi-N$  scattering, the strangeness content of the proton, and  $\pi-N$  scattering lengths. The former two issues are dealt with by Bernard, Jaffe, and Meissner (1988) in a full SU(3) calculation, which does not, however, contain a consistent expansion in  $1/N_c$  for the self-energy. We refer the reader directly to this reference for further information, and also to Gasser *et al.* (1991), who point out that low-energy precision measurements in  $\pi-N$  scattering are required for clarifying the discrepancies in the experimental data and to aid in the resolution of the theoretical conflicts on this issue. Scattering lengths for the  $\pi-N$  system have, to date, not been studied within the framework of this model.

In the next section, we shall discuss thermodynamic properties of quark matter, and we include a discussion for finite chemical potential. The application of external electromagnetic and chromoelectromagnetic fields and electromagnetic properties will be discussed in Sec. VI.

## V. EFFECTS OF EXTERNAL PARAMETERS I: TEMPERATURE AND CHEMICAL POTENTIAL

As has been seen in Sec. IV, the NJL model apparently provides a good description of the pseudoscalar mesonic sector. Of interest to us now is to see what insights we may gain from the model with regard to various aspects of hadronic relativistic many-body physics. In particular, we are interested in the response of a quark system to temperature and finite chemical potential; we therefore devote this section to a discussion of the finite density and thermodynamical aspects of the NJL model. To date, extensive work has been done on the SU(2) NJL model in this regard, whereas the SU(3) case has not been that thoroughly studied. Within the literature on the SU(2) model, there has been some confusion as to the order of the phase transition at finite density but zero temperature. In this section we give an overview of the SU(2) situation, addressing the problem of finite chemical



potential, but zero-temperature first. We then deal with the finite-temperature case and the ensuing equation of state. The generalization to SU(3) can be effected using the results of Sec. II.

### A. Finite chemical potential

Here we consider a finite baryon density within the SU(2) Lagrangian. One introduces the chemical potential  $\mu$  into the operator  $K = H - \mu N$ , where  $H$  is the Hamilton density associated with the Lagrange density  $\mathcal{L}$  of Eq. (2.15) and  $N$  is the quark number density operator  $N = \psi^\dagger \psi$ , which can be fixed since it is a constant of motion. On the other hand, the scalar density  $\langle \bar{\psi} \psi \rangle$  has to be determined from the dynamics of the system itself. Following the treatment of Asakawa and Yazaki (1989), we note that the mean-field contribution of  $\mathcal{L}_{\text{int}}$  in (2.15) to the mass term is

$$2G \langle \bar{\psi} \psi \rangle \bar{\psi} \psi \quad (5.1)$$

from the direct interaction, while that from the exchange interaction can be gleaned from the Fierz-transformed version of the Lagrangian given in (2.55) as

$$\frac{G}{2N_c} \langle \bar{\psi} \psi \rangle \bar{\psi} \psi. \quad (5.2)$$

Since  $K$  has a term proportional to the density operator, mean-field averages that are also proportional to it must also be included. From (2.55), one can construct the contribution from the exchange interaction to be

$$-\frac{G}{N_c} \langle \psi^\dagger \psi \rangle \psi^\dagger \psi. \quad (5.3)$$

One assumes that all further exchange averages that could arise from (2.55) vanish. The effective mean-field Lagrangian is then

$$\begin{aligned} \mathcal{L}_{\text{eff}} = & \bar{\psi}(i\partial - m_0)\psi + G[2 + 1/2N_c] \langle \bar{\psi} \psi \rangle \bar{\psi} \psi \\ & - \frac{G}{N_c} \langle \psi^\dagger \psi \rangle \psi^\dagger \psi + \mu \psi^\dagger \psi \\ & - \frac{1}{2}G[2 + 1/2N_c] \langle \bar{\psi} \psi \rangle^2 + \frac{G}{2N_c} \langle \psi^\dagger \psi \rangle^2, \end{aligned} \quad (5.4)$$

where the last two terms compensate for double counting of the interaction energy. One sees immediately that the chemical potential is shifted due to the average exchange field,

$$\mu' = \mu - \frac{G}{N_c} \langle \psi^\dagger \psi \rangle, \quad (5.5)$$

and the effective quasiparticle mass is given as

$$m^* = m_0 - G[2 + 1/2N_c] \langle \bar{\psi} \psi \rangle, \quad (5.6)$$

so that one may write  $\mathcal{L}_{\text{eff}} = \bar{\psi}(i\partial - m^* + \gamma^0 \mu')\psi$  plus the constant terms appearing in Eq. (5.4). The Green's function associated with this effective Lagrangian is defined through the relation

$$[i\partial - m^* + \gamma^0 \mu'] S(x, x') = \delta^4(x - x'), \quad (5.7)$$

which has the solution, in momentum space,

$$S(p) = \frac{k + m^*}{k^2 - m^{*2}} + \frac{i\pi}{E_p} (k + m^*) \theta(\mu' - E_p) \delta(k_0 - E_p) \quad (5.8)$$

with  $k = \gamma^0(p_0 + \mu') - \boldsymbol{\gamma} \cdot \mathbf{p}$ . This is the familiar result for a Green's function associated with a free particle of mass  $m^*$  in a system with chemical potential  $\mu'$ . The scalar density  $\langle \bar{\psi} \psi \rangle$  may be expressed in terms of the Green's function  $S$  as

$$\langle \bar{\psi} \psi \rangle = -i \lim_{x' \rightarrow x^+} \text{Tr} S(x, x')$$

as before, so that (5.6) reads

$$m^* = m_0 + 2iG(N_c N_f + \frac{1}{2}) \int \frac{d^4 p}{(2\pi)^4} \text{tr} S(p) \quad (5.9)$$

as the gap equation, and the vector density is given in terms of  $S$  as

$$\langle \psi^\dagger \psi \rangle = -i \lim_{x \rightarrow x'} \text{Tr} \gamma^0 S(x, x'). \quad (5.10)$$

Inserting Eq. (5.8) explicitly, we see that (5.9) and (5.10) become

$$\begin{aligned} m^* = m_0 + 4G(N_c N_f + \frac{1}{2}) m^* \left[ \int^\Lambda \frac{d^3 p}{(2\pi)^3} \frac{1}{E_p} \right. \\ \left. - \int \frac{d^3 p}{(2\pi)^3} \frac{1}{E_p} \theta(\mu' - E_p) \right] \end{aligned} \quad (5.11)$$

and

$$\langle \psi^\dagger \psi \rangle = 2N_c N_f \int \frac{d^3 p}{(2\pi)^3} \theta(\mu' - E_p), \quad (5.12)$$

respectively, and  $\mu'^2 = E_{F_f}^2 = p_F^2 + m^{*2}$  defines the Fermi energy. Here we have a regulator on the three-momentum integrals. It remains now to solve Eq. (5.11) in conjunction with (5.5) after inserting (5.12). Before undertaking this, however, one notes from (5.11) that a phase transition in which chiral symmetry is restored must occur: on the right-hand side of (5.11), it is evident that the unoccupied available phase space for exciting quarks from the negative-energy sea becomes restricted as  $\mu'$  or the density increases. The order of the transition must, however, be determined by examining the thermodynamic potential (here at zero temperature) in conjunction with a numerical solution of the equations. Writing (5.5) and (5.11) in terms of the chemical potential, one has the coupled set

$$\mu' = \mu - \frac{GN_f}{3\pi^2} (\mu'^2 - m^{*2})^{3/2} \quad (5.13)$$

and

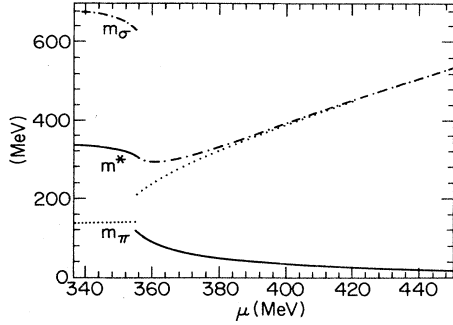


FIG. 11. Effective quark mass and the pion and sigma masses for case I (Asakawa and Yazaki, 1989).

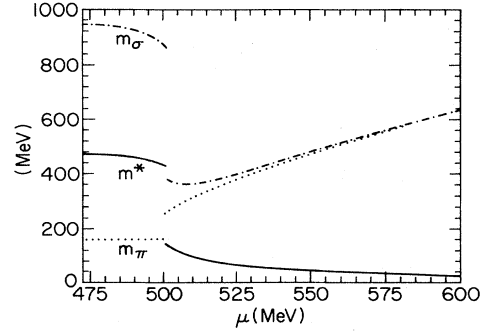


FIG. 12. Effective quark mass and the pion and sigma masses for case II (Asakawa and Yazaki, 1989).

$$m^* = m_0 + G \left[ N_c N_f + \frac{1}{2} \right] \frac{1}{\pi^2} m^* \left[ \Lambda \sqrt{m^{*2} + \Lambda^2} - m^{*2} \log(\Lambda + \sqrt{m^{*2} + \Lambda^2}) - \mu' \sqrt{\mu'^2 - m^{*2}} + m^{*2} \log(\mu' + \sqrt{\mu'^2 - m^{*2}}) \right]. \quad (5.14)$$

The solutions to (5.13) and (5.14) are displayed in Figs. 11 and 12 for two parameter sets that are commonly employed in the literature and which are listed in Table V. We refer to that employed by Hatsuda and Kunihiro (1987a) as case I, and cite that used by Bernard *et al.* (1987a) as case II. Both cases are also discussed by Asakawa and Yazaki (1989). Figures 11 and 12 also display the scalar- and pseudoscalar-meson modes, which are obtained by solving Eq. (4.9) and the associated equation for the  $\sigma$  meson, with  $\Pi_{ps}$  and  $\Pi_s$  as defined in Eqs. (4.8) and (4.13), respectively. Here, of course, the density Green's function (5.8) must be inserted.

The phase transition that one observes is first order in nature in both cases, as can be confirmed by plotting the associated thermodynamic potential density at zero temperature. This is given in Fig. 13 for the parameters of case II, with the formal development of the thermodynamic potential energy left to Sec. V.B [see Eq. (5.43)]. One sees that the energy develops three extrema, two of which are minima for certain values of the chemical potential, and the desired mass  $m^*$  corresponding to the lowest minimum must be selected.

The results warrant comment, since they differ from the results presented by other authors (Bernard *et al.*, 1987a) who have also investigated the SU(2) case and who find a second-order phase transition. In this reference, the method of characterizing the phase transition is

misleading, since these authors present the spectrum as a function of the density and not of the chemical potential. In Fig. 14, we show  $\rho$  as a function of  $\mu$ , which indicates that there is a discontinuity in the density at the critical value of  $\mu = \mu_c$ . In this case, the density jumps from normal to 5 times normal nuclear matter density,  $\rho_0 = 1.30 \times 10^6 \text{ MeV}^3$ . For case I, the jump in density is from  $0.29\rho_0$  to  $1.75\rho_0$ .

It is interesting to investigate whether the order of the phase transition is related to the order of approximation that has been made. We therefore solve the gap equation in the Hartree approximation, for comparison. If one ignores exchange, then Eq. (5.13) reduces to the simple form  $\mu' = \mu$ , while in Eq. (5.14), the factor  $N_c N_f + \frac{1}{2} \rightarrow N_c N_f$ . The results for cases I and II are given in Fig. 15. In both cases, one observes a smooth transition in the behavior of the dynamically generated quark mass from its “constituent” to its current quark value. Thus a first-order phase transition is no longer observed, and the smooth behavior that is seen is a vestige

TABLE V. Parameter values, including a current quark mass.

	$m_0$ (MeV)	$G\Lambda^2$	$\Lambda$	$m^*$ (MeV)	$\langle \bar{u}u \rangle^{1/3}$ (MeV)
Case I	5.5	2.02	631	336	-247
Case II	5.0	2.00	925	472	-359
Phenomenological values				$\sim \frac{1}{3} M_N$	$\sim -250$

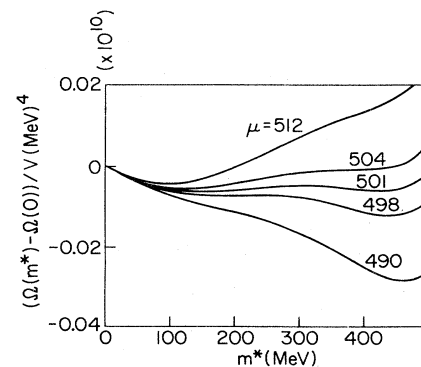


FIG. 13. Thermodynamic potential density as a function of  $m^*$  for case II (after Asakawa and Yazaki, 1989).

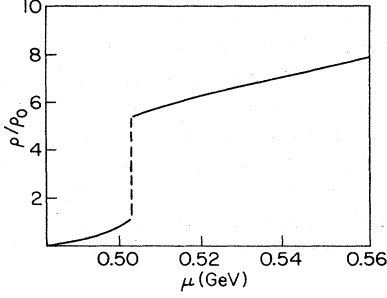


FIG. 14. Density  $\rho$ , given as a function of  $\mu$  for case II.  $\rho_0$  is normal nuclear matter density;  $\rho_0 = 1.30 \times 10^6 \text{ MeV}^3$ .

of the idealized second-order transition that would occur if  $m_0$  were zero. This result is, however, a sensitive function of the parameters employed: with a slight change in parameters, for example, using the set  $\Lambda = 643 \text{ MeV}$ ,  $m_0 = 5.5 \text{ MeV}$ , and  $G\Lambda^2 = 2.2$ , the first-order transition is recovered.

We also find that the results of the SU(2) NJL model calculated at finite density and in Hartree-Fock differ also from the results of the U(1) version taken in the same approximation. Here the Lagrange density is given as

$$\mathcal{L} = \bar{\psi} i \partial \psi - m_0 \bar{\psi} \psi + G[(\bar{\psi} \psi)^2 + (\bar{\psi} i \gamma_5 \psi)^2].$$

In this case (Klevansky and Lemmer, 1990), the gap equation obtained differs from (5.14) only in that the coupling strength

$$G(N_f N_c + \frac{1}{2}) \rightarrow G N_c N_f,$$

while Eq. (5.13) remains intact. Thus the coupled set of nonlinear equations to be solved differs slightly in its parameters from the SU(2) Hartree-Fock version. This leads again to a smoothing out of the second-order phase transition for the same parameter sets used in the previous calculation.

We mention the SU(3) situation only briefly: Kunihiro (1989b, 1991) and Klimt, Lutz and Weise (1990) find that the observed phase transition is again second order in nature for the parameter sets that they have employed.

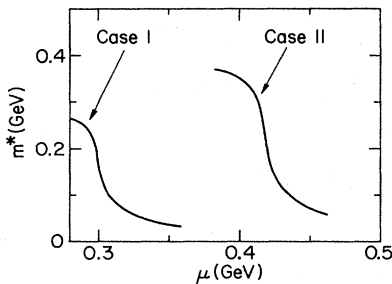


FIG. 15. Effective quark mass, calculated in the Hartree approximation for the parameters of case I and case II.

One may thus conclude that the NJL model does not uniquely specify an order for the phase transition; it is strongly dependent on the choice of parameters as well as being a function of the approximation that is made.

Finally, for completeness, we note that Eqs. (5.13) and (5.14) can be derived directly from the self-energy (Bernard *et al.*, 1987a; Klevansky and Lemmer, 1990). Equations (2.27) and (2.28) may be added and Fourier transformed into momentum space to give

$$\Sigma = m_0 + 2iG \left[ N_c N_f \int \frac{d^4 p}{(2\pi)^4} \text{tr} S(p) - \int \frac{d^4 p}{(2\pi)^4} S(p) + 3 \int \frac{d^4 p}{(2\pi)^4} \gamma_5 S(p) \gamma_5 \right], \quad (5.15)$$

since  $\text{Tr} S(p) \gamma_5 \tau$  vanishes. A direct evaluation of this using Eq. (5.8) gives

$$\Sigma = m_0 + 4(N_c N_f + \frac{1}{2}) G m^* \left[ \int^\Lambda \frac{d^3 p}{(2\pi)^3} \frac{1}{E_p} - \int \frac{d^3 p}{(2\pi)^3} \frac{1}{E_p} \theta(\mu' - E_p) \right] + 4\gamma^0 G \int \frac{d^3 p}{(2\pi)^3} \theta(\mu' - E_p), \quad (5.16)$$

indicating that the matrix form of  $\Sigma$  can no longer simply be a scalar. Writing therefore

$$\Sigma = m^* - \gamma^0 M_0, \quad (5.17)$$

one may identify

$$m^* = m_0 + 4(N_c N_f + \frac{1}{2}) G m^* \left[ \int^\Lambda \frac{d^3 p}{(2\pi)^3} \frac{1}{E_p} - \int \frac{d^3 p}{(2\pi)^3} \frac{1}{E_p} \theta(\mu' - E_p) \right] \quad (5.18)$$

and

$$-M_0 = 4G \int \frac{d^3 p}{(2\pi)^3} \theta(\mu' - E_p), \quad (5.19)$$

where  $E_{p_F} = \mu'$  as before. With (5.18), one has again recovered the gap equation as given in (5.11); and a direct calculation of the density

$$(N_q - N_{\bar{q}})/V = 2N_c N_f \int^{p_F} \frac{d^3 p}{(2\pi)^3} = \langle \psi^\dagger \psi \rangle \quad (5.20)$$

indicates that  $\langle \psi^\dagger \psi \rangle$  and  $M_0$  are directly related,

$$-M_0 = \frac{G}{N_c} \langle \psi^\dagger \psi \rangle, \quad (5.21)$$

so that (5.12) may again be recovered. One also notes that the effect of the term  $M_0$  in Eq. (5.17) for  $\Sigma$  is to shift the chemical potential  $\mu$  to  $\mu' + M_0$ , thus recovering (5.5).

## B. Finite temperature

### 1. The gap equation and thermodynamic potential

It would at first appear that the generalization of Sec. V.A to include the effects of temperature is straightforward. By denoting the grand canonical ensemble average of an operator  $\Theta$  as

$$\langle\langle \Theta \rangle\rangle = \frac{\text{Tr} \Theta e^{-\beta(H-\mu N)}}{\text{Tr} e^{-\beta(H-\mu N)}}, \quad (5.22)$$

the mean-field procedure of Sec. V.A can be effected with all averages occurring in Eqs. (5.1) through (5.6) being replaced by the corresponding ensemble averages. However, there is a problem. Strictly speaking, ensemble averages for systems of quarks should refer to states that are colorless. The grand canonical ensemble includes fluctuations in color, and a suitable projection technique is required to extract color singlet states only (Redlich and Turko, 1980; Turko, 1981; Le Yaouanc *et al.*, 1988). In the following, we ignore this problem. Then, in particular, Eq. (5.5) becomes

$$\mu' = \mu - \frac{G}{N_c} \langle\langle \psi^\dagger \psi \rangle\rangle \quad (5.23)$$

and Eq. (5.6) becomes

$$m^* = m_0 - G[2 + 1/2N_c] \langle\langle \bar{\psi} \psi \rangle\rangle. \quad (5.24)$$

At this point it is useful to introduce both the Matsubara or imaginary-time Green's function and the real-time Green's function (see, for example, Fetter and Walecka, 1971 and Dolan and Jackiw, 1974). The former is defined through

$$\mathcal{S}(\mathbf{x}, \tau; \mathbf{x}', \tau') = -\langle\langle T_\tau \psi(\mathbf{x}, \tau) \bar{\psi}(\mathbf{x}', \tau') \rangle\rangle, \quad (5.25)$$

where  $T_\tau$  orders the fermion operators in imaginary time  $\tau$ , while the real-time Green's function is defined as

$$iS(x, x') = \langle\langle T \psi(x) \bar{\psi}(x') \rangle\rangle, \quad (5.26)$$

with, as is customary,  $T$  ordering the fermion operators in real time. The Matsubara Green's function is antiperiodic for fermions over an imaginary-time interval  $\beta$ , i.e.,

$$\mathcal{S}(\mathbf{x} - \mathbf{x}', \tau - \tau')|_{\tau - \tau' = 0} = -\mathcal{S}(\mathbf{x} - \mathbf{x}', \tau - \tau')|_{\tau - \tau' = -\beta}.$$

Consequently the Fourier transform is given as

$$\mathcal{S}(\mathbf{p}, \omega_n) = \int d^3(x - x') \int_0^\infty d\tau \mathcal{S}(\mathbf{x}, \mathbf{x}', \tau) e^{i\omega_n \tau}, \quad (5.27)$$

with  $\omega_n = \pm(2n + 1)\pi/\beta$ ,  $n = 0, 1, 2, \dots$ , and we have assumed that the system is spatially homogeneous. The inverse transform follows as

$$\begin{aligned} \mathcal{S}(\mathbf{x} - \mathbf{x}', \tau - \tau') \\ = \frac{1}{\beta} \sum_n e^{-i\omega_n(\tau - \tau')} \int \frac{d^3 p}{(2\pi)^3} \mathcal{S}(\mathbf{p}, \omega_n) e^{i\mathbf{p} \cdot (\mathbf{x} - \mathbf{x}')}. \end{aligned} \quad (5.28)$$

The advantage of the Matsubara formalism is that Wick's theorem may be revised to apply to imaginary-time operators (Fetter and Walecka, 1971). Consequently there is a formal similarity between the zero-temperature theory and the finite-temperature theory at imaginary time. We exploit this to note that the Matsubara Green's function for a free particle of mass  $m^*$  in a system with chemical potential  $\mu$  described by the effective Lagrangian following Eq. (5.6) must satisfy the equation

$$(\not{p}_n - m^* + \gamma^0 \mu) \mathcal{S}(\mathbf{p}, \omega_n) = 1, \quad (5.29)$$

where  $p_n = (i\omega_n, \mathbf{p})$ . That is,

$$\mathcal{S}(\mathbf{p}, \omega_n) = [\not{p}_n - m^* + \gamma^0 \mu]^{-1}.$$

It is useful to rationalize this equation, and separate it into partial fractions as

$$\begin{aligned} \mathcal{S}(\mathbf{p}, \omega_n) = \frac{\not{p} + m^*}{2E_p} \frac{1}{i\omega_n - (E_p - \mu)} \\ + \frac{\tilde{\not{p}} - m^*}{2E_p} \frac{1}{i\omega_n + (E_p + \mu)}, \end{aligned} \quad (5.30)$$

where

$$\not{p} = \gamma^0 E_p - \boldsymbol{\gamma} \cdot \mathbf{p}$$

and

$$\tilde{\not{p}} = \gamma^0 E_p + \boldsymbol{\gamma} \cdot \mathbf{p}.$$

The real- and imaginary-time Green's functions are linked by the spectral function  $A(x, \mathbf{p})$ , where

$$A(x, \mathbf{p}) = \frac{1}{i} [\mathcal{S}(\mathbf{p}, \omega_n)|_{i\omega_n = x - i\eta} - \mathcal{S}(\mathbf{p}, \omega_n)|_{i\omega_n = x + i\eta}]. \quad (5.31)$$

Then the real-time Green's function  $S(\mathbf{p}, \omega)$  is obtained,

$$S(\mathbf{p}, \omega) = \int_{-\infty}^{\infty} \frac{d\omega'}{2\pi} \frac{A(\mathbf{p}, \omega')}{\omega - \omega' + i\eta} + i f(\omega) A(\mathbf{p}, \omega), \quad (5.32)$$

with  $f(\omega) = [1 + \exp \beta \omega]^{-1}$ . Using Eqs. (5.30) and (5.31), one finds the explicit form

$$\begin{aligned} S(p) = \frac{k + m^*}{k^2 - m^{*2} + i\epsilon} \\ + 2\pi i (k + m^*) \delta(k_0^2 - E_p^2) \\ \times [\theta(k^0) f^-(\mathbf{p}, \mu) + \theta(-k^0) f^+(\mathbf{p}, \mu)] \end{aligned} \quad (5.33)$$

for  $S(p)$  with

$$f^\pm(\mathbf{p}, \mu) = [1 + \exp \beta(E_p \pm \mu)]^{-1}$$

and

$$k = \gamma^0(p_0 + \mu) - \boldsymbol{\gamma} \cdot \mathbf{p}.$$

The single argument  $p$  of  $S$  in Eq. (5.33) refers to the four-momentum  $(p^0, \mathbf{p})$ .

The choice of which Green's function to use—Matsubara or real-time—is now a matter of taste. The mean-field procedure developed in this section so far fares better than the latter, while the self-energy approach can only be effected with the former, since perturbation theory and Feynman diagram techniques are only applicable in this case. We shall have cause to examine the self-energy anyway, since, as will be seen, it can be used in a sophisticated method to evaluate the thermodynamic potential. First, however, let us return to developing the gap equation, for which we use the real-time Green's function. As before, the scalar density is

$$\langle\langle \bar{\psi}\psi \rangle\rangle = -i \lim_{x' \rightarrow x^+} \text{Tr} S(x, x'),$$

while the quark density can be expressed as

$$\langle\langle \psi^\dagger \psi \rangle\rangle = \langle\langle [\psi^\dagger, \psi] \rangle\rangle = -i \lim_{x' \rightarrow x^+} \text{Tr} \gamma^0 S(x, x').$$

Inserting (5.33) into these equations and integrating out the  $p_0$  and angular components, one has

$$\langle\langle \psi^\dagger \psi \rangle\rangle = \frac{N_c N_f}{\pi^2} \int_0^\Lambda dp p^2 [f^-(\mathbf{p}, \mu') - f^+(\mathbf{p}, \mu')] \quad (5.34)$$

and

$$\langle\langle \bar{\psi}\psi \rangle\rangle = -m^* \frac{N_c N_f}{\pi^2} \int_0^\Lambda dp \frac{p^2}{E_p} [1 - f^-(\mathbf{p}, \mu') - f^+(\mathbf{p}, \mu')]. \quad (5.35)$$

Recognizing the fact that

$$1 - f^-(\mathbf{p}, \mu') - f^+(\mathbf{p}, \mu') = \frac{1}{2} (\tanh \frac{1}{2} \beta \omega_p^- + \tanh \frac{1}{2} \beta \omega_p^+) \quad (5.36)$$

while the difference in Fermi functions is given as

$$f^-(\mathbf{p}, \mu') - f^+(\mathbf{p}, \mu') = \frac{1}{2} (\tanh \frac{1}{2} \beta \omega_p^+ - \tanh \frac{1}{2} \beta \omega_p^-) \quad (5.37)$$

in terms of  $\omega_p^\pm = E_p \pm \mu'$ , one can construct the gap equation from (5.24) and (5.35),

$$m^* = m_0 + G [N_c N_f + \frac{1}{2}] \frac{m^*}{\pi^2} \times \int_0^\Lambda dp \frac{p^2}{E_p} (\tanh \frac{1}{2} \beta \omega_p^- + \tanh \frac{1}{2} \beta \omega_p^+), \quad (5.38)$$

and from Eqs. (5.23) and (5.34)

$$\mu' = \mu - G \frac{1}{\pi^2} \int_0^\Lambda dp p^2 (\tanh \frac{1}{2} \beta \omega_p^+ - \tanh \frac{1}{2} \beta \omega_p^-); \quad (5.39)$$

the mass  $m^*$  obtained in this fashion must be shown to lead to a value of the thermodynamic potential

$$\Omega = -\frac{1}{\beta} \log(\text{Tr} e^{-\beta(H - \mu N)}) \quad (5.40)$$

that is lower in the chirally broken phase. The evaluation of  $\Omega$  is a technical exercise that is relegated to Appendix D. One finds

$$\frac{\Omega}{N_c N_f} = \frac{(m^* - m_0)^2}{4[N_c N_f + \frac{1}{2}]G} - \frac{M_0^2}{4G} - 2 \int \frac{d^3 p}{(2\pi)^3} E_p - \frac{2}{\beta} \int \frac{d^3 p}{(2\pi)^3} \log(1 + e^{-\beta(E_p + \mu')})(1 + e^{-\beta(E_p - \mu')}), \quad (5.41)$$

which has been given by Asakawa and Yazaki (1989). The zero-temperature limit of this equation,

$$\frac{\Omega_{T \rightarrow 0}}{N_c N_f} = \frac{(m^* - m_0)^2}{4G[N_c N_f + \frac{1}{2}]} - \frac{M_0^2}{4G} - \int \frac{d^3 p}{(2\pi)^3} E_p + 2 \int \frac{d^3 p}{(2\pi)^3} E_p \theta(\mu' - E_p) - 2\mu' \int \frac{d^3 p}{(2\pi)^3} \theta(\mu' - E_p), \quad (5.42)$$

leads to the simple analytic form

$$\begin{aligned} \Omega_{T \rightarrow 0} = & \frac{N_c (m^* - m_0)^2}{2[N_c N_f + \frac{1}{2}]G} - \frac{2G}{3\pi^2} (\mu'^2 - m^{*2})^3 \\ & - \frac{N_c N_f}{\pi^2} 8[-m^{*4} \log(\Lambda + \sqrt{\Lambda^2 + m^{*2}}) + \sqrt{\Lambda^2 + m^{*2}} (m^{*2} \Lambda + 2\Lambda^3) \\ & + m^{*4} \log(\mu' + \sqrt{\mu'^2 - m^{*2}}) + \mu' m^{*2} \sqrt{\mu'^2 - m^{*2}} + \frac{2}{3} \mu' (\mu'^2 - m^{*2})^{3/2}] \end{aligned} \quad (5.43)$$

that has been used for Fig. 13.

Finally, one may recognize that the last integral occurring in Eq. (5.42) is related to  $M_0$ , via Eq. (5.19). Using this, and writing its cofactor out explicitly,  $\mu' = \mu + M_0$ , enables one to write

$$\begin{aligned} \Omega_{T \rightarrow 0} = & N_c N_f \left[ \frac{N_c (m^* - m_0)^2}{4G[N_c N_f + \frac{1}{2}]} + \frac{M_0^2}{4G} + 2 \int \frac{d^3 p}{(2\pi)^3} E_p \theta(\mu' - E_p) - 2 \int \frac{d^3 p}{(2\pi)^3} E_p \right] - \mu \langle \psi^\dagger \psi \rangle \\ = & U - \mu N, \end{aligned} \quad (5.44)$$

from which the internal energy  $U$  may be identified.

## 2. Mesonic excitations

We turn now to the particle-hole propagator to examine the mesonic excitations. As in Sec. IV, it suffices to examine the lowest-order term for the proper polarization, which we denote, in the imaginary-time formalism, as  $\Pi(\mathbf{q}, i\nu_n)$ . This term is illustrated diagrammatically in Fig. 16.

Once again, in the random-phase approximation, the bubbles must be summed. The meson modes may be obtained by examining the function  $1 - 2G\Pi(\mathbf{q}, \omega) = 0$  as before, where  $\Pi(\mathbf{q}, \omega)$  refers to the analytically continued function  $\Pi(\mathbf{q}, i\nu_n)$  onto the real frequency axis. For clarity, we examine the scalar mode in detail in Appendix E. Here we list only the final results, evaluated at  $\mathbf{q} = 0$ . In this limit, the equations for  $\Pi_s(0, \omega)$  and  $\Pi_{ps}(0, \omega)$  become particularly simple,

$$\Pi_s(0, \omega) = 2N_c N_f \int \frac{d^3p}{(2\pi)^3} \frac{1}{E_p} \frac{E_p^2 - m^{*2}}{E_p^2 - \omega^2/4} \tanh \frac{1}{2} \beta E_p \quad (5.45)$$

and

$$\Pi_{ps}(0, \omega) = 2N_c N_f \int \frac{d^3p}{(2\pi)^3} \frac{1}{E_p} \frac{E_p^2}{E_p^2 - \omega^2/4} \tanh \frac{1}{2} \beta E_p. \quad (5.46)$$

The temperature dependence of the dynamically generated mass, together with the meson modes, has been calculated by Hatsuda and Kunihiro (1985b, 1987a) and is shown in Fig. 17.

The parameters used by these authors are  $\Lambda = 631$  MeV and  $G\Lambda^2 = 2.02$  to reproduce the pion-decay constant and the quark condensate  $\langle \bar{u}u \rangle = (-250 \text{ MeV})^3$  (case I of Table V). The current quark mass used is  $m_0 = 5.5$  MeV. One sees from the figure a pattern, indicated by the solid curves, that occurs repeatedly in the restoration of chiral symmetry. The mass drops rapidly but continuously to the current quark mass value. The scalar mode drops, while the pseudoscalar mode rises to meet it in the chiral limit. Both modes continue to rise in energy as the temperature is increased, since the thermal energy now dominates the spectrum. The dashed curves shown in this figure represent the calculated modes where  $m^*$  is kept constant (Wigner-Weyl mode). One

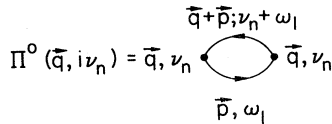


FIG. 16. Lowest-order contribution to the polarization propagator in imaginary time. The frequencies  $\nu_n$  are even,  $\nu_n = \pm 2n\pi/\beta$ ,  $n = 0, 1, 2, 3, \dots$ , while the fermion frequencies  $\omega_1$  can take odd values only,  $(\omega_1)_m = \pm(2m+1)\pi/\beta$ ,  $m = 0, 1, 2, 3, \dots$ .

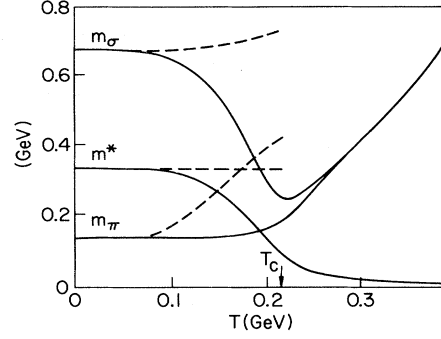


FIG. 17. Variation of the dynamically generated mass  $m^*$ ,  $m_\pi$ , and  $m_\sigma$  as a function of temperature. The solid curves indicate the Nambu-Goldstone mode, whereas the dashed curves give the Wigner-Weyl modes, where  $m^*$  is kept constant (after Hatsuda and Kunihiro, 1987a).

sees in this case that both meson modes rise, a feature that can be understood as due to Pauli blocking: the thermally excited quarks and antiquarks partially block available states for the formation of the  $\bar{q}q$  coherent modes, thereby reducing the collectiveness of the  $\sigma$  and  $\pi$ . In the Nambu-Goldstone mode, the fact that the observed phase transition is smeared out means that no critical point in the temperature can be uniquely defined. Following Asakawa and Yazaki (1989), we define it to be the temperature at which  $m^*$  has reached half its zero-temperature value and denote this as  $T_c$ . Then a phase-transition line can be drawn for the parameter sets employed in this section, and this is shown in Fig. 18. In this diagram, the solid lines refer to the occurrence of a first-order phase transition, while the dashed lines represent smooth transition regions as defined above. We note that the transition temperature at  $\mu = 0$  lies at about  $T = 180$  MeV for case I, which represents a more realistic parameter set than case II. This value lies close to the estimate  $T_c = 190$  MeV of chiral perturbation theory (Gerber and Leutwyler, 1989). A closer comparison between the NJL model and chiral perturbation theory at finite temperature has to date not been made.

It is interesting to note that, for the case of a zero current quark mass and zero chemical potential, an ap-

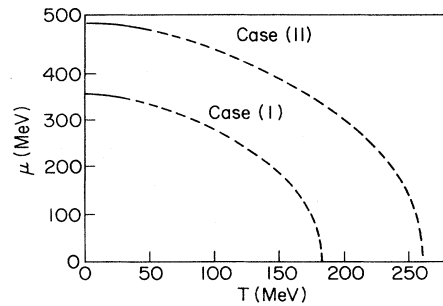


FIG. 18. Phase-transition line for cases I and II (Asakawa and Yazaki, 1989).

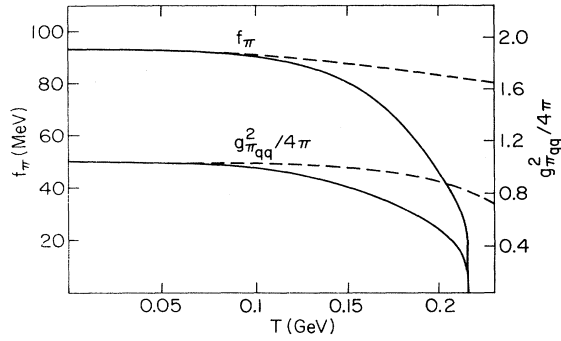


FIG. 19. Temperature dependence of  $f_\pi$  and  $g_{\pi qq}^2$  is shown for the Nambu-Goldstone mode (solid curve) and the Wigner-Weyl model (dashed line); (after Hatsuda and Kunihiro, 1987a).

proximate estimate for  $T_c$  can be obtained directly from the gap equation. From Eqs. (5.38) and (3.28), one obtains

$$T_c \simeq \Lambda \left[ \frac{3}{\pi^2} \right]^{1/2} \left[ 1 - \frac{\pi^2}{GN_c N_f \Lambda^2} \right]^{1/2} \\ = \sqrt{2} f_\pi = 135 \text{ MeV} \quad (5.47)$$

provided that  $m^{*2} \ll \Lambda^2$ .

The dependence of the coupling constants on temperature may be calculated along the lines developed in Sec. IV.A. One finds (Hatsuda and Kunihiro, 1987a) the result shown in Fig. 19. One sees that an increase in temperature leads to a decrease in the coupling strengths, indicating that the mesons decouple from the surrounding matter in the chiral limit.

One may wish to contrast the results obtained here with the findings of lattice gauge theory. Here thermodynamic Monte Carlo studies have been made, primarily with  $\mu=0$  (see, for example, Christ, 1991 and Kogut *et al.*, 1991, and references cited therein). These references tell us, however, that the nature of the phase transition as determined via lattice gauge theory is not yet clear. The results of Kogut *et al.* (1991) indicate that the initial evidence for a first-order transition is considerably weakened when a larger lattice is used. The transition is less abrupt and could simply be a crossover phenomenon for the quark masses used in their simulations. These authors have studied a three-flavor model. Christ (1991) confirms this tendency for the two-flavor model, while the three-flavor-model results depend rather sensitively on the quark mass parameters that are used.

## VI. EFFECTS OF EXTERNAL PARAMETERS II: MAXWELL AND COLOR FIELDS

Up to this point, the self-interactions of quarks with one another have been modeled via an interaction that is four-point in SU(2), or, in SU(3), both four- and six-point. Quarks, possessing a flavor-dependent electric charge,

however, couple to electromagnetic fields and, via their color charge, also to chromoelectromagnetic fields. The effects of such fields on a system of quarks that interact via the NJL Lagrangian is the subject of this section (Bernard and Vautherin, 1989; Klevansky and Lemmer, 1989; Klevansky *et al.*, 1991; Suganuma and Tatsumi, 1990, 1991).

We first take a look at the coupling of quarks to Maxwellian fields. One can solve this problem *exactly*, for arbitrary values of the field strengths, provided that constant electromagnetic configurations are considered. This is important, since it lays the foundation for the study in which color electromagnetic fields are considered instead: these fields are strong and cannot be handled perturbatively. Furthermore, by using the Pauli-Villars regularization scheme, we are able to perform calculations while preserving both gauge and Lorentz invariance. The response of the condensate, the meson modes, and the coupling strengths can all be calculated. The results are at first sight somewhat surprising: the influence of an electric field serves to restore chiral symmetry, while the magnetic field tends to enhance its breaking. We can understand this physically, since we may imagine that the electric field destroys the condensate by pulling the pairs apart, while the magnetic field aids in antialigning the helicities which are bound by the NJL interaction. This is in contrast to the influence of electromagnetic fields in standard BCS theory, but we can understand this by recalling that in that case, *like* particles (electrons) of opposite spin are paired, whereas in the NJL model, the pairing is between particles and their antiparticles.

We then present small-field results, i.e., the electromagnetic polarizabilities of the pion (Sec. VI.A.3). The pion form factor, which can also be calculated analytically in the NJL model, is examined in Sec. VI.A.4.

It turns out that, in practice, the electromagnetic fields that are generated in heavy-ion collisions are too weak for an effect of chiral symmetry breaking to be observed, and so we turn our attention to chromoelectromagnetic fields in Sec. VI.B. In QED, background fields can be kept under laboratory control. In QCD, however, this is not the case: external color electric and magnetic fields exist only in the interior of hadrons. This concept has formed the basis of the schematic flux tube models (Kogut and Susskind, 1975; Casher *et al.*, 1979; Gatoff *et al.*, 1987; see also Low, 1975) and is useful in describing the early stages of ultrarelativistic heavy-ion collisions, where flux tubes with strong chromoelectric fields are supposed to be formed in the central collision region. This latter picture is also suggested by lattice QCD calculations (Giacomo *et al.*, 1990). The evaluation of the pair-production rate in the presence of external fields for a flux tube could in principle then be effected using Schwinger's formula (see, for example, Itzykson and Zuber, 1980; Cox and Yildiz, 1985; Martin and Vautherin, 1988, Klevansky, 1991; and Suganuma and Tatsumi,

1991). It is with this rather rough picture in mind that the constant or homogeneous background SU(3) color field in the NJL model is reviewed.

### A. Maxwell fields

#### 1. Gap equation

To investigate the effects of minimally coupling a U(1) gauge field into the NJL Lagrangian, we consider the modified SU(2) Lagrange density

$$\mathcal{L} = \mathcal{L}_{\text{NJL}} - q\bar{\psi}\gamma_\mu A^\mu\psi - \frac{1}{4}F_{\mu\nu}F^{\mu\nu} + \mathcal{L}_{\text{mass}}, \quad (6.1)$$

where  $\mathcal{L}_{\text{NJL}}$  is given by Eq. (2.15). If we consider the fields  $A_\mu$  to be electromagnetic fields, then  $F^{\mu\nu} = \partial^\mu A^\nu - \partial^\nu A^\mu$  and

$$q_F = \frac{1}{2}e(\tau_f + \frac{1}{3}), \quad (6.2)$$

where  $\tau_f = \pm 1$  refers to up and down quarks, respectively. We note that the presence of this term in (6.1) breaks chiral symmetry explicitly. This is in contrast to the coupling of chromoelectric fields into the QCD Lagrangian: in that case, the associated coupling constant is both flavor and color independent, thereby maintaining the chiral symmetry of the QCD Lagrangian.

In general, the electromagnetic potential is a function of the four-dimensional space-time vector  $x$ ,  $A_\mu = A_\mu(x)$ . We are thus led to consider the representation of all quantities in  $x$  space. We begin once again with the self-energy, which is given in Hartree as

$$\Sigma = m = m_0 + 2iG \text{Tr}S(x, x) + 2iG(i\gamma_5)\tau \cdot \text{Tr}i\gamma_5 S(x, x)\tau, \quad (6.3)$$

and is again independent of position. The trace of the pseudoscalar term does not in general vanish when fields are present, so that  $\Sigma$  has the structure

$$\Sigma^f = m + i\gamma_5\tau_fm_1$$

in flavor space.  $S^f$  and therefore  $\Sigma^f$  are flavor diagonal, this dependence arising solely from the different charge states, since the current quark masses are assumed equal. For notational ease, we temporarily suppress the flavor labels. The propagator  $S(x, x')$  satisfies

$$(i\partial_x - qA - \Sigma)S(x, x') = \delta^{(4)}(x - x'), \quad (6.4)$$

which can be solved either within the path-integral formalism of Feynman (1950); or through the proper-time procedure of Schwinger (1951). We choose the latter, summarizing the procedure only briefly here. One introduces an auxiliary function  $G(x, x')$  via

$$S(x, x') = [i\partial - qA + \Sigma^\dagger]G(x, x'), \quad (6.5)$$

so that  $G(x, x')$  satisfies the scalar equation

$$\left[ (i\partial - qA)^2 - \frac{q}{2}\sigma_{\mu\nu}F^{\mu\nu} - M^2 \right] G(x, x') = \delta^{(4)}(x - x'), \quad (6.6)$$

where  $M^2 = m^2 + m_1^2$  is the square of the quark mass in the presence of the electromagnetic field and is flavor independent. One may write this equation in operator form as

$$[\mathcal{H} - M^2]G = 1, \quad (6.7)$$

with the identification

$$\mathcal{H} = (i\partial - qA)^2 - \frac{q}{2}\sigma_{\mu\nu}F^{\mu\nu} - M^2. \quad (6.8)$$

Equation (6.7) may be expressed as

$$G = -i \int_{-\infty}^0 d\tau e^{-i(\mathcal{H} - M^2)\tau}, \quad (6.9)$$

and one is required to find the matrix element

$$\langle x|G|x' \rangle = -i \int_{-\infty}^0 d\tau \langle x|e^{-iq(\mathcal{H} - M^2)\tau}|x' \rangle. \quad (6.10)$$

This is determined if

$$U(x, x', \tau) = \langle x|e^{-i\tau\mathcal{H}}|x' \rangle \quad (6.11)$$

is known. Equation (6.11) can be evaluated by drawing an analogy with quantum mechanics.  $U$  can be regarded as an evolution operator if one considers  $\mathcal{H}$  to be a Hamiltonian that describes the evolution of a system in the “proper time”  $\tau$ .  $U(x, x', \tau)$  satisfies the differential equation

$$i\frac{\partial U}{\partial \tau} = HU \quad (6.12)$$

and is subject to the boundary condition

$$\lim_{\tau \rightarrow 0} U(x, x', \tau) = \delta^{(4)}(x - x').$$

It is interesting to note that Eq. (6.12), when analytically continued to the Euclidean variable,  $t = i\tau$ , is identical with the heat-kernel equation (Stephens, 1988), which is discussed by Ebert and Reinhardt (1986), in connection with bosonization techniques.

The equations of motion for the “coordinates”  $x_\mu$  and “momenta”  $\pi_\mu$  are

$$\frac{\partial x_\mu}{\partial \tau} = \frac{1}{i}[x_\mu, \mathcal{H}] = -2\pi_\mu \quad (6.13)$$

and

$$\begin{aligned} \frac{\partial \pi_\mu}{\partial \tau} &= \frac{1}{i}[\pi_\mu, \mathcal{H}] \\ &= -2qF_{\mu\nu}\pi^\nu - iq\partial^\nu F_{\mu\nu} - \frac{q}{2}\partial_\mu\sigma_{\rho\nu}F^{\rho\nu}, \end{aligned} \quad (6.14)$$

respectively, where  $\tau_\mu = (i\partial - qA)_\mu$ . These equations can be solved exactly for certain field configurations, in particular when the field strengths are constant. One finds (Schwinger, 1951; Itzykson and Zuber, 1980)



$$U(x, x', \tau) = -\frac{i}{(4\pi\tau)^2} \exp \left[ -iq\phi(x, x') - L(\tau) + \frac{i}{4}(x - x')K(\tau)(x - x') + \frac{iq}{2}\sigma_{\mu\nu}F^{\mu\nu}\tau \right], \quad (6.15)$$

using the abbreviations

$$\phi(x, x') = \int_{x'}^x d\xi^\mu [A_\mu(\xi) + \frac{1}{2}F_{\mu\nu}(\xi - x')^\nu], \quad (6.16)$$

$$L(\tau) = \frac{1}{2} \text{tr} \log[(qF\tau)^{-1} \sinh(qF\tau)] \quad (6.17)$$

and

$$K(\tau) = qF \coth qF\tau \quad (6.18)$$

using an obvious matrix notation. We require, however,  $S(x, x')$ , which can now be obtained on combining Eqs. (6.5) and (6.10) to give

$$iS(x, x') = \int_{-\infty}^0 d\tau e^{iM^2\tau} \left[ -\frac{1}{2}\gamma^\mu M_{\mu\nu}(\tau)(x - x')^\nu + \Sigma^\dagger \right] U(x, x', \tau), \quad (6.19)$$

where  $M(\tau) = K(\tau) - qF$ , and  $U(x, x', \tau)$  is obtained from (6.15). It is now a straightforward matter to obtain the self-consistency condition or gap equation for  $\Sigma$  by inserting Eq. (6.19) into Eq. (6.3). We summarize the details here in a form somewhat different from that given in the literature, which is, however, more transparent for the present discussion.

Since only the trace of  $S$  at equal space-time points enters the determination of  $\Sigma$ , one has some simplification. One requires, however, the values of  $\exp[-L(\tau)]$  and the value of the spinor trace operation on  $\exp[iq\tau\sigma F/2]$  and  $\gamma_5 \exp[iq\tau\sigma F/2]$ . The former two quantities have been calculated in Schwinger's original paper (Schwinger, 1951) using an elegant eigenvalue argument to give their values in terms of the Lorentz and

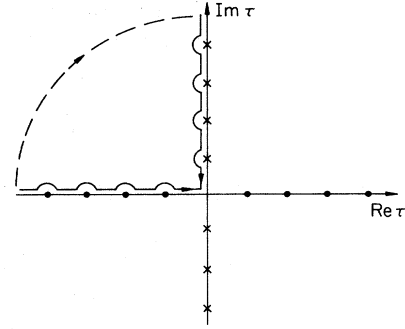


FIG. 20. Integration contour for the evaluation of the gap equation (6.23).

gauge-invariant combination  $\chi^2 = (\mathbf{B} + i\mathbf{E})^2 = 2(\mathcal{F} + i\mathcal{G})$  of the field strength. Here

$$\mathcal{F} = -\frac{1}{2}(\mathbf{E}^2 - \mathbf{B}^2), \quad \mathcal{G} = \mathbf{B} \cdot \mathbf{E} \quad (6.20)$$

are field invariants  $\frac{1}{4}F_{\mu\nu}F^{\mu\nu}$  and  $-\frac{1}{4}F_{\mu\nu}\tilde{F}^{\mu\nu}$ , respectively, and  $\tilde{F}^{\mu\nu}$  is the field tensor dual to  $F^{\mu\nu}$ . Alternatively, one can express these quantities explicitly in terms of the four eigenvalues  $\pm iF'$  and  $\pm F''$  (two real and two pure imaginary) of the field tensor  $F_{\mu\nu}$ . We present a detailed discussion of the eigenvalues of  $F^{\mu\nu}$  and the representation of functions of the field tensor in terms of its eigenvalues in Appendix F. Here, we simply give the final equations,

$$e^{-L(\tau)} = \frac{(qF'\tau)(qF''\tau)}{\sinh(qF'\tau)\sin(qF''\tau)}, \quad (6.21)$$

$$\text{tr} e^{iq\tau\sigma F/2} = 4 \cosh(qF'\tau) \cos(qF''\tau), \quad (6.22a)$$

and

$$\text{tri} \gamma_5 e^{iq\tau\sigma F/2} = -4 \sinh(qF'\tau) \sin(qF''\tau). \quad (6.22b)$$

Gathering the results together, one can reorganize Eq. (6.3) to read

$$\Sigma^f = m_0 - \frac{iGN_c}{2\pi^2} \Sigma^f \int_{-\infty}^0 \frac{d\tau}{\tau^2} e^{iM^2\tau} \left[ \sum_g q_g F'\tau \coth(q_g F'\tau) q_g F''\tau \cot(q_g F''\tau) - i\gamma_5 \tau_f \sum_g \tau_g (q_g \tau F') (q_g \tau F'') \right], \quad (6.23)$$

where  $g$  is a flavor label. The integrand appearing in the first term has simple poles at  $\pm in\pi/qF$  due to the hyperbolic cotangent, and at  $\pm n\pi/qF''$  due to the cotangent, where  $n = 1, 2, 3, \dots$ . The point  $\tau=0$  is always a double pole, whether the field is present or not, and reflects the standard divergence of the gap equation in the NJL model in the proper-time scheme. The  $\tau$ -integration contour in Eq. (6.23) runs infinitesimally above the negative real axis, since  $m^2$  has a negative imaginary part. It is useful to deform the  $\tau$ -integration path to consist of a large quarter circle in the upper-left quadrant of the complex  $\tau$  plane, plus a straight-line path parallel, but infinitesimally close, to the left of the positive imaginary axis, in order to avoid the poles of  $qF'\tau \coth qF'\tau$ . This deformation of contour is shown in Fig. 20. The quarter circle makes no contribution, and one can rewrite Eq. (6.23) as

$$\Sigma^f = m_0 + \frac{GN_c}{2\pi^2} \Sigma^f \left[ \sum_g \int_0^\infty \frac{ds}{s^2} e^{-M^2s} q_g F's \cot(q_g F's) q_g F''s \coth(q_g F''s) + i\gamma_5 \tau_f \frac{F'F''}{M^2} (q_u^2 - q_d^2) \right] \quad (6.24)$$

after setting  $\tau = is$  on the positive imaginary  $\tau$  axis. The second term has been explicitly evaluated. In the first term of this equation, the  $s$ -integration path lies infinitesimally above the real  $s$  axis and, except in the case of a pure magnetic field ( $F'=0$ ,  $F''=B$ ), results in a finite negative imaginary contribution to the integral from simple poles along the real

axis. Consequently, the quasiparticles acquire a complex mass that reflects the nonpermanence of the vacuum under the action of a constant field with respect to pair production (Schwinger, 1951). One can show that the second term that is proportional to  $F'F'' = \mathcal{G}$  also contributes mainly to the quasiparticle width. These effects are ignored here, so that only the principle value of integrals such as those occurring in (6.24) is considered, and the second term of Eq. (6.24) is dropped, which in turn is equivalent to setting  $m_1 = 0$ ,  $M = m$ . In any event, this latter term falls away for the field configurations that will be considered, where either  $F'$  or  $F''$  are set to zero.

For the discussion of regularization, it is convenient to split up the gap equation as

$$m = m_0 + \frac{GN_c m}{2\pi^2} \left[ \sum_f \int_0^\infty \frac{ds}{s^2} e^{-m^2 s} + \sum_f \int_0^\infty \frac{ds}{s^2} e^{-m^2 s} [q_f F' s \cot(q_f F' s) q_f F'' s \coth(q_f F'' s) - 1] \right], \quad (6.25)$$

thereby isolating the divergence in the first term. The original procedure of Nambu and Jona-Lasinio of cutting off the zero-field version of Eq. (6.25) in Euclidean four-momentum becomes intractable when fields are present. Instead, we follow the procedure of Pauli and Villars of coupling in massive auxiliary fields to regularize Eq. (6.25), as discussed in Sec. III. Calling  $B_R(m^2)$  the regularized version of the divergent integral in (6.25), one finds that

$$\begin{aligned} B_R(m^2) &= \lim_{\rho \rightarrow 0} \sum_a C_a \int_\rho^\infty \frac{ds}{s^2} e^{-M_a^2 s} \\ &= \sum_a C_a M_a^2 \log \frac{M_a^2}{m^2}, \end{aligned} \quad (6.26)$$

with the weights  $C_a$  and auxiliary masses  $M_a$  satisfying  $\sum C_a = 0$  and  $\sum C_a M_a^2 = 0$ , with  $C_0 = 1$  and  $M_0 = m$ . Implementing these conditions as in Sec. III, one chooses  $C_1 = 1$ ,  $C_2 = -2$ , and  $M_1^2 = m^2 + 2\Lambda^2$ ,  $M_2^2 = m^2 + \Lambda^2$ , where  $\Lambda^2$  is an arbitrary cutoff mass squared. Then

$$\begin{aligned} B_R(m^2) &= \Lambda^2 \left[ \left( 2 + \frac{m^2}{\Lambda^2} \right) \log \left( 1 + 2 \frac{\Lambda^2}{m^2} \right) \right. \\ &\quad \left. - 2 \left( 1 + \frac{m^2}{\Lambda^2} \right) \log \left( 1 + \frac{\Lambda^2}{m^2} \right) \right]. \end{aligned} \quad (6.27)$$

In this equation,  $m$  is the field-dependent dynamical mass. We consider now Eq. (6.25) for the case of a constant electric field. Then  $F' = \sqrt{2|\mathcal{F}|}$  and  $F'' = 0$ , in terms of the Lorentz invariant  $\mathcal{F} = -\frac{1}{2}E^2$ . The gap equation now takes the form

$$\begin{aligned} \frac{2\pi^2}{GN_c} \left[ 1 - \frac{m_0}{m} \right] &= N_f B_R(m^2) \\ &\quad + \sum_f q_f E \operatorname{Re} J(im^2/2q_f E), \end{aligned} \quad (6.28)$$

upon taking the principal value of the integral

$$\int_0^\infty \frac{ds}{s^2} e^{-m^2 s} [q_f E s \cot q_f E s - 1] = q_f E J[im^2/2q_f E] \quad (6.29)$$

where

$$J(z) = 2i \left[ (z - \frac{1}{2}) \log z - z - \log \Gamma(z) + \frac{1}{2} \log 2\pi \right]. \quad (6.30)$$

For a pure magnetic field, the eigenvalues  $F'$  and  $F''$  interchange, with the field invariant  $\mathcal{F}$  given by  $\mathcal{F} = \frac{1}{2}B^2$ . The resulting gap equation is again given by Eq. (6.28) with the replacement  $\mathbf{E} \rightarrow i\mathbf{B}$ .

For purposes of illustration, we ignore the charge difference of  $u$  and  $d$  quarks and solve Eq. (6.25) for an average common charge  $q$  (Klevansky and Lemmer, 1989). The solutions of the respective gap equations are shown in Fig. 21 as a function of  $q\sqrt{|\mathcal{F}|}$  for both a zero current quark mass and for  $m_0 = 5.2$  MeV. The other parameters used are  $\Lambda = 851$  MeV and  $G\Lambda^2 = 2.87$ , to fix  $f_\pi = 94$  MeV and  $\langle \bar{q}q \rangle = (-250 \text{ MeV})^3$  at zero field in the chirally symmetric case. Then at zero field  $m = 248$  MeV for  $m_0 = 0$  or  $m = 265$  MeV for  $m_0 = 5.2$  MeV.

One notices the following features. For a zero current quark mass,  $m$  displays a second-order phase transition as a function of  $q\sqrt{|\mathcal{F}|}$  to the chirally symmetric phase at the critical-field strength given by

$$\begin{aligned} qE_c &= 2\Lambda'^2 \pi^{-1} (1 - 2\pi^2 / GN_c N_f \Lambda'^2) \\ &= 0.56 \text{ GeV fm}^{-1}, \end{aligned}$$

with  $\Lambda'^2 = 2\Lambda^2 \log 2$ , in the case of a pure electric field. (The approximate analytic form  $qE_c \simeq 8\pi f_\pi^2/3 = 0.38 \text{ GeV fm}^{-1}$  obtained in the limit  $m^* \ll \Lambda$  in the Pauli-Villars scheme gives the correct order of magnitude for this quantity, but underestimates it somewhat.) This

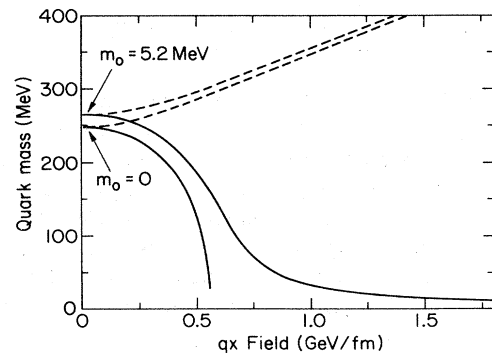


FIG. 21. Behavior of the dynamically generated quark mass in a constant electric or magnetic field. The solid curves refer to the effect of a pure electric field for both a zero current quark mass and for the choice  $m_0 = 5.2$  MeV. The dashed curves give the corresponding behavior in a magnetic field.

phase transition is washed out in the presence of a current quark mass. By contrast, the effect of a  $B$  field is to stabilize the chirally asymmetric vacuum. In this case, the gap equation always has a nontrivial solution for finite  $B$ . The different behavior in the response of a condensate in these two situations can be understood as follows. While the  $E$  field opposes condensate formation by polarizing the bound  $\bar{q}q$  pairs, the  $B$  field facilitates the binding by antialigning the helicities of the quark and antiquark, which are then bound by the NJL interaction. We note that this contrasts with the behavior of the BCS ground state of an ordinary superconductor. There the application of an external magnetic field favors the spin alignment of the electron pairs and consequently opposes BCS condensate formation, with the result that the magnetic field tends to restore the spontaneously broken symmetry. The contrasting behavior in the response of a quark system to electric and magnetic fields has recently also been confirmed by other authors (Suganuma and Tatsumi, 1991) who work with the linear sigma model. These authors point out that this result has consequences in weak-interaction physics, too, in particular, in resolving the longstanding issue as to whether the Cabibbo angle vanishes and strangeness is conserved in the weak interactions in a strong electromagnetic field, as may be expected in some nuclei or hadrons. This possibility was first indicated by Salam and Strathdee, who, however, assumed that the effects of a strong magnetic field are symmetry restoring (Salam and Swathdee, 1975; see also Suganuma and Tatsumi, 1991, and references cited therein). In the model presented by these authors, the Cabibbo angle  $\theta_c$  is not considered as a constant, but arises rather as a consequence of spontaneous symmetry breaking due to a Higgs field.

## 2. Meson modes

The response of the scalar-scalar and pseudoscalar-isovector modes to an external  $U(1)$  field can be obtained using the methods described in Sec. IV. For simplicity, we consider here a common charge until we calculate the polarizabilities of the mesons, when it is essential to recognize the charge difference. Here, as was the case for the Green's function in Sec. IV, the proper polarization

must be expressed in terms of space-time variables. One has

$$\frac{1}{i}\Pi_{ps}(x, x') = -\text{Tr}[i\gamma_5 TiS(x, x')i\gamma_5 iS(x', x)] \quad (6.31)$$

for the  $0^{-+}$  mode, in analogy to Eq. (4.8), while the  $0^{++}$  mode is obtained by constructing the appropriate analogy to Eq. (4.13),

$$\frac{1}{i}\Pi_s(x, x') = -\text{Tr}[iS(x, x')iS(x', x)] \quad (6.32)$$

One sees from Eq. (6.19) that  $S(x, x')$  is a function of the relative coordinate  $x - x'$ , apart from the phase factor  $\phi(x, x')$  that occurs in  $U$ . This phase factor will cancel in the construct required by (6.31) and (6.32), so that one may write

$$\frac{1}{i}\Pi_{ps}(k) = \int d^4(x - x') e^{ik(x - x')} \times \text{Tr}[\gamma_5 TiS(x, x')\gamma_5 TiS(x', x)] \quad (6.33)$$

for the Fourier transform of the pseudoscalar polarization of  $\Pi_{ps}$ , for example. Once again, the dispersion relation is given by solving

$$1 - 2G\Pi_{ps}(k) = 0, \quad (6.34)$$

and the effective coupling strength of the pseudoscalar mode to quarks,  $g_{\pi qq}$ , is given as before, via the relation

$$g_{\pi qq}^{-2}(\mathcal{F}) = \left. \frac{\partial \Pi_{ps}}{\partial k_0^2} \right|_{k_0^2 = m_\pi^2} \quad (6.35)$$

The mass of the scalar mode, and the coupling of this mode to quarks, is given, for finite field strengths, by the dispersion relation

$$1 - 2G\Pi_s(k) = 0 \quad (6.36)$$

and the corresponding relation

$$g_{\sigma qq}^{-2} = \left. \frac{\partial \Pi_s}{\partial k_0^2} \right|_{k_0^2 = m_\pi^2} \quad (6.37)$$

The evaluation of  $\Pi_{ps}$  and  $\Pi_s$  is rather a difficult technical exercise and is relegated to Appendix G, where it is briefly sketched for  $\Pi_{ps}$ . We find

$$\frac{1}{i}\Pi_{ps} = -N_c N_f \frac{4}{(4\pi)^2} \sum_a C_a \int_0^\infty \frac{d\lambda}{\lambda^2} qE\lambda \coth qE\lambda e^{-iM_a^2\lambda} - 2N_c N_f I(k)(k_0^2 - k_3^2) + 2N_c N_f I'(k)k_1^2, \quad (6.38)$$

where

$$I(k) = \frac{i}{(4\pi)^2} \sum_a C_a \int_0^\infty \frac{d\lambda}{\lambda} qE\lambda \coth qE\lambda e^{-iM_a^2\lambda} \int_0^1 du e^{ikK_{12}^{-1}k} \frac{\cosh qE\lambda u}{\cosh qE\lambda} \quad (6.39)$$

and

$$I'(k) = \frac{i}{(4\pi)^2} \sum_a C_a \int_0^\infty \frac{d\lambda}{\lambda} qE\lambda \coth qE\lambda e^{-iM_a^2\lambda} \int_0^1 du e^{ikK_{12}^{-1}k}. \quad (6.40)$$

The first term of (6.38) may be simplified by making use of the gap equation. By choosing a suitable contour deforma-

tion, one may write

$$\sum_a C_a \int_0^\infty \frac{d\lambda}{\lambda^2} qE\lambda \coth qE\lambda e^{-M_a^2 \lambda} = i \lim_{\rho \rightarrow 0} \sum_a C_a \int_\rho^\infty e^{-M_a^2 s} + i \int_0^\infty \frac{ds}{s^2} e^{-m^2 s} [qE \cot qEs - 1] \quad (6.41)$$

and use the identifications (6.26), (6.28), and (6.29) to write the simplified form

$$1 - 2G\Pi_{ps}(k) = \frac{m_0}{m} + 4N_c N_f G i (k_0^2 - k_3^2) I(k) - 4GN_c N_f i k_1^2 I'(k), \quad (6.42)$$

which is valid for all  $qE$  for  $m_0 \neq 0$  and for  $qE < qE_c$  for  $m_0 = 0$ .

Let us examine the results that we obtain. Firstly, one finds that, as before, an explicit equation for  $m_\pi$  can be obtained, which is the generalized version of Eq. (4.21),

$$m_\pi^2 = \frac{m_0}{m(\mathcal{F})} \frac{1}{4GN_c N_f I(m_\pi^2)}, \quad (6.43)$$

given here for a pure electric or magnetic field, and is characterized by  $\mathcal{F}$ . Correspondingly, the coupling strength scales as

$$g_{\pi qq}^{-2} = -2iN_f N_c I(m_\pi^2). \quad (6.44)$$

In a fashion analogous to the arguments given in Sec. IV.A.3, the pion-decay strength  $f_\pi(\mathcal{F})$  may also be calculated in the presence of a field  $\mathcal{F}$ , and again one can directly confirm the Goldberger-Treiman relation  $f_\pi(\mathcal{F}) = g_{\pi qq}^{-1}(\mathcal{F})m(\mathcal{F})$  and the current-algebra result  $m_\pi^2(\mathcal{F})f_\pi^2(\mathcal{F}) = -m_0 \langle \bar{\psi}\psi \rangle$ , if one again assumes that  $I$  is slowly varying.

The scalar-meson mode can be treated in a fashion similar to that of the pseudoscalar mode; the mass of this mode is found to be

$$m_\sigma^2(\mathcal{F}) = -\frac{m_q}{m(\mathcal{F})} \frac{1}{4iGN_c N_f I(m_\sigma)} + 4m^2 \quad (6.45)$$

with coupling strength

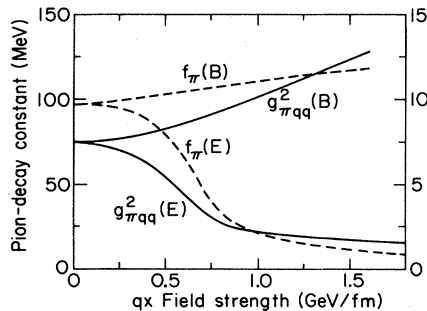


FIG. 22. Variation of the coupling constants  $g_{\pi qq}^2 \approx g_{\pi qq}^2$  (solid lines) and the pion-decay constant  $f_\pi$  (dashed lines) with applied field. The nature (electric or magnetic) of the field is indicated by the appropriate argument. The left-hand scale refers to  $f_\pi$ , whereas the right-hand scale refers to the coupling constants  $g_{\pi qq}^2$  (Klevansky, Jaenicke, and Lemmer, 1991).

$$g_{\sigma qq}^{-2} = -2N_c N_f i I(m_\sigma). \quad (6.46)$$

To the extent that the variation of  $I$  with four-momentum is unimportant,

$$g_{\sigma qq}^{-2} \approx g_{\pi qq}^{-2} \approx f_\pi^2(\mathcal{F})m^{-2}(\mathcal{F}), \quad (6.47)$$

and the scalar and pseudoscalar masses are connected by the relation

$$m_\sigma^2(\mathcal{F}) = 4m^2(\mathcal{F}) + m_\pi^2(\mathcal{F}). \quad (6.48)$$

In Fig. 22 we show the variation of the coupling constants as a function of the field strength, having set  $I(m_\pi) \approx I(m_\sigma) = I(0)$ . Since

$$I(0) = \frac{i}{(4\pi)^2} \left[ 2 \ln \left[ 1 + \frac{\Lambda^2}{m^2} \right] - \ln \left[ 1 + 2 \frac{\Lambda^2}{m^2} \right] \right], \quad (6.49)$$

one sees that the variation of the coupling strengths with external field is contained solely in the variation of the dynamical mass  $m = m(\mathcal{F})$ . This holds true also for the variation of  $f_\pi$ , which is also shown in this figure. In this section, all the calculations were performed with the choice  $m_0 = 5.2$  MeV for the current quark mass. The remaining parameters are the same as those used for Fig. 21.

The collective modes are shown in Fig. 23. At zero field, one has  $m_\sigma = 546$  MeV, while  $m_\pi = 135$  MeV for the parameters chosen. The important features that one observes from this calculation are (i) the slow variation of meson mass with magnetic field: one sees that the  $\pi$  meson hardly moves at all; and (ii) the behavior of the two modes, which in the electric case is complementary. The mass  $m_\sigma$  falls to a minimum before turning up to

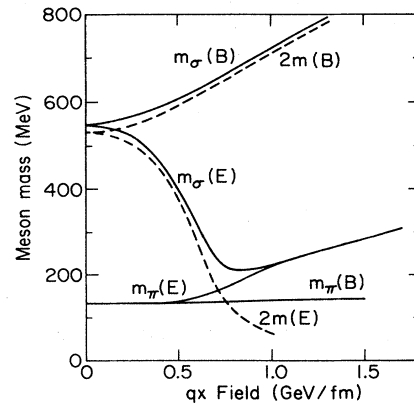


FIG. 23. Variation of  $m_\sigma$  and  $m_\pi$  as a function of the applied field (solid curve). The dashed curves illustrate the behavior of the pair-production threshold  $2m(\mathcal{F})$ . A small current quark mass,  $m_0 = 5.2$  MeV, has been assumed.

merge with  $m_\pi$  and appears as a common excitation of the vacuum in which chiral symmetry has been restored. The turning point of  $m_\sigma$  can be used to identify the critical-field strength  $\sim 0.8 \text{ GeV fm}^{-1}$  that always lies above the pair continuum threshold, so that this mode is unstable with respect to its decay into  $\bar{q}q$  pairs. By contrast, the pion is stable in the chirally asymmetric region, but is unstable in the chirally restored phase where its mass has moved into the pair continuum. It is also noteworthy that the features that are observed with regard to the inclusion of electric fields are common to the response of other external parameters in the NJL Lagrangian that tend to restore chiral symmetry. For example, a similar variation of meson masses and coupling constants was shown in Sec. V as temperature and/or baryon density was varied, the increase in either of which favors a chirally restored vacuum.

### 3. Polarizabilities

From Fig. 23, one sees that the collective modes have masses that vary quadratically with the applied field in the vicinity of the origin. One can thus introduce electric and magnetic polarizabilities  $\alpha$  and  $\beta$  according to the change in mass with field,

$$\Delta m_{\pi,\sigma} = -\frac{1}{2}\alpha_{\pi,\sigma}E^2 \text{ or } \frac{1}{2}\beta_{\pi,\sigma}B^2. \quad (6.50)$$

In addition,  $\alpha$  contains a classical contribution due to the acceleration of the charge (Ericson and Hüfner, 1973; Bernard and Vautherin, 1989), which we do not consider further here. Since the behavior of the meson masses with applied field is completely determined by the variation of the dynamically generated mass with  $\mathcal{F}$ , see Eqs. (6.43) and (6.48), one can give simple expressions for  $\alpha$  or  $\beta$  by expanding the right-hand member of the gap equation (6.25). One finds that  $m(\mathcal{F})$  varies as

$$m(\mathcal{F}) \simeq m(0) + \frac{\mathcal{F}}{8\pi^2 m(0)f_\pi^2} \sum_f q_f^2 \quad (6.51)$$

to first order in  $\mathcal{F}$ . Since  $m$  is solely a function of the Lorentz invariant  $\mathcal{F}$ , it follows that the electric and magnetic polarizabilities necessarily sum to zero,  $\alpha + \beta = 0$ . One can see this from Fig. 23, in the symmetric forked behavior of  $m_\sigma$  near the origin. The effect is too small to be seen for the  $\pi$  meson, with the graphical accuracy employed. Analytically, one deduces that

$$\begin{aligned} \alpha_\pi &= \frac{3}{16\pi^4 f_\pi^4 N_f} \sum_f q_f^2 m_\pi \left[ 1 - \frac{2\pi^2 f_\pi^2}{3m^2} \right] \\ &= \frac{5}{96} \frac{e^2 m_\pi}{\pi^4 f_\pi^4} \left[ 1 - \frac{2\pi^2 f_\pi^2}{3m^2} \right] \end{aligned} \quad (6.52)$$

for the  $\pi$  meson. Note that this vanishes in the chiral limit,  $\alpha = \beta = 0$ . The symbols  $m_\pi$  and  $f_\pi$  refer to the zero-field values. Since  $e^2/4\pi = 1/137$ , and the other quantities have been calculated previously, one can calculate the polarizability. Since we have assumed a common charge coupling for the quarks, the calculation thus far corresponds to that for the neutral pion. One finds

$$\alpha_{\pi_0} = -\beta_{\pi_0} \simeq 6 \times 10^{-5} \text{ fm}^3.$$

The polarizabilities for the charged pions have been calculated together with those of the neutral pion and the  $K$  mesons within the SU(3) NJL model in a perturbative approach (Bernard and Vautherin, 1989). These authors obtain the results listed in Table VI for the parameter sets (i)  $G\Lambda^2 = 2.35$ ,  $K\Lambda^5 = 27.83$  and (ii)  $G\Lambda^2 = 2.74$  and  $K\Lambda^5 = 43.29$ . In both cases, they set  $m_u = m_d \simeq 7 \text{ MeV}$  and  $m_s = 175 \text{ MeV}$ . Experimentally, the polarizability for charged pions is  $\alpha_{\pi^\pm} + \beta_{\pi^\pm} = (1.4 \pm 5.5) \times 10^{-4} \text{ fm}^3$  (Antipov *et al.*, 1985), while nothing is known about the polarizability of the neutral pions.

### 4. Electromagnetic form factor of the pion

The electromagnetic vertex function  $\Gamma_\mu(k, k')$  of the pion considered as a composite object is given by the sum of the diagrams shown in Fig. 24 (Brodsky and Primack, 1969), where the incoming and outgoing mesons are on-shell,  $k^2 = k'^2 = m_\pi^2$ .

One finds, after a short calculation, that

$$\Gamma_\mu(k', k) = -N_c N_f (q_i + q_j) g_{\pi qq}^2 I_\mu(k', k), \quad (6.53)$$

where

$$I_\mu(k', k) = \int \frac{d^4 p}{(2\pi)^4} \text{tr}[\gamma_5 iS(p + k') \gamma_\mu iS(p + k) \gamma_5 iS(p)], \quad (6.54)$$

and  $q_i + q_j$  makes up the charge on the pion. One can show that the on-shell version of  $I_\mu(k', k)$ , evaluated at  $k^2 = k'^2 = m_\pi^2$ , is given by

TABLE VI. Electromagnetic polarizabilities of the charged (neutral) particles in units of  $10^{-4}$  ( $10^{-5}$ )  $\text{fm}^3$  (Bernard and Vautherin, 1989).

	$\alpha_{\pi^\pm}$	$\beta_{\pi^\pm}$	$\alpha_{K^\pm}$	$\beta_{K^\pm}$	$\alpha_{\pi^0}$	$\beta_{\pi^0}$	$\alpha_{K^0}$	$\beta_{K^0}$
(i)	12.5	-11.8	3.88	-1.74	1.24	9.97	3.50	6.35
(ii)	10.5	-10.3	3.14	-2.45	2.30	1.93	3.42	0.14

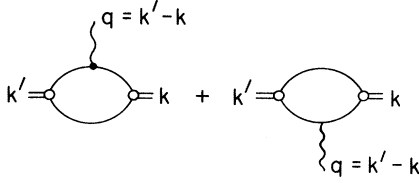


FIG. 24. Electromagnetic vertex function for the pion.

$$I_\mu(k', k) = 2 \left[ iI(0) - \frac{1}{(4\pi)^2} R(q^2) \right] (k_\mu + k'_\mu) \quad (6.55)$$

in the chiral limit, where  $m_\pi = 0$ . Here  $I(k^2)$  has been defined in Eq. (4.17) and

$$R(q^2) = \int_0^1 dx \int_0^1 dy \frac{\frac{1}{2} q^2 y^2}{m^2 - q^2 y^2 x(1-x)}. \quad (6.56)$$

Inserting  $g_{\pi qq}^{-2} = -2iN_c N_f I(0)$ , from Eq. (4.25), and Eq. (6.55) into Eq. (6.53), one finds

$$\Gamma_\mu(k', k) = (q_i + q_j) F_\pi(q^2) (k_\mu + k'_\mu) \quad (6.57)$$

where the form factor  $F_\pi(q^2)$  is given by

$$F_\pi(q^2) = 1 - \frac{1}{(4\pi)^2} R(q^2) / iI(0). \quad (6.58)$$

For small values of  $q^2$ ,  $R(q^2) \simeq \frac{1}{6} q^2 / m^2$ , so that

$$\begin{aligned} F_\pi(q^2) &\simeq 1 + \frac{1}{8\pi^2} \frac{q^2}{f_\pi^2} \\ &= 1 - \frac{1}{8\pi^2} \frac{Q^2}{f_\pi^2}, \end{aligned} \quad (6.59)$$

using Eq. (4.26).  $Q^2$  is spacelike. From the standard relation for the rms radius of a charged particle,

$$\langle r^2 \rangle = -6 \frac{dF(Q^2)}{dQ^2} \Big|_{Q^2=0}, \quad (6.60)$$

one identifies  $\langle r^2 \rangle = 3f_\pi^{-2} / 4\pi^2 = (0.58 \text{ fm})^2$  (Bernard and Meissner, 1988b; Bernard and Vautherin, 1989), which concurs with the result quoted by Tarrach (1979) from the direct photon-quark coupling in the soft-pion limit. This underestimates the experimental value of  $(0.66 \text{ fm})^2$ . An extension of this calculation in flavor SU(3) that includes  $\rho$ -meson intermediate states (Bernard and Meissner, 1988b) is required to bring this number to its experimental value. A plot of  $|F_\pi(Q^2)|^2$  that has been extended to include the coupling of the  $\rho$  meson as well is given in Fig. 25 for spacelike values of  $q^2 = -Q^2$ . The electromagnetic form factor of the kaon, including intermediate  $\omega$  and  $\phi$  states, is also given in this reference. Here the kaon radius  $\langle r_K^2 \rangle^{1/2} = 0.56 \text{ fm}$  is underestimated by four percent.

The reader is also referred to Lutz and Weise (1990) and Vogl and Weise (1991), who also calculate the form

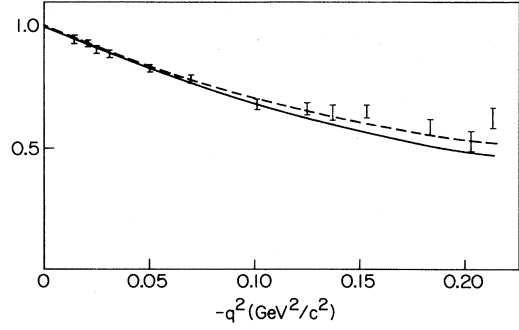


FIG. 25. Pion charge form factor  $|F_\pi(q^2)|^2$  in the spacelike region for  $-q^2 = Q^2 \leq 0.2 \text{ GeV}^2$ . The solid line is the NJL model calculation. The data are taken from Amendolia *et al.* (1984), Amendolia, Arik, *et al.* (1986), and Amendolia, Batignani, *et al.* (1986). The dashed line gives the best constrained fit of these authors, with  $\langle r_\pi^2 \rangle = 0.431 \text{ fm}^2$  (Bernard and Meissner, 1988b).

factors in an SU(3) flavor generalization of the NJL model.

## B. Chromoelectromagnetic fields

At this point, it is reasonable to ask if such strong electromagnetic fields could be so generated in heavy-ion collisions as to indicate the features observed in the previous section. To this end, it is instructive to make a simple model of two colliding ions, both, say, of radius  $R$ . Let us assume further that the distance of closest approach is limited by their radii, as is illustrated schematically in Fig. 26.

The electric field along the  $z$  axis, generated by this configuration, is

$$eE(z) = \frac{(2Z\alpha)z}{(R^2 + z^2)^{3/2}}, \quad (6.61)$$

which has its maximum value

$$eE_{\text{max}} = \frac{2Z\alpha}{R^2} \left[ \frac{2}{3^{3/2}} \right] \quad (6.62)$$

at  $z = R/\sqrt{2}$ . Here  $Z$  is the charge of each ion, and  $\alpha$  is the fine-structure constant  $\alpha \simeq 1/137$ . Assuming that  $R \simeq 1.2 A^{1/3} \text{ fm}$ , an estimate for  $eE_{\text{max}}$  for two uranium ions, for which  $Z = 92$ , gives  $eE = 0.003 \text{ GeV/fm}$ . This

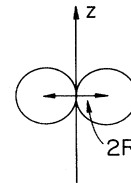


FIG. 26. Heavy ions, with centers separated by  $2R$ .

value is considerably less than the lowest possible critical strength  $qE_c \sim 0.55$  GeV/fm (see Fig. 21) that is obtained for the parameter set used, with zero current quark mass. The large value of the critical-field strength and the scale over which chiral symmetry is restored indicate that the phenomenon may well be relevant for gluonic systems. (An estimate given later on in this section indicates that a field strength  $\sim 5.3$  GeV/fm could be expected in the interior of a flux tube.) One could naively regard the U(1) field as an effective gluonic field, and the coupling constant  $q$  occurring in (6.1) as an effective flavor-independent color charge. It is of course more realistic to examine the case of coupling in an SU(3) gauge field to the NJL model, and this is discussed in what follows.

The generalization of Schwinger's arguments (Schwinger, 1951) for a U(1) background field to describe a constant or homogeneous background SU(3) color field has been investigated by Yildiz and Cox (1980) and Claudson, Yildiz, and Cox (1980). Their arguments have been expanded by Suganuma and Tatsumi (1990,1991) to investigate the couplings of such external fields into the SU(2) NJL Lagrangian. In this case, Eq. (6.1) is altered to read

$$\mathcal{L} = \bar{\psi}(i\mathcal{D} - m)\psi + G[(\bar{\psi}\psi)^2 + (\bar{\psi}i\gamma_5\tau\psi)^2] - \frac{1}{4}F_{\mu\nu}^a F_a^{\mu\nu} \quad (6.63)$$

with

$$F_a^{\mu\nu} = \partial^\mu A_a^\nu - \partial^\nu A_a^\mu - gf_{abc} A_b^\mu A_c^\nu \quad (6.64)$$

and

$$D^\mu = \partial^\mu + igA^\mu; \quad A^\mu = \frac{1}{2}\lambda^a A_\mu^a. \quad (6.65)$$

The dynamics of the gluon fields can now be disregarded, since the effects due to these are assumed to be already incorporated in the form of the four-fermion interaction of the NJL model. The presence of the gluon fields is

thought of solely as being due to the presence of a quark and antiquark placed at opposite ends of a flux tube. The condition of a constant background field,  $\partial_\mu F_{\pi\rho} = 0$ , is not gauge invariant; the condition

$$D_\mu^{ab} F_{\pi\rho}^b = 0 \quad (6.66)$$

that presumes that the field is covariantly constant is gauge invariant, however, and is used to define what is meant by “constant” or “homogeneous” field in this instance (Claudson, Yildiz, and Cox, 1980; Yildiz and Cox, 1980). By introducing a matrix notation  $(F_{\mu\nu})^{ab} = if^{acb} F_{\mu\nu}^c$ , this can be written in a matrix form

$$i[D_\mu, F_{\pi\rho}] = 0, \quad (6.67)$$

together with the relation  $[D_\mu, D_\nu] = -igF_{\mu\nu}$ , with the consequence that

$$[F_{\mu\nu}, F_{\pi\rho}] = 0. \quad (6.68)$$

This in turn has the consequence that  $F$  can be diagonalized as a Lorentz matrix, without problems due to the non-Abelian nature induced by color. As for the Maxwellian case given in Sec. VI.A,  $gF_\mu^\nu$  will again have two real and two imaginary eigenvalues (here for each color component),  $\pm gF'$  and  $\pm igF''$  where  $F'$  and  $F''$  are the same as those given for the Maxwellian field by Eq. (F5). As usual,  $\mathcal{F} = -\frac{1}{2}(E^2 - B^2)$  and  $\mathcal{G} = \mathbf{B} \cdot \mathbf{E}$ , with  $E_i = F^{0i}$  and  $B_i = \frac{1}{2}\epsilon_{ijk} F^{jk}$ . This formal similarity of the solution to the SU(3) background field problem with the Maxwellian constant field problem has the consequence that the equations arising in the SU(3) case bear formal similarity to that case with only minor differences (Claudson *et al.*, 1980): in SU(3), the trace over color does not appear trivially, and the fields naturally refer to the combinations  $\mathbf{E} = \mathbf{E}_a \lambda^a/2$ ,  $\mathbf{B} = \mathbf{B}_a \lambda^a/2$ . In particular, the self-energy is given, as before, by Eq. (6.3), and the gap equation is given as (Suganuma and Tatsumi, 1991)

$$m = m_0 + \frac{N_f G}{2\pi^2} m \text{tr}_c \int_{1/\Lambda^2}^\infty \frac{ds}{s^2} e^{-m^2 s} (gF's) \cot(gF's) (gF''s) \coth(gF''s), \quad (6.69)$$

in direct analogy with (6.24). Here  $\text{tr}_c$  refers to a trace over color alone, and a lower limit cutoff on the proper-time integral has been introduced, as has been presented by these authors. Following their treatment, we specialize to the case of a constant  $E$  field only, considered in a flux-tube model. It is useful to label the chargeless gauge fields  $A_3^\mu = \mathcal{A}^\mu$  and  $A_8^\mu = \mathcal{B}^\mu$ . These have associated with them a color isotopic charge  $Q_{\mathcal{A}}$  and a color hypercharge  $Q_{\mathcal{B}}$ , respectively (see, for example, Huang, 1982), which are listed in Table VII.

Since the external field is homogeneous, it may be expressed solely in terms of fields due to  $\mathcal{A}^\mu$  and  $\mathcal{B}^\mu$ ,

$$E = E_{\mathcal{A}} \lambda_3/2 + E_{\mathcal{B}} \lambda_8/2. \quad (6.70)$$

To obtain  $E_{\mathcal{A}}$  and  $E_{\mathcal{B}}$ , one can apply Gauss's law independently to each of these charges, so that

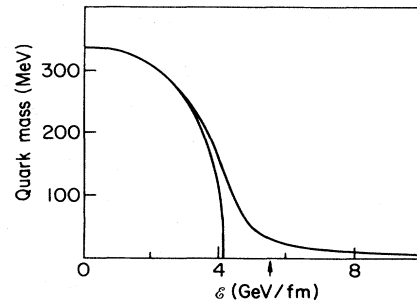


FIG. 27. Dynamical quark mass  $m$  as a function of  $\mathcal{E} = g^2/\sigma$ . The value of  $\mathcal{E}$  expected in a mesonic system is indicated by the arrow (Suganuma and Tatsumi, 1990).

$Q_{\mathcal{A}} = E_{\mathcal{A}} \sigma$ ,  $Q_{\mathcal{B}} = E_{\mathcal{B}} \sigma$ , where  $\sigma$  is the cross section of the flux tube. One has, for example, from (6.70) for the choice  $R\bar{R}$ ,

$$E = \begin{pmatrix} \frac{1}{3} & 0 & 0 \\ 0 & -\frac{1}{6} & 0 \\ 0 & 0 & -\frac{1}{6} \end{pmatrix} \frac{g}{\sigma}, \quad (6.71)$$

and the Dyson equation, on explicitly performing the color trace, becomes

$$m = m_0 + m \frac{GN_f}{2\pi^2} N_c \int_{1/\Lambda^2}^{\infty} \frac{ds}{s^2} + m \frac{GN_f}{2\pi^2} \left\{ \int_0^{\infty} \frac{ds}{s^2} e^{-sm^2} \left[ \left[ \frac{\mathcal{E}}{3} s \right] \cot \left[ \frac{\mathcal{E}}{3} s \right] - 1 \right] + 2 \int_0^{\infty} \frac{ds}{s^2} e^{-sm^2} \left[ \left[ \frac{\mathcal{E}}{6} s \right] \cot \left[ \frac{\mathcal{E}}{6} s \right] - 1 \right] \right\}, \quad (6.72)$$

where  $\mathcal{E} = g^2/\sigma$ , to be compared with Eq. (6.25) for an electric field. This result holds for any color configuration. The solution to (6.72) for the dynamical quark mass is given in Fig. 27 and indicates that a critical strength for the restoration of chiral symmetry is  $\mathcal{E}_c \simeq 4$  GeV/fm, a value that lies somewhat higher than that for the U(1) case. These authors use the parameter set  $G = 0.21 \text{ fm}^2$ ,  $\Lambda = 950 \text{ MeV}$ , and  $m_0 = 5.5 \text{ MeV}$  or  $m_0 = 0$  in the chiral limit.

Suganuma and Tatsumi (1990) estimate the physical value of  $\mathcal{E}$  in a flux tube due to a quark and antiquark pair by considering the total energy per unit length,

$$k = \frac{1}{2}(E_{\mathcal{A}}^2 + E_{\mathcal{B}}^2)\sigma = \frac{1}{2\sigma}(Q_{\mathcal{A}}^2 + Q_{\mathcal{B}}^2) = \frac{g^2}{6\sigma}.$$

Here, a volume energy has not been considered (see, for example, Low, 1975). Using a value  $k = 0.177 \text{ GeV}^2$  from Casher *et al.* (1979), one has

$$\mathcal{E} = \frac{g^2}{\sigma} \simeq 5.3 \text{ GeV/fm} > \mathcal{E}_c.$$

This indicates that chiral symmetry should be restored in the interior of mesons, and thereby provides support for the chiral bag model picture.

## VII. BOSONIZATION

Up until this point, the NJL Lagrangian has been considered in its original form, which considers quark degrees of freedom and their interactions that are determined to be consistent with the symmetries of QCD. One may, however, attempt to parallel some of the developments made in the understanding of QCD. In particular, the work of 't Hooft (1974) showed that in the limit of a large number of colors, QCD can be regarded as an effective theory of mesons and glueballs. Subsequently, it was shown (Witten, 1979, 1983) that the baryons could be viewed as the solitons of the meson theory. One thus arrives at the question, what effective meson theory does the NJL Lagrangian approximately represent? Mesonic

TABLE VII. Color isotopic charge and color hypercharge  $Q_{\mathcal{A}}$  and  $Q_{\mathcal{B}}$  for quarks, given in units of the coupling strength  $g$ .

	$Q_{\mathcal{A}}$	$Q_{\mathcal{B}}$
Red	1/2	$1/2\sqrt{3}$
Blue	-1/2	$1/2\sqrt{3}$
Green	0	$-1/\sqrt{3}$

theories of different natures have been well studied over the past few decades. These include, for example, the linear and nonlinear sigma models of chiral symmetry breaking (see, for example, Lee, 1981 and Pokorski, 1989), the Skyrme model (Skyrme, 1961), and the Walecka model (Serot and Walecka, 1986), all of which have enjoyed considerable success since their inception.

At this stage, it should be clearly stated that all the models in question suffer from a common flaw: all are simply models, none of which have been derived from QCD, and the parentage of any one of them has not been rigorously established. It is of course highly desirable to do so. In this regard, the bosonization of QCD *per se* is required to arbitrate between models, and some steps toward performing this difficult task have already been taken (Reinhardt, 1991).<sup>3</sup> In this section, however, we shall deal solely with bosonization of the NJL model. This should then reveal the nature of the effective meson theory. More importantly, however, since bosonization is generally introduced via the Feynman path-integral formalism, one can attempt to make contact with the renormalization constants of chiral perturbation theory (Gasser and Leutwyler, 1984, 1985, 1987). Since these constants are determined from experiment, this gives some criterion as to the validity of the model, and it is with this in mind that this section is written. We stress that the bosonized (or effective) NJL Lagrangian must also, as a model of chiral symmetry, necessarily allow for the current-algebra results to be fulfilled. We do not repeat these standard arguments here in this framework, but refer the reader to papers in this field (see, for example, Ebert and Reinhardt, 1986 and Volkov, 1984, 1986).

To date, bosonization of the original (flavor) U(1) form of the NJL Lagrangian has been undertaken by Eguchi and Sugawara (1974) and Kikkawa (1974). The non-Abelian U( $N_f$ ) form has been discussed by Chakrabarti

<sup>3</sup>An approach relating the results of the NJL model to those from QCD sum rules can be found in Adami and Brown (1990).



and Hu (1976), and in particular, the SU(2) version has received attention from Ebert and Volkov (1984,1986) and Ebert and Reinhardt (1986). Unfortunately, no direct bosonization of an SU(3) Lagrangian that includes a 't Hooft term, as indicated in Eq. (2.9), exists in the literature, although some authors (see, for example, Volkov, 1984) account for the nonappearance of the  $U_A(1)$  symmetry by hand at a later stage. We deal therefore with the SU(2) situation in detail and discuss the U(3) version only briefly, suggesting appropriate literature.

Historically, the procedure of bosonization was first developed by Eguchi and Sugawara (1974), who extended the BCS model of superconductivity, which has been applied to elementary particles in the NJL model, to spatially inhomogeneous systems. They present a field-theoretical model that is based on an analogy with the Ginzburg-Landau theory of superconductivity. (Ginzburg and Landau, 1950) that generalizes the BCS theory to describe spatially inhomogeneous systems such as type-II superconductors or superconductors with magnetic impurities. In the field-theoretical analog, Eguchi and Sugawara describe mesons as extended objects by identifying inhomogeneous (but local) terms occurring in the self-energy as the mesonic fields. The resulting equations of motion derived for the fields bear strong resemblance to the Ginzburg-Landau equation of superconductivity: their derivation is performed in analogy with Gor'kov's derivation from the microscopic theory of superconductivity (Gor'kov, 1959; see also Fetter and Walecka, 1971). From the equations of motion that are obtained for the fields, an effective Lagrangian for the meson fields may be inferred, thus completing the bosonization procedure. We comment that this method is also used by Chakrabarti and Hu (1976).

An alternative approach of reformulating bosonization in terms of the Feynman path-integral method was first introduced by Kikkawa (1976) and taken over by subsequent authors. Today, this enjoys the most popularity, as it is easier to handle systematically, although the Ginzburg-Landau-like derivation, like the Bogoliubov-Valatin transformation, offers a simple intuitive and physical insight. In what follows, we shall briefly discuss

the Ginzburg-Landau approach, using, however, a simple Lagrangian in order to emphasize the methods and not to generate long equations. We then discuss the SU(2) model via the path-integral formalism and comment on the further development in the U(3) model.

### A. Ginzburg-Landau description for quarks

We return again to the two-flavor model Lagrangian given by Eq. (2.7),

$$\mathcal{L} = \bar{\psi} i \not{\partial} \psi + G [(\bar{\psi} \psi)^2 + (\bar{\psi} i \gamma_5 \tau \psi)^2] . \quad (7.1)$$

Following the method of Eguchi and Sugawara (1974), we go beyond the Hartree approximation in assuming that the self-energy is inhomogeneous, but local. That is, the Green's function satisfies the equation

$$[i \not{\partial}_x - m(x)] S(x, y) = \delta^{(4)}(x - y) . \quad (7.2)$$

The Green's function for an infinite system in the Hartree approximation is denoted as  $S_0(x, y)$  and satisfies, as before,

$$[i \not{\partial}_x - m^*] S_0(x, y) = \delta^{(4)}(x - y) . \quad (7.3)$$

Note that  $S_0(x, y) = S_0(x - y)$ , but that this is not true of  $S(x, y)$ . The lowest-order term in the calculation of the self-energy is given as

$$m(x) = 2Gi [\text{Tr} S(x, x) + i \gamma_5 \tau \cdot \text{Tr} \tau (i \gamma_5) S(x, x)] , \quad (7.4)$$

where the second term need no longer vanish. Upon introducing the abbreviations

$$m_s(x) = 2Gi \text{Tr} S(x, x) , \quad (7.5)$$

$$m_{ps}(x) = 2Gi \text{Tr} \tau (i \gamma_5) S(x, x) ,$$

one may write

$$m(x) = m_s(x) + i \gamma_5 \tau \cdot m_{ps} \quad (7.6)$$

for the effective quark mass in Eq. (7.2). A formal solution to Eq. (7.5) can be obtained by expanding the full propagator about  $S_0(x, y)$ , i.e.,

$$S(x, y) = S_0(x, x) + \int d^4 x' S_0(x, x') \delta m(x') S_0(x', y) + \int d^4 x' \int d^4 x'' S_0(x, x') \delta m(x') S_0(x', x'') \delta m(x'') S_0(x'', y) + \dots , \quad (7.7)$$

where  $m(x) = m^* + \delta m(x)$ . Seen in diagrams, this series represents the sum shown in Fig. 28.

The series that occurs in Eq. (7.7) can be evaluated in the limit of large  $\Lambda$ , where terms up to order  $\log \Lambda$  only are retained. One sees that the tadpole (or second) term in the expansion for  $m_s(x)$  can be written as

$$m_s^{(1)} = 2iG \int d^4 x' \delta m_s(x') \frac{1}{i} \Pi_s(x', x) , \quad (7.8)$$

with  $\delta m_s(x) = m_s(x) - m^*$ , since the pseudoscalar part of  $\delta m(x)$  does not contribute in building the trace.  $\Pi_s$  is

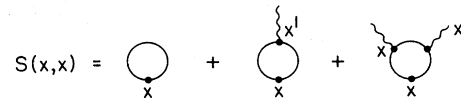


FIG. 28. Diagrammatic representation of the expansion of the single-particle propagator. The continuous lines represent quark propagators, while the wavy lines refer to the scalar or pseudoscalar fields.

the scalar polarization, which is given in Eq. (4.27). For zero current quark mass, this is

$$2G\Pi_s(k^2) = 1 - 4iGN_cN_f(k^2 - 4m^{*2})I(k^2). \quad (7.9)$$

The leading log expansion is given by evaluating the function  $I$  at the value  $k^2=0$  [see Eqs. (3.36) and (3.40)]. This is consistent with our earlier assumption that  $I(k^2)$  is slowly varying. Inserting this into Eq. (7.8), one ob-

tains the Fourier transform

$$m_s^{(1)}(k) = \delta m_s(k) - 4N_cN_f iI(0)\delta m_s(k)[k^2 - 4m^{*2}] \quad (7.10)$$

for this contribution to  $m_s(x)$ . The following terms in the expansion for  $m_s(x)$  are best evaluated directly in momentum space. The next term is given as

$$m_s^{(2)}(k) = 2iG \text{Tr} \int \frac{d^4p}{(2\pi)^4} \int \frac{d^4q}{(2\pi)^4} S_0(p)\delta m(q)S_0(p-q)\delta m(k-q)S_0(p-k). \quad (7.11)$$

In order to calculate terms to leading order in  $\log\Lambda$ , we immediately evaluate the propagator  $S_0$  everywhere at the argument  $p$ , so that one has

$$m_s^{(2)}(k) \simeq 2iG \text{Tr} \int \frac{d^4p}{(2\pi)^4} \int \frac{d^4q}{(2\pi)^4} \frac{1}{(p^2 - m^{*2})^3} (\not{p} + m^*) [\delta m_s(q) + i\gamma_5 \mathbf{m}_s(q) \cdot \boldsymbol{\tau}] \\ \times (\not{p} + m^*) [\delta m_s(k-q) + i\gamma_5 \mathbf{m}_s(k-q) \cdot \boldsymbol{\tau}] (\not{p} + m^*), \quad (7.12)$$

which, upon performing the trace, simplifies to

$$m_s^{(2)}(k) = 2iG \int \frac{d^4p}{(2\pi)^4} \int \frac{d^4q}{(2\pi)^4} 4N_cN_f [(3m^{*2}p^2 + m^{*3})\delta m_s(q)\delta m_s(k-q) \\ + (m^{*2}p^2 - m^{*3})\mathbf{m}_{ps}(q) \cdot \mathbf{m}_{ps}(k-q)] \frac{1}{(p^2 - m^{*2})^3}. \quad (7.13)$$

Again, since only leading terms in the expansion are to be considered, convergent terms may be discarded. Furthermore, by writing

$$\int \frac{d^4p}{(2\pi)^4} \frac{p^2}{(p^2 - m^{*2})^3} = \int \frac{d^4p}{(2\pi)^4} \left[ \frac{1}{(p^2 - m^{*2})^2} + \frac{m^{*2}}{(p^2 - m^{*2})^3} \right], \quad (7.14)$$

one may neglect the second term in leading order and write

$$\int \frac{d^4p}{(2\pi)^4} \frac{p^2}{(p^2 - m^{*2})^3} \simeq I(0), \quad (7.15)$$

with the consequence that

$$m_s^{(2)}(k) = 8iGN_cN_f I(0)m^* \int \frac{d^4q}{(2\pi)^4} [3\delta m_s(q)\delta m_s(k-q) + \mathbf{m}_{ps}(q) \cdot \mathbf{m}_{ps}(k-q)]. \quad (7.16)$$

The third divergent term in the expansion for  $S$  can be evaluated analogously. One has, to leading order,

$$m_s^{(3)}(k) = 2iG4N_cN_f \int \frac{d^4p}{(2\pi)^4} \int \frac{d^4q}{(2\pi)^4} \int \frac{d^4q'}{(2\pi)^4} \frac{p^4}{(p^2 - m^{*2})^4} \\ \times [\delta m_s(q)\delta m_s(q')\delta m_s(k-q'-q) + \mathbf{m}_{ps}(q)\delta m_s(q')\delta m_s(k-q'-q) \\ + \mathbf{m}_{ps}(q) \cdot \mathbf{m}_{ps}(q')\delta m_s(k-q'-q)]. \quad (7.17)$$

Decomposing

$$p^4/(p^2 - m^{*2})^4 = 1/(p^2 - m^{*2})^2 + 2m^{*2}/(p^2 - m^{*2})^3 + m^4/(p^2 - m^{*2})^4$$

and again discarding the last two terms, which when integrated over are convergent, one has

$$m_s^{(3)}(k) = 8iGN_cN_f I(0) \int \frac{d^4q}{(2\pi)^4} \int \frac{d^4q'}{(2\pi)^4} [\delta m_s(q)\delta m_s(q')\delta m_s(k-q'-q) + \mathbf{m}_{ps}(q) \cdot \mathbf{m}_{ps}(q')\delta m_s(k-q'-q)]. \quad (7.18)$$

The  $x$ -space representation of the terms in the expansion for  $S(x, x')$  are now obtained upon Fourier-transforming the results of Eqs. (7.10), (7.16), and (7.18). The corresponding three terms that make up  $m_s(x)$  from Eq. (7.5) are

$$\begin{aligned}
m_s^{(1)}(x) &= \delta m_s(x) + 4GN_c N_f I(0)(\partial^\mu \partial_\mu + 4m^{*2})\delta m_s(x), \\
m_s^{(2)}(x) &= 8iGN_c N_f I(0)m^{*2}[3(\delta m_s(x))^2 + \mathbf{m}_{ps}(x) \cdot \mathbf{m}_{ps}(x)], \\
m_s^{(3)}(x) &= 8iGN_c N_f I(0)[(\delta m_s(x))^3 + \mathbf{m}_{ps}(x) \cdot \mathbf{m}_{ps}(x)\delta m_s(x)],
\end{aligned} \tag{7.19}$$

which can be combined with the first term that occurs from the expansion (7.7) for  $S$  to give the equation of motion for the scalar field that reads

$$(\partial_\mu \partial^\mu - 2m^{*2})m_s(x) + 2m_s(x)\mathbf{m}_{ps}(x) \cdot \mathbf{m}_{ps}^*(x) + 2m_s^3(x) = 0, \tag{7.20}$$

on replacing  $\delta m_s(x)$  by  $m_s(x) - m^*$ . Analogously, the equation of motion for the pseudoscalar field is

$$(\partial_\mu \partial^\mu - 2m^{*2})\mathbf{m}_{ps}(x) + 2m_s^2(x)\mathbf{m}_{ps} + 2(\mathbf{m}_{ps} \cdot \mathbf{m}_{ps})\mathbf{m}_{ps} = 0. \tag{7.21}$$

Using the fact that  $g_{\sigma qq} \simeq g_{\pi qq}$ , we scale  $m_s = g_{\sigma qq}\sigma$  and  $\mathbf{m}_\pi = g_{\sigma qq}\boldsymbol{\pi}$  to find that the set of coupled equations (7.20) and (7.21) can be summarized in the form

$$\partial_\mu \partial^\mu \Psi - 2m^* \Psi + 2g_{\sigma qq}^2 |\Psi|^2 \Psi = 0, \tag{7.22}$$

where the complex field  $\Psi$  is defined as  $\Psi = \sigma + i\gamma_5 \boldsymbol{\tau} \cdot \boldsymbol{\pi}$ . For a static field  $\Psi$ , Eq. (7.22) has precisely the form of the Ginzburg–Landau equation (Ginzburg and Landau, 1950; see also Fetter and Walecka, 1971). This again leads to the physical interpretation of mesonic states as particle-antiparticle pairs that are correlated over a finite region in space. Furthermore, one can describe this theory of mesons by constructing a Lagrangian that would give rise to the above equations of motion. In this case,

$$\mathcal{L} = \frac{1}{2}\partial_\mu \sigma \partial^\mu \sigma + \frac{1}{2}\partial_\mu \boldsymbol{\pi} \partial^\mu \boldsymbol{\pi} - \frac{1}{2}g_{\sigma qq}^2 (\sigma^2 + \boldsymbol{\pi}^2 - \sigma_0^2)^2, \tag{7.23}$$

with  $m^* = g_{\sigma qq}\sigma_0$  sufficing.

For completeness, we comment that in the work of Eguchi and Sugawara (1974), a U(1)-invariant NJL Lagrangian that includes both vector and axial-vector terms is included,

$$\begin{aligned}
\mathcal{L} &= \bar{\psi} i \not{\partial} \psi + G[(\bar{\psi} \psi)^2 + (\bar{\psi} i \gamma_5 \psi)^2] \\
&\quad - G'[(\bar{\psi} \gamma_\mu \psi)^2 + (\bar{\psi} \gamma_5 \gamma_\mu \psi)^2].
\end{aligned} \tag{7.24}$$

This has the consequence that the breakdown of the self-energy into meson fields includes vector and axial-vector fields; here, one has

$$m(x) = m_s(x) + i\gamma_5 m_p(x) + \gamma^\mu m_\mu^V(x) + \gamma_5 \gamma^\mu m_\mu^A(x). \tag{7.25}$$

Clearly, equations of motion for  $m^V(x)$  and  $m^A(x)$  can be derived in the same fashion as that for the scalar and pseudoscalar fields, and the corresponding Lagrangian can be inferred. We only quote the final result,

$$\begin{aligned}
L(x) &= |[\partial_\mu + 2im_\mu^A(x)]\Psi|^2 - \frac{1}{3}F_{\mu\nu}(x)F^{\mu\nu}(x) \\
&\quad + \frac{2G}{3(4G' - G)L'} m_\mu^A(x)^2 \\
&\quad + 2m^* |\Psi(x)|^2 - |\Psi(x)|^4,
\end{aligned} \tag{7.26}$$

with  $F_{\mu\nu} = \partial_\mu m_\nu^A - \partial_\nu m_\mu^A$ . A feature of this calculation is that the axial field couples in as an external field would do. In this case, however, it is not an external field, but describes the collective excitations of the quasiparticle pairs just as the scalar and pseudoscalar fields do. This constitutes a major difference between the derivation of the superconducting Ginzburg–Landau equation and that for a theory of mesons, since in the former case, the term containing  $F_{\mu\nu}$  would represent the inclusion of an external electromagnetic field.

## B. Path-integral formulation in flavor SU(2) and the derivative expansion

Starting with the SU(2) NJL Lagrange density of Eq. (2.7) for massless quarks,

$$\mathcal{L} = \bar{\psi} i \not{\partial} \psi + G[(\bar{\psi} \psi)^2 + (\bar{\psi} i \gamma_5 \boldsymbol{\tau} \psi)^2], \tag{7.27}$$

one may introduce the generating functional

$$\begin{aligned}
Z[\eta, \bar{\eta}] &= \frac{1}{N} \int \mathcal{D}\psi \int \mathcal{D}\bar{\psi} \exp \left\{ i \int d^4x [\mathcal{L}(\bar{\psi}, \psi) \right. \\
&\quad \left. + \bar{\psi} \eta + \bar{\eta} \psi] \right\},
\end{aligned} \tag{7.28}$$

where  $\mathcal{D}\psi$ ,  $\mathcal{D}\bar{\psi}$  are the fermion functional measures, and  $\bar{\eta}$  and  $\eta$  are fermion and antifermion sources, respectively. As is well known, the path integral of Gaussian functions can be performed exactly,

$$\begin{aligned}
\int \mathcal{D}\Phi \exp \left[ i \int d^4x (\pm A \Phi - B \Phi^2) \right] \\
= \frac{1}{N'} \exp \left[ i \int d^4x A^2 / 4B \right].
\end{aligned} \tag{7.29}$$

$N'$  is an (infinite) normalization constant that need not be known explicitly. In particular, introducing a single scalar field  $\sigma$  and triplet of pseudoscalar fields  $\boldsymbol{\pi}$ , according to

$$\begin{aligned} \frac{1}{N'} \exp \left[ i \int d^4x G (\bar{\psi}\psi)^2 \right] &= \int \mathcal{D}\sigma \exp \left[ i \int d^4x \left[ -(\bar{\psi}\psi)\sigma - \frac{1}{4G} \sigma^2 \right] \right] \\ \frac{1}{N'} \exp \left[ i \int d^4x G (\bar{\psi}i\gamma_5\tau\psi)^2 \right] &= \int \mathcal{D}\pi \exp \left[ i \int d^4x \left[ -(\bar{\psi}i\gamma_5\tau\pi) - \frac{1}{4G} \pi^2 \right] \right], \end{aligned} \quad (7.30)$$

one may write

$$Z[\eta, \bar{\eta}] = \frac{1}{N} \int \mathcal{D}\psi \mathcal{D}\bar{\psi} \mathcal{D}\sigma \mathcal{D}\pi \exp \left[ i \int d^4x \left[ \bar{\psi} [i\partial - (\sigma + i\gamma_5\tau\pi)] \psi - \frac{1}{4G} (\sigma^2 + \pi^2) + \bar{\psi}\eta + \bar{\eta}\psi \right] \right]. \quad (7.31)$$

Defining

$$\{i\partial - (\sigma + i\gamma_5\tau\pi)\} \delta^{(4)}(x-y) = S^{-1}(x,y)$$

as the inverse fermion propagator, one may decompose the functional into fermionic and bosonic sectors,

$$Z[\eta, \bar{\eta}] = \int \mathcal{D}\sigma \mathcal{D}\pi \exp \left[ i \int d^4x \left[ -\frac{1}{4G} (\sigma^2 + \pi^2) \right] \right] Z_f[\eta, \bar{\eta}], \quad (7.32)$$

with the fermionic sector described by

$$Z_f[\eta, \bar{\eta}] = \int \mathcal{D}\psi \mathcal{D}\bar{\psi} \exp \left[ i \int d^4x \left[ \int d^4y \bar{\psi}(x) S^{-1}(x,y) \psi(y) + \bar{\psi}(x) \eta + \bar{\eta} \psi(x) \right] \right], \quad (7.33)$$

which, when integrated out, gives

$$Z_f[\eta, \bar{\eta}] = \exp(-i \text{Tr} \log S^{-1}|_{y=x}) \exp \left[ -i \int d^4x \int d^4y \bar{\eta}(x) S(x,y) \eta(y) \right]. \quad (7.34)$$

We recall at this point that the symbol  $\text{Tr}$  has been reserved to describe the trace over color, flavor, and spinor indices. In keeping with the standard literature, we introduce the functional trace, which we denote  $\tilde{\text{Tr}}$ ,

$$\tilde{\text{Tr}} \hat{\mathcal{O}} = \text{Tr} \int d^4x \langle x | \hat{\mathcal{O}} | x \rangle, \quad (7.35)$$

where  $\hat{\mathcal{O}}$  is any operator. Then, with  $S(x,y)$  written as

$$S(x,y) = [i\partial - (\sigma + i\gamma_5\tau\pi)]^{-1} \delta^{(4)}(x-y), \quad (7.36)$$

the generating functional can be written as

$$\begin{aligned} Z[\eta, \bar{\eta}] &= \int \mathcal{D}\sigma \mathcal{D}\pi \exp \left[ i\mathcal{S} + \int d^4x \bar{\eta} \frac{1}{i\partial - (\sigma + i\tau\pi)} \eta \right], \\ &\quad (7.37) \end{aligned}$$

where the action  $\mathcal{S}$  is

$$\mathcal{S} = \int d^4x \left[ -\frac{1}{4G} (\sigma^2 + \pi^2) \right] - i \tilde{\text{Tr}} \log [i\partial - (\sigma + i\tau\pi)]. \quad (7.38)$$

We note that the fields  $\sigma$  and  $\pi$  may be scaled by a coupling strength  $g_0$ , i.e.,  $\sigma, \pi \rightarrow g_0(\sigma, \pi)$ , so that one has

$$\begin{aligned} \mathcal{S} &= \int d^4x \left[ -\frac{1}{2} \delta\mu_0^2 (\sigma^2 + \pi^2) \right] \\ &\quad - i \tilde{\text{Tr}} \log [i\partial - g_0(\sigma + i\tau\pi)], \end{aligned} \quad (7.39)$$

with  $\delta\mu_0 = g_0^2/2G$ . Assuming that only  $\sigma$  has a nonvanishing vacuum expectation value  $v_0$ , we write

$$\sigma = s + v_0; \quad (7.40)$$

varying  $\delta\mathcal{S}/\delta\phi = 0$ ,

$$\phi = \{ \langle \sigma \rangle = v_0, \langle \pi \rangle = 0 \},$$

one recovers the gap equation

$$m^* = 2iG \tilde{\text{Tr}} \frac{1}{i\partial - m^*} \quad (7.41)$$

with  $m^* = g_0 v_0$ , written here in terms of the functional trace. This result can be compared with the Hartree limit of Eq. (2.31), after recognizing that the functional trace is invariant under a change of basis.

Our major interest here, however, is in deriving an effective local action for the mesonic degrees of freedom. Equation (7.39) contains, however, the highly nonlocal term due to the fermionic determinant. For the above purpose, it is desirable to localize it in a systematic fashion. One such procedure is to deal with this term in a derivative expansion of the fields. Now, since the parts of the action that are free of boson fields only contribute to the normalization of the generating functional, the essential piece of the action due to the nonlocal fermionic determinant term, from Eq. (7.39), is given as

$$S_{\text{fd}} = -i \text{Tr} \log \left[ 1 - \frac{1}{i\partial - m^*} g_0 (s + i\gamma_5 \tau \cdot \pi) \right] \\ = \sum_{n=1}^{\infty} U^{(n)}, \quad (7.42)$$

subdivided into both divergent and convergent pieces in the manner that will be illustrated explicitly in the derivative expansion for the scalar field. Consider, for example,  $n=2$ . The scalar contribution to  $U^{(2)}$  is

where

$$U^{(n)} = \frac{i}{n} \text{Tr} \left[ \frac{1}{i\partial - m^*} g_0 (s + i\gamma_5 \tau \cdot \pi) \right]^n. \quad (7.43)$$

$$U_s^{(2)} = g_0^2 \frac{i}{2} \text{Tr} \int \frac{d^4 p}{(2\pi)^4} \left\langle p \left| \frac{1}{i\partial - m^*} s \frac{1}{i\partial - m^*} s \right| p \right\rangle, \quad (7.44)$$

One notes that  $U^{(n)}, n \geq 5$ , are convergent integrals, while  $U^{(n)}, n=1 \dots 4$ , diverge. These divergent terms are now

which, on introducing appropriate intermediate states, leads to the result

$$U_s^{(2)} = 4g_0^2 i N_c \int \frac{d^4 p}{(2\pi)^4} \int \frac{d^4 p'}{(2\pi)^4} \int d^4 x \int d^4 y e^{i(p-p')(x-y)} \frac{[p \cdot p' + m^{*2}]}{(p^2 - m^{*2})(p'^2 - m^{*2})} s(x) s(y). \quad (7.45)$$

It is convenient to move to Euclidean space for intermediate calculations:  $p \rightarrow p_E$ ,  $x \rightarrow x_E$ , and dropping the subscript, one has

$$U_s^{(2)} = 4i N_c g_0^2 \int \frac{d^4 p}{(2\pi)^4} \int \frac{d^4 p'}{(2\pi)^4} \int d^4 x \int d^4 y e^{-i(p-p')(x-y)} \frac{[-p \cdot p' + m^{*2}]}{(p^2 + m^{*2})(p'^2 + m^{*2})} s(x) s(y). \quad (7.46)$$

One now makes a local expansion in the field

$$s(y) \simeq s(x) + (y-x)_\mu \partial_\mu s(x) + \frac{1}{2} (y-x)_\mu (y-x)_\nu \partial_\mu \partial_\nu s(x) + \dots \quad (7.47)$$

The first term of the series can be simply evaluated and reduced to the (Minkowski) space form,

$$\text{Term}(1) = (g_0^2 I_2 - 2m^{*2} g_0^2 I_0) \int d^4 x s^2(x), \quad (7.48)$$

where

$$I_2 = 4N_c i \int \frac{d^4 p}{(2\pi)^4} \frac{1}{p^2 - m^{*2}} \quad (7.49)$$

and

$$I_0 = -4N_c i \int \frac{d^4 p}{(2\pi)^4} \frac{1}{(p^2 - m^{*2})^2}. \quad (7.50)$$

The second term of the expansion can be shown to vanish. The third term in the series, in which two spatial derivatives of the field occur, is

$$\text{Term}(3) = 2N_c g_0^2 i \int \frac{d^4 p}{(2\pi)^4} \int \frac{d^4 p'}{(2\pi)^4} \int d^4 x (s \partial_\mu \partial_\nu s) \int d^4 z e^{i(p-p')z} z_\mu z_\nu \frac{1}{p^2 + m^{*2}} \frac{-p \cdot p' + m^{*2}}{p'^2 + m^{*2}}. \quad (7.51)$$

Noting that

$$\exp[i(p-p')z] z_\mu = i \partial_\mu^{p'} \exp[i(p-p')z],$$

one has

$$\text{Term}(3) = -2N_c g_0^2 i \int \frac{d^4 p}{(2\pi)^4} \frac{1}{p^2 + m^{*2}} \int d^4 x (s \partial_\mu \partial_\nu s) \int \frac{d^4 p'}{(2\pi)^4} \int d^4 z \frac{-p \cdot p' + m^{*2}}{p'^2 + m^{*2}} \partial_\mu^{p'} \partial_\nu^{p'} e^{i(p-p')z}. \quad (7.52)$$

But the last two integrals can be easily evaluated,

$$\int \frac{d^4 p}{(2\pi)^4} \int d^4 z \left[ \frac{-p \cdot p' + m^{*2}}{p'^2 + m^{*2}} \right] \partial_\mu^{p'} \partial_\nu^{p'} e^{i(p-p')z} = \partial_\mu^{p'} \partial_\nu^{p'} \left[ \frac{-p \cdot p' + m^{*2}}{p'^2 + m^{*2}} \right] \Big|_{p=p'}, \quad (7.53)$$

so that

$$\text{Term}(3) = -2i N_c g_0^2 \int d^4 x (s \partial_\mu \partial_\nu s) \int \frac{d^4 p}{(2\pi)^4} \left[ \frac{4p_\mu p_\nu}{(p^2 + m^{*2})^3} + 8p_\mu p_\nu \frac{(-p^2 + m^{*2})}{(p^2 + m^{*2})^4} - 2\delta_{\mu\nu} \frac{-p^2 + m^{*2}}{(p^2 + m^{*2})^3} \right]. \quad (7.54)$$

This equation may now be evaluated in a straightforward manner following the philosophy of the previous section, in which the convergent terms are separated out. The divergent remainder can be evaluated, using relations such as (7.14), to give

$$\text{Term}(3) = \frac{1}{2} I_0 g_0^2 \int d^4x (\partial_\mu s)(\partial^\mu s). \quad (7.55)$$

One is now in a position from (7.55) to distill the contribution from  $U_s^{(2)}$  to the effective Lagrange density that displays the kinetic energy of the  $\sigma$  field. This can be seen explicitly in Eq. (7.59), which will follow, on remembering the connection (7.40). For completeness, we note that the term occurring in the Lagrange density that will be proportional to  $\sigma^2$  contains not only the contribution from Eq. (7.48) due to the scalar portion of  $U^{(2)}$ , but also a piece due to the scalar sectors of  $U^{(3)}$  and  $U^{(4)}$ . The leading term in the derivative expansion for

the scalar sector of  $U^{(3)}$  is

$$U_s^{(3)} \simeq -2m^* g_0^3 I_0 \int d^4x s^3(x), \quad (7.56)$$

while that from  $U^{(4)}$  is

$$U_s^{(4)} \simeq -\frac{1}{2} I_0 g_0^4 \int d^4x s^4(x). \quad (7.57)$$

In combination with Eq. (7.40), the term proportional to  $\sigma^2$  may be isolated. One has, from adding the contributions from  $U_s^{(4)}$ , that the term contributing to the action and proportional to  $\sigma^2$  is

$$g_0^2 I_2 + m^* g_0^2 I_0. \quad (7.58)$$

For a full calculation, this procedure is applied to the pseudoscalar field also. The resulting local Lagrange density, obtained after summing up all divergent contributions, is given as (Eguchi, 1976)

$$\begin{aligned} \mathcal{L} = & -\frac{1}{2}(\delta\mu_0^2 - 2I_2 g_0^2)(\sigma^2 + \pi^2) + I_0 g_0^2 \frac{1}{2}[(\partial_\mu \sigma)^2 + (\partial_\mu \pi)^2] + I_0 g_0^2 (g_0 v_0)^2 (\sigma^2 + \pi^2) \\ & - \frac{1}{2} I_0 g_0^4 (\sigma^2 + \pi^2)^2 + \mathcal{L}_c(g_0, v_0) + \bar{\eta} \frac{1}{i\partial - g_0(\sigma + i\gamma_5 \tau \cdot \pi)} \eta, \end{aligned} \quad (7.59)$$

where

$$\mathcal{L}_c = \sum_{i=2}^4 U_c^{(i)} + \sum_{i=5}^{\infty} U^{(i)} \quad (7.60)$$

reflects the contribution of the convergent terms  $U^{(n)}$  to the Lagrangian. The sum for  $U$  from Eq. (7.43) can also be seen in a diagrammatic fashion similar to the Green's-function expansion of Fig. 28. In this case, the direct diagrammatic translation of the fermionic determinant is expressed in Fig. 29.

As has been pointed out by Eguchi (1976), renormalization of the terms occurring in Eq. (7.59) can be effected along the lines of the linear sigma model, which is defined as

$$\mathcal{L}_\sigma = \bar{\psi}[i\gamma \cdot \partial - g_0'(\sigma + i\gamma_5 \tau \cdot \pi)]\psi + \frac{1}{2}[(\partial_\mu \sigma)^2 + (\partial_\mu \pi)^2 - \mu'^2(\sigma^2 + \pi^2)] - \frac{1}{4}\lambda_0'(\sigma^2 + \pi^2)^2 - \frac{1}{2}\delta\mu_0'^2(\sigma^2 + \pi^2). \quad (7.61)$$

The fermionic fields may again be integrated out of the generating functional to give an effective Lagrangian in meson degrees of freedom only that may be compared with the effective Lagrangian of the bosonized NJL model. Although there is a formal similarity between the two models, there are fundamental differences in philosophy. In particular, the  $\sigma$  model introduces quark and meson fields simultaneously. This implies that there is a dual role assigned to the mesons: either they can be conceived of as fermionic bound states, or as independent fields. No such conceptual difficulty arises in the bosonizing procedure for the NJL model, since the original Lagrang-

ian contained only fermionic degrees of freedom. One then sees clearly how the mesons are obtained; i.e., the kinetic terms for the meson fields are generated via radiative corrections to the fermion loops, while the meson interaction potential arises directly from the four-fermion interactions.

We make some comments in conclusion. Firstly, it is clear that the wealth of knowledge obtained from the study of  $\sigma$  models can now be applied to an effective Lagrangian of this kind, and the hadronic degrees of freedom can be studied as the corresponding solitonic states. Further expansion of this model would include the vector and axial-vector contributions to the original NJL Lagrangian (see, for example, Ebert and Volkov, 1983) that would consequently require the introduction of sufficient corresponding mesonic fields. Such terms are necessary to achieve a sufficiently attractive force in the axial-vector channel. Finally, we comment that the results of Ebert and Volkov (1983) differ from those of Eguchi (1976) in describing the scalar and pseudoscalar sectors.

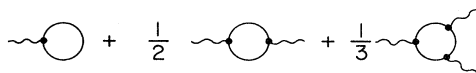


FIG. 29. Feynman diagram representation of the series contained in Eq. (7.43) (after Kikkawa, 1976). Wavy lines represent meson fields.

The treatment given here is in agreement with the latter paper.

### C. Developments in flavor U(3)

Several authors (Kikkawa, 1976; Volkov, 1984, 1986; Ebert and Reinhardt, 1986) have studied the bosonized effective Lagrange density in flavor U(3), written here as

$$\mathcal{L} = \bar{\psi}(i\not{\partial} - m_0)\psi + \frac{1}{2}G_1 \sum_{i=0}^8 [(\bar{\psi}\lambda_i\psi)^2 + (\bar{\psi}i\gamma_5\lambda_i\psi)^2] - \frac{1}{2}G_2 \sum_{i=0}^8 [(\bar{\psi}\gamma^\mu\lambda_i\psi)^2 + (\bar{\psi}\gamma^\mu\gamma_5\lambda_i\psi)^2], \quad (7.62)$$

which is identical with the Lagrangian (2.14) with  $G_3$  and  $G_4$  set to zero and with color octet terms suppressed. The six-fermion-interaction term is not included here, with the consequence that the model does not contain the problem of the  $U_A(1)$  anomaly and the splitting of the  $\eta$  and  $\eta'$  mesons. A bosonization procedure can, of course, once again be performed through the introduction of vectors of nine scalar fields, nine pseudoscalar, nine vector, and nine axial-vector fields. Since this exactly parallels the development of Sec. VII.B, we do not go into detail here. Instead, we refer the reader directly to the work of Ebert and Reinhardt (1986), who have studied this in detail. We point out that these authors used an expansion technique different from, but equivalent to, the derivative expansion described in the previous section, in order to evaluate the ensuing nonlocal functional of the mesonic fields. That is, a heat-kernel expansion is performed. The resulting effective Lagrangian, as in the SU(2) case, can be subdivided into finite and divergent contributions.

In addition, these authors indicated that the presence of the axial-vector coupling leads to an imaginary part of the effective action, as was considered by Wess and Zumino (1979), and thus the effective Lagrange density gains a Wess-Zumino term. For a discussion of the current-algebra properties that relate to the vector-meson spectrum [Weinberg and KSRF (Kawarabayashi-Suzuki-Riazuddin-Fayyazuddin) relations], we refer the reader directly to Ebert and Reinhardt (1986) and Meissner (1988).

### D. Correspondence with chiral perturbation theory

In a series of articles, Gasser and Leutwyler (1984, 1985) derive an effective low-energy mesonic Lagrangian for two and three flavors, to order  $p^4$ . They show that in the two-flavor case, the  $O(p^2)$  general effective Lagrangian consistent with Lorentz invariance, parity, and chiral symmetry involves only two constants,  $F$  and  $B$ , and can be written as

$$\mathcal{L}_1 = \frac{1}{2}F^2 \nabla_\mu U^T \nabla^\mu U + 2BF^2(s^0 U^0 + p^i U^i). \quad (7.63)$$

In Eq. (7.63),  $U^A(x)$  is defined to be a four-component real  $O(4)$  vector field of unit length  $U^T U = 1$ , and  $s(x)$  and  $p(x)$  are external scalar and pseudoscalar fields, respectively, the former of which is understood to contain a mass matrix  $M$ .

A general effective Lagrange density of order  $p^4$ , consistent with the same symmetries as  $\mathcal{L}_1$ , requires the introduction of ten constants,  $l_1 \dots l_7$  and  $h_1 \dots h_3$ , reflecting low- and high-energy properties, respectively. The Lagrange density in this order reads

$$\begin{aligned} \mathcal{L}_2 = & l_1(\nabla^\mu U^T \nabla_\mu U)^2 + l_2(\nabla^\mu U^T \nabla^\nu U)(\nabla_\mu U^T \nabla_\nu U) + l_3(\chi^T U)^2 + l_4(\nabla^\mu \chi^T \nabla_\mu U) + l_5(U^T F^{\mu\nu} F_{\mu\nu} U) \\ & + l_6(\nabla^\mu U^T F_{\mu\nu} \nabla^\nu U) + l_7(\tilde{\chi}^T U)^2 + h_1 \chi^T \chi + h_2 \text{tr} F_{\mu\nu} F^{\mu\nu} + h_3 \tilde{\chi}^T \chi. \end{aligned} \quad (7.64)$$

In this equation the vector  $\chi^a$  is given as  $\chi^a = 2B(s^0, p^i)$ . Evaluating the action to one loop (see, for example, Ramond, 1981 and 't Hooft, 1973), one obtains ultraviolet divergences that may be removed on effecting the renormalization

$$\begin{aligned} l_i &= l_i' + \gamma_i \lambda, \quad i = 1, \dots, 7 \\ h_i &= h_i' + \delta_i \lambda_i, \quad i = 1, 2, 3 \end{aligned} \quad (7.65)$$

for which

$$\lambda = (4\pi)^{-2} \mu^{d-4} \left\{ 1/(d-4) - \frac{1}{2} [\log 4\pi + \Gamma'(1) + 1] \right\}, \quad (7.66)$$

for which  $d$  is the dimensionality, and  $\gamma_1 = \frac{1}{3}$ ,  $\gamma_2 = \frac{2}{3}$ ,  $\gamma_3 = -\frac{1}{2}$ ,  $\gamma_4 = 2$ ,  $\gamma_5 = -\frac{1}{6}$ ,  $\gamma_6 = -\frac{1}{3}$ , and  $\gamma_7 = 0$ . The constants  $\delta_i$  are given as  $\delta_1 = 2$ ,  $\delta_2 = \frac{1}{12}$ , and  $\delta_3 = 0$ , and  $\mu$  is the renormalization scale. The renormalized constants  $l_i'$  and  $h_i'$  depend logarithmically on the scale  $\mu$ , so that it is

useful to define the *scale-independent* quantities  $\tilde{l}_i$  and  $\tilde{h}_i$  via

$$\begin{aligned} l_i' &= \frac{\gamma_i}{32\pi^2} \left[ \tilde{l}_i + \log \frac{M^2}{\mu^2} \right] \quad i = 1, \dots, 6 \\ h_i' &= \frac{\delta_i}{32\pi^2} \left[ \tilde{h}_i + \log \frac{M^2}{\mu^2} \right] \quad i = 1, 2. \end{aligned} \quad (7.67)$$

The values of  $\tilde{l}_i$  can be extracted from experiment and are listed in Table VIII.

It is useful to note that physical quantities, expanded in the current quark mass to  $O(p^4)$ , can be obtained. In particular, the pion mass and pion-decay constant are given as

$$m_\pi^2 = m_0^2 \left[ 1 - \frac{m_0^2}{32\pi^2 F^2} \tilde{l}_3 + O(m_0^4) \right] \quad (7.68)$$

and

$$f_\pi = F \left[ 1 + \frac{m_0^2}{16\pi^2 F^2} \bar{I}_4 + O(m_0^4) \right], \quad (7.69)$$

where  $m_0$  is the average SU(2) current quark mass.

For three quark flavors, the general effective Lagrangian of order  $p^2$  again requires only two constants, while that to  $O(p^4)$  requires ten additional low-energy constants  $L_1 \dots L_{10}$  and two high-energy constants  $H_1$  and  $H_2$ . The effective Lagrangian for this order takes the form

$$\begin{aligned} \mathcal{L}_2 = & L_1 \langle \nabla^\mu U^\dagger \nabla_\mu U \rangle^2 + L_2 \langle \nabla_\mu U^\dagger \nabla_\nu U \rangle \langle \nabla^\mu U^\dagger \nabla^\nu U \rangle + L_3 \langle \nabla^\mu U^\dagger \nabla_\mu U \nabla^\nu U^\dagger \nabla_\nu U \rangle + L_4 \langle \nabla^\mu U^\dagger \nabla_\mu U \rangle \langle \chi^\dagger U + \chi U^\dagger \rangle \\ & + L_5 \langle \nabla^\mu U^\dagger \nabla_\mu U (\chi^\dagger U + U^\dagger \chi) \rangle + L_6 \langle \chi^\dagger U + \chi U^\dagger \rangle^2 + L_7 \langle \chi^\dagger U - \chi U^\dagger \rangle^2 \\ & + L_8 \langle \chi^\dagger U \chi^\dagger U + \chi U^\dagger \chi U^\dagger - i L_9 \langle F_{\mu\nu}^R \nabla^\mu U \nabla^\nu U^\dagger + F_{\mu\nu}^L \nabla^\mu U^\dagger \nabla^\nu U \rangle \\ & + L_{10} \langle U^\dagger F_{\mu\nu}^R U F^{\mu\nu L} \rangle + H_1 \langle F_{\mu\nu}^R F^{\mu\nu R} + F_{\mu\nu}^L F^{\mu\nu L} \rangle + H_2 \langle \chi^\dagger \chi \rangle. \end{aligned} \quad (7.70)$$

Here, the bracket  $\langle A \rangle$  denotes the trace of the matrix  $A$ . The field-strength tensors are defined as

$$F_{\mu\nu}^{R,L} = \partial_\mu F_\nu^{R,L} - \partial_\nu F_\mu^{R,L} - i[F_\mu^{R,L} F_\nu^{R,L}],$$

with  $F_\mu^{R,L} = v_\mu \pm a_\mu$ .

Taking one-loop graphs into account in the generating functional, one is again led to a renormalization prescription,

$$\begin{aligned} L_i &= L_i' + \Gamma_i \lambda_i \quad i=1, \dots, 10 \\ H_i &= H_i' + \Delta_i \lambda_i, \quad i=1, 2 \end{aligned} \quad (7.71)$$

where  $\lambda$  is given as before by Eq. (7.67), and the values of the  $\Delta_i$  are  $\Delta_1 = -\frac{1}{8}$  and  $\Delta_2 = \frac{5}{24}$ . The values of the  $L_i'$ , inferred from experiment, are listed in Table IX. As before, the  $L_i'$  are scale dependent, and the change in  $L_i'$  with the scale is given by

$$L_i'(\mu_2) = L_i'(\mu_1) + \frac{\Gamma_i}{16\pi^2} \log \frac{\mu_1}{\mu_2}. \quad (7.72)$$

The renormalized coupling constants of SU(2) can be re-

TABLE VIII. Values of the low-energy constants (Gasser and Leutwyler, 1984).

Constant	Value	Obtained from	$\gamma_i$
$\bar{I}_1$	$-2.3 \pm 3.7$	$D$ wave	$\frac{1}{3}$
$\bar{I}_2$	$6.0 \pm 1.3$	scattering lengths	$\frac{2}{3}$
$\bar{I}_3$	$2.94 \pm 2.4$	SU(3) mass formula	$-\frac{1}{2}$
$\bar{I}_4$	$4.3 \pm 0.9$	$f_K/f_\pi$	2
$\bar{I}_5$	$13.9 \pm 1.3$	$\pi \rightarrow e \nu \gamma$	$-\frac{1}{6}$
$\bar{I}_6$	$16.5 \pm 1.1$	$\langle r^2 \rangle_\pi^V$	$-\frac{1}{3}$
$l_7$	$O(5 \times 10^{-3})$	$\pi^0$ - $\eta$ mixing	0

lated to those of SU(3). The reader is referred to Gasser and Leutwyler (1985).

There are two methods in which a comparison of the NJL model with chiral perturbation theory has been undertaken. In the work of Hansson, Prakash, and Zahed (1990), a direct expansion of the self-energy in terms of powers of the current quark mass is made, i.e.,

$$m^* = \Sigma = \Sigma_0 + \Sigma_1 m_0 + \Sigma_2 (m_0^2/2) + \dots, \quad (7.73)$$

and the expansion coefficients  $\Sigma_0, \Sigma_1$ , and  $\Sigma_2$  are determined from the Hartree-Fock gap equation, Eq. (2.31), in the SU(2) case. One finds that

$$\begin{aligned} 1 &= \Delta \int \frac{d^3 p}{(2\pi)^3} \frac{1}{(p^2 + \Sigma_0^2)^{1/2}}, \\ \Sigma_1 &= \Delta \Sigma_0^2 \int \frac{d^3 p}{(2\pi)^3} \frac{1}{(p^2 + \Sigma_0^2)^{3/2}}, \\ \Sigma_2 &= 3\Delta (\Sigma_0 \Sigma_1)^3 \int \frac{d^3 p}{(2\pi)^3} \frac{1}{(p^2 + \Sigma_0^2)^{5/2}} - \frac{\Sigma_1^2}{\Sigma_0}, \end{aligned} \quad (7.74)$$

TABLE IX. Values of the low-energy constants taken at the scale  $\mu = m_\eta$  (Gasser and Leutwyler, 1985).

Constant	Value	Source	$\Gamma_i$
$L_1'$	$(0.9 \pm 0.3) \times 10^{-3}$	$\pi\pi D$ waves, Zweig rule	$\frac{3}{32}$
$L_2'$	$(1.7 \pm 0.7) \times 10^{-3}$	$\pi\pi D$ waves	$\frac{3}{16}$
$L_3'$	$(-4.4 \pm 2.5) \times 10^{-3}$	$\pi\pi D$ waves, Zweig rule	0
$L_4'$	$(0 \pm 0.5) \times 10^{-3}$	Zweig rule	$\frac{1}{8}$
$L_5'$	$(2.2 \pm 0.5) \times 10^{-3}$	$f_K/f_\pi$	$\frac{3}{8}$
$L_6'$	$(0 \pm 0.3) \times 10^{-3}$	Zweig rule	$\frac{11}{144}$
$L_7'$	$(-0.4 \pm 0.15) \times 10^{-3}$	Gell-Mann–Okubo, $L_5 L_8$	0
$L_8'$	$(1.1 \pm 0.3) \times 10^{-3}$	$K^0 - K^+, R, L_5$	$\frac{5}{48}$
$L_9'$	$(7.4 \pm 0.7) \times 10^{-3}$	$\langle r^2 \rangle_{\pi}^{\text{e.m.}}$	$\frac{1}{4}$
$L_{10}$	$(-6.0 \pm 0.7) \times 10^{-3}$	$\pi \rightarrow e \nu \gamma$	$-\frac{1}{4}$



where the abbreviation  $\Delta = 2G(2N_c N_f + 1)$  has been introduced and a cutoff on the three-momentum has been employed. A similar expansion for the quark condensate follows from Eq. (3.25) on setting

$$\langle \bar{q}q \rangle = \langle \bar{q}q \rangle_0 + \langle \bar{q}q \rangle_1 m_0 + \langle \bar{q}q \rangle_2 (m_0^2/2) + \dots \quad (7.75)$$

One finds

$$\langle \bar{q}q \rangle_0 = -(2N_f N_c / \Delta) \Sigma_0,$$

$$\langle \bar{q}q \rangle_1 = -(2N_f N_c / \Delta) (\Sigma_1 - 2),$$

and

$$\langle \bar{q}q \rangle_2 = -(2N_f N_c / \Delta) (\Sigma_2 + 2/\Sigma_0).$$

For the pion, the expansion

$$m_\pi^2 = 0 + m_{\pi,1}^2 m_0 + m_{\pi,2}^2 (m_0^2/2) + \dots \quad (7.76)$$

has coefficients that are determined from Eqs. (4.9) and (4.21) to be  $m_{\pi,1}^2 = 4\Sigma_0 \Sigma_1$  and

$$m_{\pi,2}^2 = 8(2\Sigma_0 \Sigma_2 / 3 + \Sigma_1^2).$$

Finally, the pion-decay constant can also be expanded in powers of the current quark mass as

$$f_\pi = f_{\pi,0} + f_{\pi,1} m_0 + \dots, \quad (7.77)$$

with the expansion coefficients  $f_{\pi,0}$  and  $f_{\pi,1}$  determined via Eq. (4.26) for the chosen regularization scheme. A comparison of Eqs. (7.76) and (7.77) with Eqs. (7.68) and (7.69) leads to the identification

$$\frac{1}{2} m_{\pi,2}^2 = -\frac{B^2}{8\pi^2 F^2} \tilde{I}_3 = -\frac{\langle \bar{q}q \rangle_0^2}{32f_{\pi,0}^6} \tilde{I}_3, \quad (7.78)$$

where the last step follows on identifying  $B = 1408$  MeV and  $F = 88$  MeV as the values of  $-\langle \bar{q}q \rangle / 2f_\pi^2$  and  $f_\pi$ , extrapolated to the chiral limit. Thus  $\tilde{I}_3$  may be determined in terms of the values calculated within the NJL model. In a similar fashion  $\tilde{I}_4$  may be obtained,

$$\tilde{I}_4 = -8\pi^2 \frac{f_{\pi,0}^3}{\langle \bar{u}u \rangle_0} f_{\pi,1}. \quad (7.79)$$

The calculation of these (scale-independent) values gives

$$\tilde{I}_3^{\text{NJL}} = 0.37, \quad \tilde{I}_4^{\text{NJL}} = 0.85, \quad (7.80)$$

which, for the parameter set chosen,  $G\Lambda^2 = 2.09$ ,  $\Lambda = 615$  MeV, and  $m_0 \approx 5.8$  MeV, is not particularly good. For a four-momentum cutoff  $\Lambda = 859$  MeV,  $G\Lambda^2 = 4.25$ , and a larger current quark mass  $m_0 = 7$  MeV, these values are somewhat improved,

$$\tilde{I}_3^{\text{NJL}} = 0.98, \quad \tilde{I}_4^{\text{NJL}} = 1.17. \quad (7.81)$$

These results should be carefully considered. It may perhaps be more useful to work strictly to first order in the number of flavors, considering as such only the Har-

tree contribution. It would certainly also be of interest to see if one could reproduce the broad spectrum of parameters of chiral perturbation theory by using the full SU(3) NJL Lagrangian of Eq. (2.32).

An alternative approach has been taken by Ebert and Reinhardt (1986) and, following this work, by Schüren, Ruiz Arriola, and Goeke (1991) and Ruiz Arriola (1991). Ebert and Reinhardt consider the effective Lagrange density that they have obtained via bosonization and reconstruct this in a form analogous to that of Gasser and Leutwyler (1985). In this calculation, the renormalized constants are calculated neglecting the pion loops that are responsible for chiral logarithms. The full fourth-order term in the heat-kernel expansion has not been calculated in this approach. In the papers of Schüren, Ruiz Arriola, and Goeke (1991) and Ruiz Arriola (1991) that commence with the SU(2) and U(3) NJL models, respectively, the philosophy of Ebert and Reinhardt is followed, but the evaluation of the fermion determinant is undertaken to fourth order using a derivative expansion in the fields. The results obtained are compared with the renormalized values  $L_i', i = 1 \dots 10$ , at the scale  $m_\rho = 776$  MeV. A typical set of results quoted by these authors seems in fair agreement with the low-energy constants. They obtain, for example, in the Pauli-Villars regularized scheme with  $m_0 = 7.0$  MeV,  $\Lambda = 911$  MeV, the values

$$\begin{aligned} L_1 &= 0.77, \quad L_2 = 1.54, \quad L_3 = -3.08, \quad L_4 = 0, \\ L_5 &= 1.21, \quad L_6 = 0, \quad L_7 = 0, \quad L_8 = 0.34, \\ L_9 &= 4.72, \quad L_{10} = -3.08 \end{aligned}$$

in comparison with the empirical values taken at the scale  $m_\rho = 776$  MeV,

$$\begin{aligned} L_1 &= 0.7 \pm 0.3, \quad L_2 = 1.3 \pm 0.7, \quad L_3 = -4.4 \pm 2.5, \\ L_4 &= -0.3 \pm 0.5, \quad L_5 = 1.4 \pm 0.5, \quad L_6 = -0.2 \pm 0.3, \\ L_7 &= -0.4 \pm 0.15, \quad L_8 = 0.9 \pm 0.3, \quad L_9 = 6.9 \pm 0.7, \\ L_{10} &= -5.2 \pm 0.3. \end{aligned}$$

In a treatment of the U(3) NJL Lagrangian that includes vector mesons, Ruiz Arriola (1991) performs a chi-squared fit to the renormalized low-energy constants. In this paper, the  $U_A(1)$  breaking is introduced by including an extra term in the NJL Lagrangian, which is, however, not flavor mixing, as is the 't Hooft term in the standard version of the model as given in Eqs. (2.32). It is therefore not strictly equivalent to the SU(3) NJL model as presented in Sec. II. In addition, it should also be noted that the bosonization procedure, strictly speaking, leads to a version of the linear sigma model and, moving onto the chiral circle to construct a nonlinear sigma model, is done by hand. The least-squares fit, while representing the constants  $L_1 \dots L_{10}$  well,

$$\begin{aligned}
L_1 &= 0.96, \quad L_2 = 1.25, \quad L_3 = -5.21, \quad L_4 = 0, \\
L_5 &= 1.23, \quad L_6 = 0, \quad L_7 = -0.40, \quad L_8 = 0.62, \\
L_9 &= 6.27, \quad L_{10} = -5.42,
\end{aligned}$$

leads to a somewhat higher value of the Pauli-Villars regularization cutoff  $\Lambda = 1370$  MeV and somewhat too low values of the current quark masses  $(m_u^0 + m_d^0)/2 = 2.44$  MeV. The condensate value  $\langle \bar{u}u \rangle = -(325 \text{ MeV})^3$  differs from the value extracted via sum rules  $\langle \bar{u}u \rangle = -(240 \pm 25 \text{ MeV})^3$  by roughly a factor of 2. With their parametrization, the renormalization-group-invariant product,  $-(m_u^0 + m_d^0)\langle \bar{u}u + \bar{d}d \rangle$ , remains at the physical value that one would expect, viz., at  $2f_\pi^2 m_\pi^2$ . The dynamically generated mass in the SU(2) sector is quoted as  $m = 300$  MeV.

We conclude this section by remarking that the conclusions regarding the connection of the NJL model to chiral perturbation theory remain open. We substantiate this comment by summarizing the situation. In the fermionic version of the NJL model, which has been studied in the flavor SU(2) version in the Hartree-Fock approximation, the scale-independent quantities  $\tilde{L}_3$  and  $\tilde{L}_4$  are not in particularly good agreement with the empirical values. On the other hand, the bosonized form of the NJL Lagrangian appears to give a good fit to the scale-dependent values  $L_1 \dots L_{10}$  at the scale of the  $\rho$ -meson mass. In this calculation, however, the usual parameters of the model ( $\langle \bar{u}u \rangle, m_u^0, m_d^0$ ) do not lie within the standard bounds. Furthermore, the procedure invoked by these authors is to move onto the chiral circle. This is a procedure which is put in by hand, in an *ad hoc* fashion, and which therefore distances this effective boson model from the original fermionic NJL model. It is thus desirable within the framework of the (fermion) SU(3) NJL Lagrange density of Eq. (2.32) either to establish the scale-independent low-energy parameters or to extract in a complete fashion the renormalized constants from a fully equivalent SU(3) bosonized effective Lagrangian. We comment, too, that a detailed comparison of the NJL model with chiral perturbation theory at finite temperatures (Gasser and Leutwyler, 1987; Gerber and Leutwyler, 1989) has not yet been undertaken.

### VIII. CONCLUDING REMARKS

We have demonstrated that the NJL model is a technically useful field-theoretical framework for modeling chiral symmetry breaking, since it facilitates calculation. The basis of solution rests on obtaining a self-consistent solution for the self-energy in either the Hartree or Hartree-Fock approximation that can be carried out exactly because of the simple contact nature of the four- or six-point fermion interactions. Physically, this corresponds to constructing a trial BCS-like vacuum state of zero total helicity and momentum in which particles and antiparticles are paired. This is in contrast to the theory of superconductivity in which like particles (electrons) of

opposite helicities are paired.

The inclusion of the flavor symmetries of QCD in the construction of the NJL Lagrangian has the consequence that the relations of current algebra, such as the Goldberger-Treiman and Gell-Mann–Oakes–Renner relations, must hold and can easily be demonstrated to do so explicitly. The NJL model has further been used to study effects of including external parameters such as temperature, chemical potential, and applied Maxwell and color fields on a system of quarks that are governed by a chirally symmetric Lagrangian. The static properties of mesons are also studied. One finds that, in addition to the relations of current algebra, approximate regularization-free results can be established for several other quantities of physical significance. These include the  $\sigma$ -meson mass, the condensation energy, and the critical parameters of the phase transition, such as the critical transition temperature and the critical-field strength for chiral symmetry restoration.

We have also noted that the path-integral formalism may be employed to construct an effective Lagrangian that contains only bosonic degrees of freedom. This bosonized form of the NJL model may be linked to the well-known phenomenological meson models, which have been well studied over the past few decades.

One must of course draw a balance by also listing the negative features of the model. To the extent that it has been investigated, the connections and predictions of this model in comparison with chiral perturbation theory are in partial agreement at best. The relationship of this model with QCD is not known, and it would be interesting to establish whether such a connection exists. Next, the contact nature of the fermion interaction has the consequence that the model is not renormalizable, in the sense that an infinite number of renormalization constants would be required for its complete specification. In practice, one uses only one regularization constant when working at the one-loop level, so that care must be taken in performing any mathematical procedures, to ensure that the symmetries of the model are maintained. We have mentioned this only cursorily in this article. A further criticism is that the contact four-fermion interaction does not allow for confinement, so that the decay of mesonic states into free  $\bar{q}q$  states occurs. This is rather a feature of states that lie high in energy with respect to the scale of the theory. It is assumed in constructing the NJL model that, for low-energy mass spectra and properties, the role of symmetries overrides that of confinement, which is expected to affect the high-energy behavior of the theory. In actual calculations, mesonic states that lie in the continuum must have a narrow width in order to be considered as physical in this model, which has been assumed to be the case.

### ACKNOWLEDGMENTS

The author wishes to thank the many people who have contributed in some way to this article, either with pro-

vocative questions or with useful discussions. You know of course who you all are. In particular, I wish to thank Klaus Werner and Matthias Neubert for useful discussions. I am also most indebted to Jörg Hüfner for his support and critical comments on this work. Finally, I wish to thank August Nüchter, for making every computer convenience available to me for the preparation of the manuscript and the figures. This work was supported in part by the Federal Ministry of Research and Technology (BMFT) under Contract number 06 HD 710, and by the Deutsche Forschungsgemeinschaft (DFG) under contract number Hu 233/4-1.

## APPENDIX A: THE SIX-FERMION INTERACTION

In this appendix we obtain the self-energy that arises from the six-fermion interaction in the mean-field approximation. We also derive an effective four-fermion form for this interaction term.

The self-energy due to the six-fermion interaction can be obtained by Wick-contracting all possible pairs of creation and destruction operators in this term of the Lagrangian, such that only two remain. Introducing the abbreviation  $\Gamma^\pm = 1 \pm \gamma_5$ , this term, taken from Eq. (2.32),

can be written as

$$\begin{aligned} \mathcal{L}^{(6)} &= -K(\det \bar{\psi} \Gamma^+ \psi + \det \bar{\psi} \Gamma^- \psi) \\ &= -\frac{K}{6} \epsilon_{ijk} \epsilon_{lmn} [(\bar{\psi}^i \Gamma^+ \psi^l)(\bar{\psi}^j \Gamma^+ \psi^m) \\ &\quad \times (\bar{\psi}^k \Gamma^+ \psi^n) + (+ \rightarrow -)] , \end{aligned} \quad (\text{A1})$$

where  $\epsilon_{ijk}$  is the Levi-Civita antisymmetric tensor, and the flavor indices  $i, j, k, \dots$  are now explicitly displayed. Consider a generic term for which  $\Gamma$  can be either  $\Gamma^+$  or  $\Gamma^-$ . There are 18 possible ways of contracting two creation and two destruction field operators of the six available that will give rise to four distinct terms,

$$\begin{aligned} \bar{\psi}^j [3\Gamma(\hat{\text{Tr}} \Gamma S^{jm})(\hat{\text{Tr}} \Gamma S^{kn}) + 6\Gamma S^{jm} \Gamma(\hat{\text{Tr}} \Gamma S^{kn}) \\ + 3\Gamma(\hat{\text{Tr}} \Gamma S^{kn} \Gamma S^{jm}) + 6\Gamma S^{jm} \Gamma S^{kn} \Gamma] \psi^i . \end{aligned} \quad (\text{A2})$$

The symbol  $\hat{\text{Tr}}$  refers to the sum over color and spinor indices only, and the particle propagators are all understood to be in  $x$  space,  $S^{ij}(x, x) = S^i(x, x) \delta^{ij}$ . Thus the effective contracted six-fermion Lagrangian is given by Eq. (A1) with Eq. (A2) inserted and with  $\Gamma \rightarrow \Gamma^+$  and  $\Gamma \rightarrow \Gamma^-$ . One now adds pairwise the terms of the same structure that contain  $\Gamma^+$  and  $\Gamma^-$ , to obtain an effective six-fermion mean-field Lagrangian

$$\begin{aligned} \mathcal{L}_{\text{eff}}^{(6)} &= \bar{\psi}^i K \sum_{jk} \epsilon_{ijk} \epsilon_{ljk} \{ N_c^2 (\text{tr} S^j)(\text{tr} S^k) + 2N_c [S^j(\text{tr} S^k) + \gamma_5 S^j \gamma_5 (\text{tr} S^k)] + N_c \text{tr} (S^j S^k + \gamma^5 S^j \gamma^5 S^k) \\ &\quad + 2(S^j S^k + \gamma^5 S^j \gamma^5 S^k + \gamma^5 S^j S^k \gamma^5 + S^j \gamma^5 S^k \gamma^5) \} \psi^i . \end{aligned} \quad (\text{A3})$$

The epsilon tensor has the consequence that  $i \neq j \neq k$ , and it always brings in a factor of 2 if one performs the sums explicitly, as can be seen by examining, for example, the first term on the diagonal  $i = l = u$ :

$$\begin{aligned} \sum_{jk} \epsilon_{ijk} \epsilon_{ljk} (\text{tr} S^j)(\text{tr} S^k) &= \epsilon_{uds} \epsilon_{uds} (\text{tr} S^d)(\text{tr} S^s) + \epsilon_{usd} \epsilon_{usd} (\text{tr} S^s)(\text{tr} S^d) \\ &= 2(\text{tr} S^j)(\text{tr} S^k), \quad \text{where } j \neq k \neq u . \end{aligned} \quad (\text{A4})$$

Every term can be handled in this way. Furthermore, the remaining three terms can be written as  $\text{factor} \times (\text{tr} S^j)(\text{tr} S^k)$ , with the direct insertion of Eq. (2.30) into (A3): the second term of (A3) is proportional to

$$\begin{aligned} (S^j + \gamma^5 S^j \gamma^5)(\text{tr} S^k) &= \int \frac{d^4 p}{(2\pi)^4} \left[ \frac{\not{p} + m^*}{p^2 - m^{*2}} + \frac{\gamma^5 (\not{p} + m^*) \gamma^5}{p^2 - m^{*2}} \right] (\text{tr} S^k) \\ &= \int \frac{d^4 p}{(2\pi)^4} \frac{2m^*}{p^2 - m^{*2}} (\text{tr} S^k) \\ &= \frac{1}{2} (\text{tr} S^j)(\text{tr} S^k) . \end{aligned} \quad (\text{A5})$$

Similarly,

$$\text{tr} (S^j S^k + \gamma^5 S^j \gamma^5 S^k) = \frac{1}{2} (\text{tr} S^j)(\text{tr} S^k) \quad (\text{A6})$$

and

$$S^j S^k + \gamma^5 S^j \gamma^5 S^k + \gamma^5 S^j S^k \gamma^5 + S^j \gamma^5 S^k \gamma^5 = \frac{1}{4} (\text{tr} S^j)(\text{tr} S^k) , \quad (\text{A7})$$

with the consequence that the effective six-fermion-

interaction Lagrangian reduces to a simple form,

$$\mathcal{L}^{(6)} \rightarrow \bar{\psi}^i K (2N_c^2 + 3N_c + 1) (\text{tr} S^j)(\text{tr} S^k) \psi^i . \quad (\text{A8})$$

One may therefore identify

$$\begin{aligned} \Sigma_i^{(6)} &= -K (2N_c^2 + 3N_c + 1) (\text{tr} S^j)(\text{tr} S^k) , \\ i &\neq j \neq k . \end{aligned} \quad (\text{A9})$$

Equations (A8) and (A9) were quoted as (2.36) and (2.37) of the main text.

Let us now construct an effective four-fermion interaction from  $\mathcal{L}^{(6)}$  that would yield the same self-energy. We do this by contracting out one quark and one antiquark field operator in all possible variations, such that four

field operators are always remaining.

Since there are nine different, possible ways of contracting out one pair of creation and destruction operators, the effective Lagrangian that must be used to evaluate the self-energy must be half that obtained via this procedure. One finds

$$\frac{1}{2}\mathcal{L}^{(6)\rightarrow(4)} = \frac{1}{2}K\epsilon_{ijk}\epsilon_{lmn}[\frac{1}{2}i\text{Tr}(S^{li}\Gamma^+)(\bar{\psi}^j\Gamma^+\psi^m)(\psi^k\Gamma^+\psi^n) - i(\bar{\psi}^i\Gamma^+S^{lj}\Gamma^+\psi^m)(\bar{\psi}^k\Gamma^+\psi^n) + (+\rightarrow-)] \quad (\text{A10})$$

from Eq. (A1). Writing  $\Gamma^+$  and  $\Gamma^-$  out in full and combining like terms, one finds that

$$\frac{1}{2}\mathcal{L}^{(6)\rightarrow(4)} = \frac{1}{2}K\epsilon_{ijk}\epsilon_{lmn}(N_c + 1)i\text{tr}S^i[(\bar{\psi}^j\psi^m)(\bar{\psi}^k\psi^n) + (\bar{\psi}^j\gamma_5\psi^m)(\bar{\psi}^k\gamma_5\psi^n)] \quad (\text{A11})$$

We have made use of the identity

$$S^{ij}\gamma_5 + \gamma_5 S^{ij} = \frac{1}{2}\delta^{ij}\gamma_5\text{tr}S^l.$$

Equation (A11) represents the six-fermion interaction reduced to a four-fermion form. As it stands, however, it is unappealing, and we therefore rewrite (A11) in terms of the basis of Gell-Mann matrices  $\lambda^1 \dots \lambda^8$ , and  $\lambda^0 = \sqrt{2/3}I$ , so that the flavor labels are not explicitly displayed. After some tedious algebra, we obtain the result, Eq. (2.40) quoted in the main text.

## APPENDIX B: CROSSING MATRICES FOR THE FIERZ TRANSFORMATION

The purpose of this appendix is to calculate the crossing matrices in Dirac, SU(2) flavor, and SU(3) color or flavor space. In Dirac space, the crossing matrix is well known (see, for example, Itzykson and Zuber, 1980). Using a notation that differs slightly from this reference, we quote only the final results that we use,

$$\begin{aligned} [s]_{\alpha\beta';\alpha'\beta} &= \frac{1}{4}[s + v + \frac{1}{2}t - a - p]_{\alpha\beta;\alpha'\beta'}, \\ [p]_{\alpha\beta';\alpha'\beta} &= -\frac{1}{4}[s - v + \frac{1}{2}t + a - p]_{\alpha\beta;\alpha'\beta'}, \\ [v]_{\alpha\beta';\alpha'\beta} &= \frac{1}{4}[4s - 2v - 2a + 4p]_{\alpha\beta;\alpha'\beta'}, \\ [a]_{\alpha\beta';\alpha'\beta} &= -\frac{1}{4}[4s + 2v + 2a + 4p]_{\alpha\beta;\alpha'\beta'}, \end{aligned} \quad (\text{B1})$$

where the symbols  $s, v, t, a$ , and  $p$  are defined as

$$\begin{aligned} s_{\alpha\beta;\alpha'\beta'} &= 1_{\alpha\beta}1_{\alpha'\beta'}, \\ p_{\alpha\beta;\alpha'\beta'} &= (i\gamma_5)_{\alpha\beta}(i\gamma_5)_{\alpha'\beta'}, \\ v_{\alpha\beta;\alpha'\beta'} &= (\gamma_\mu)_{\alpha\beta}(\gamma^\mu)_{\alpha'\beta'}, \\ a_{\alpha\beta;\alpha'\beta'} &= (\gamma_\mu\gamma_5)_{\alpha\beta}(\gamma^\mu\gamma_5)_{\alpha'\beta'}, \\ t_{\alpha\beta;\alpha'\beta'} &= (\sigma^{\mu\nu})_{\alpha\beta}(\sigma_{\mu\nu})_{\alpha'\beta'}. \end{aligned} \quad (\text{B2})$$

The crossing matrix for isospin, flavor, and color can be obtained directly from the definition (2.48). For isospin, for example, the coefficients  $c_i$  and  $c'_i$  must be obtained that relate

$$\sum_{i=1}^3 (\tau^i)_{fg}(\tau^i)_{gf'} = c_0(1)_{ff'}(1)_{gg'} + \sum_{i=1}^3 c_i(\tau^i)_{ff'}(\tau^i)_{gg'} \quad (\text{B3})$$

and

$$(1)_{fg'}(1)_{gf'} = c'_0(1)_{ff'}(1)_{gg'} + \sum_{i=1}^3 c'_i(\tau^i)_{ff'}(\tau^i)_{gg'}. \quad (\text{B4})$$

To determine the  $c_i$  from Eq. (B3), one recalls the completeness relation

$$\sum_i (\tau^i)_{ab}(\tau^i)_{cd} = 2(\delta_{bc}\delta_{ad} - \frac{1}{2}\delta_{ab}\delta_{cd})$$

to evaluate the left-hand side of this equation:

$$\begin{aligned} 2(\delta_{gg'}\delta_{ff'} - \frac{1}{2}\delta_{fg'}\delta_{gf'}) &= c_{00}(1)_{ff'}(1)_{gg'} \\ &+ \sum_{i=1}^3 c_i(\tau^i)_{ff'}(\tau^i)_{gg'}. \end{aligned} \quad (\text{B5})$$

Multiplying by  $\sum_{f'}(1)_{f'f}\sum_{g'}(1)_{g'g}$  and performing the flavor sums enable one to extract  $c_0 = \frac{3}{2}$ . The remaining coefficients  $c_i = -\frac{1}{2}$  are obtained by multiplying Eq. (B5) by  $\sum_{f'}\sum_{g'}(\tau^i)_{f'f}(\tau^i)_{g'g}$  and performing the flavor sums, noting that the Pauli matrices are traceless and  $\text{tr}(\tau^i\tau^j) = 2\delta_{ij}$ . This procedure may also be applied to Eq. (B4) to reveal  $c'_0 = c'_1 = \frac{1}{2}$ , so that the SU(2) flavor relations analogous to (B1) become

$$1_{fg'}1_{gf'} = \frac{1}{2}1_{ff'}1_{gg'} + \frac{1}{2}\sum_{i=1}^3 (\tau^i)_{ff'}(\tau^i)_{gg'}, \quad (\text{B6})$$

$$\sum_{i=1}^3 (\tau^i)_{fg'}(\tau^i)_{gf'} = \frac{3}{2}(1)_{ff'}(1)_{gg'} - \frac{1}{2}\sum_{i=1}^3 (\tau^i)_{ff'}(\tau^i)_{gg'}.$$

The SU(3) color condition can be set up in the same fashion as Eqs. (B3) and (B4), with the  $\tau^i$  being replaced by the color matrices  $\lambda_i^c, i=1 \dots 8$  and  $1 \rightarrow 1^c$  (Klimt *et al.*, 1990). Since the Gell-Mann matrices are normalized also according to  $\text{tr}(\lambda_k^c\lambda_l^c) = 2\delta_{lk}$ , the same procedure can be followed, to obtain

$$1_{cd'}^c 1_{dc'}^c = \frac{1}{3}1_{cc'}^c 1_{dd'}^c + \frac{1}{2}\sum_{i=1}^8 (\lambda_i^c)_{cc'}(\lambda_i^c)_{dd'} \quad (\text{B7})$$

and

$$\sum_{i=1}^8 (\lambda_i^c)_{cd'} \lambda_{dc'}^c = \frac{16}{9} 1_{cc'}^c 1_{dd'}^c - \frac{1}{3} \sum_{i=1}^8 (\lambda_i^c)_{cc'} (\lambda_i^c)_{dd'}.$$

Finally, the flavor SU(3) group can be obtained trivially from Eqs. (B7). Here it is conventional to introduce  $\lambda^0 = (2/3)^{1/2} I$ , so that (B7) in flavor space reads

$$(\lambda^0)_{fg'} (\lambda^0)_{gf'} = \frac{1}{3} (\lambda^0)_{ff'} (\lambda^0)_{gg'} + \frac{1}{3} \sum_{i=1}^8 (\lambda^i)_{ff'} (\lambda^i)_{gg'}, \quad (\text{B8})$$

and

$$\sum_{i=1}^8 (\lambda^i)_{fg'} (\lambda^i)_{gf'} = \frac{8}{3} (\lambda^0)_{ff'} (\lambda^0)_{gg'} - \frac{1}{3} \sum_{i=1}^8 (\lambda^i)_{ff'} (\lambda^i)_{gg'}.$$

These results are summarized as Eqs. (2.49) and (2.50) of the main text.

### APPENDIX C: THE TOTAL ENERGY

For completeness, we give a sophisticated method for evaluating the total energy per unit volume in the noncovariant cutoff scheme.<sup>4</sup> This method relies solely on a knowledge of the single-particle Green's function. Our starting point is the energy-momentum tensor

$$T^{\mu\nu} = i \bar{\psi} \gamma^\mu \partial^\nu \psi - g^{\mu\nu} \mathcal{L}. \quad (\text{C1})$$

For a two-body interaction, the average value of  $T^{\mu\nu}$  can be expressed solely in terms of the single-particle propagator. One notes, from its definition preceding Eq. (2.29), that the required kinetic term average is given as

$$\begin{aligned} \langle \bar{\psi}_\alpha(x) \gamma^\mu_{\alpha\beta} \partial^\nu_x \psi_\beta(x) \rangle &= \lim_{x' \rightarrow x^+} \gamma^\mu_{\alpha\beta} \partial^\nu_x \langle \bar{\psi}_\alpha(x) \psi_\beta(x') \rangle \\ &= -i \lim_{x' \rightarrow x^+} \partial^\nu_x \gamma^\mu_{\alpha\beta} S_{\beta\alpha}(x', x) \\ &= -i \lim_{x' \rightarrow x^+} \text{Tr} \gamma^\mu \partial^\nu_x S(x', x), \end{aligned} \quad (\text{C2})$$

while the average of the interaction terms of the Lagrangian (2.15) is given, in the Hartree approximation, as

$$\langle \mathcal{L}_{\text{int}} \rangle = G \langle \bar{\psi} \psi \rangle^2 = G [-i \text{Tr} S(x, x)]^2, \quad (\text{C3})$$

so that the energy-momentum tensor is given as

$$\begin{aligned} \langle T^{\mu\nu} \rangle &= \lim_{x' \rightarrow x} \text{Tr} \gamma^\mu \partial^\nu_x S(x, x) \\ &\quad - g^{\mu\nu} \left[ \lim_{x' \rightarrow x} \text{Tr} \partial_x S(x, x') - G [\text{Tr} S(x, x)]^2 \right]. \end{aligned} \quad (\text{C4})$$

The energy-momentum tensor is more familiar in momentum space, where it can be written as

$$\langle T^{\mu\nu} \rangle = -\text{Tr} \int \frac{d^4 p}{(2\pi)^4} i p^\nu \gamma^\mu S(p) + g^{\mu\nu} \left[ \text{Tr} \int \frac{d^4 p}{(2\pi)^4} \not{p} S(p) - G \left[ \text{Tr} \int \frac{d^4 p}{(2\pi)^4} S(p) \right]^2 \right], \quad (\text{C5})$$

and, after performing the trace, we have

$$\frac{\langle T^{\mu\nu} \rangle}{N_c N_f} = -4i \int \frac{d^4 p}{(2\pi)^4} \frac{p^\mu p^\nu}{p^2 - m^{*2}} + g^{\mu\nu} \left[ 4i \int \frac{d^4 p}{(2\pi)^4} \frac{p^2}{p^2 - m^{*2}} + 16 G N_c N_f m^{*2} g^{\mu\nu} \left[ \int \frac{d^4 p}{(2\pi)^4} \frac{1}{p^2 - m^{*2}} \right]^2 \right]. \quad (\text{C6})$$

In particular,

$$\frac{\langle T^{00} \rangle}{N_c N_f} = -4i \int \frac{d^4 p}{(2\pi)^4} \frac{p_0^2}{p^2 - m^{*2}} + 4i \int \frac{d^4 p}{(2\pi)^4} \frac{p^2}{p^2 - m^{*2}} + 16 G N_c N_f m^{*2} \left[ \int \frac{d^4 p}{(2\pi)^4} \frac{1}{p^2 - m^{*2}} \right]^2, \quad (\text{C7})$$

or

$$\frac{\langle T^{00} \rangle}{N_c N_f} = -4i \int \frac{d^4 p}{(2\pi)^4} \frac{p^2}{p^2 - m^{*2}} + 16 G N_c N_f m^{*2} \left[ \int \frac{d^4 p}{(2\pi)^4} \frac{1}{p^2 - m^{*2}} \right]^2. \quad (\text{C8})$$

Integrating out the  $p_0$  component, one obtains the result quoted as Eq. (3.4).

### APPENDIX D: THE THERMODYNAMIC POTENTIAL

The thermodynamic potential can be calculated, for example, via the method of coupling-constant integration

(Fetter and Walecka, 1971), which is sketched briefly here. One divides the thermodynamic potential  $K$  into  $K(\lambda) = K_0 + \lambda K_1$ , where, in this case, one identifies

$$\begin{aligned} K_0 &= H_0 - \mu N \\ &= \bar{\psi} (i \not{\partial} - m_0) \psi - \mu \psi^\dagger \psi \end{aligned}$$

and

$$K_1 = H_1 = -G [(\bar{\psi} \psi)^2 + (\bar{\psi} i \gamma_5 \tau \psi)^2].$$

<sup>4</sup>We note that the arguments of Nambu and Jona-Lasinio (1961a) with regard to the calculation of the total energy are incomplete (Suzuki, 1963).

The partition function associated with  $K$  is

$$Z_\lambda = e^{-\beta\Omega_\lambda} = \text{Tr} e^{-\beta K(\lambda)}, \quad (\text{D1})$$

from which one may deduce that

$$\frac{d\Omega_\lambda}{d\lambda} = -\frac{1}{\beta} \frac{1}{Z_\lambda} \frac{\partial Z_\lambda}{\partial \lambda}. \quad (\text{D2})$$

A direct evaluation of  $\partial Z_\lambda / \partial \lambda$  can be made by inserting  $K(\lambda)$  explicitly into the definition of  $Z$  and expanding the exponential function. One finds

$$\frac{\partial Z_\lambda}{\partial \lambda} = \sum_{n=1}^{\infty} (n!)^{-1} (-\beta)^n \text{Tr}[(K_0 + \lambda K_1)^{n-1} K_1], \quad (\text{D3})$$

which may be manipulated to give (see, for example, Fetter and Walecka, 1971)

$$\frac{\partial Z_\lambda}{\partial \lambda} = -\frac{\beta}{\lambda} e^{-\beta\Omega} \langle \lambda K_1 \rangle. \quad (\text{D4})$$

One now inserts this into Eq. (D2); integrating on  $\lambda$  from 0 to 1 gives

$$\Omega - \Omega_0 = \int_0^1 \frac{d\lambda}{\lambda} \langle \lambda K_1 \rangle. \quad (\text{D5})$$

Thus a knowledge of the thermodynamic average of the interaction energy suffices to determine the thermodynamic potential. Moreover, for a two-body interaction of the form of  $K_1$ , this interaction energy can be expressed in terms of the single-particle Matsubara Green's function and the self-energy. Generalizing the nonrelativistic result of Fetter and Walecka (1971), one has

$$\langle \lambda K_1 \rangle = \int \frac{d^3 p}{(2\pi)^3} \frac{1}{\beta} \sum_n e^{i\omega_n \eta_1 / 2} \text{Tr} \Sigma^\lambda(\mathbf{p}, \omega_n) \mathcal{S}^\lambda(\mathbf{p}, \omega_n). \quad (\text{D6})$$

All that remains is to determine  $\mathcal{S}^\lambda(\mathbf{k}, \omega_n)$  and  $\Sigma^\lambda(\mathbf{k}, \omega_n)$ . The former is given by Eq. (5.30). There is no explicit  $\lambda$  dependence. Rather, the  $\lambda$  dependence arises implicitly through the dependence of  $m$  on  $\lambda$ .  $\Sigma^\lambda(\mathbf{k}, \omega_n)$  can be obtained, in analogy with Eq. (5.15), from the Feynman rules for finite temperature. In the Hartree-Fock approximation,

$$\Sigma^\lambda = -2G\lambda \frac{1}{\beta} \sum_n e^{i\omega_n \eta} \int \frac{d^3 p}{(2\pi)^3} [N_c N_f \text{tr} \mathcal{S}(\mathbf{p}, \omega_n) - \mathcal{S}(\mathbf{p}, \omega_n) - 3i\gamma^5 \mathcal{S}(\mathbf{p}, \omega_n) i\gamma_5]; \quad (\text{D7})$$

making the same subdivision as that in (5.17),

$$\Sigma^\lambda = m^*(\lambda) - \gamma^0 M_0(\lambda),$$

one recovers the gap equation, Eq. (5.35) for  $m^*(\lambda)$ , with  $G \rightarrow G\lambda$ , and

$$M_0(\lambda) = -2G\lambda \int \frac{d^3 p}{(2\pi)^3} (\tanh \tfrac{1}{2}\beta\omega_p^+ - \tanh \tfrac{1}{2}\beta\omega_p^-), \quad (\text{D8})$$

after renormalizing away the density divergence that arises from the negative-energy sea. As in Eq. (5.21),  $M_0(\lambda)$  is related to the quark density via

$$-M_0(\lambda) = G\lambda \langle \psi^\dagger \psi \rangle / N_c \quad (\text{D9})$$

and

$$\mu'(\lambda) = \mu + M_0(\lambda). \quad (\text{D10})$$

Inserting Eqs. (D9) and (5.30) into (D6), and making

use of Eq. (D8) and the gap equation, leads to an equation,

$$\langle \lambda K_1 \rangle = \frac{N_c N_f}{4} \left[ \frac{M_0^2(\lambda)}{G\lambda} - \frac{[m^*(\lambda) - m_0]^2}{G\lambda(N_c N_f + \frac{1}{2})} \right], \quad (\text{D11})$$

for the average interaction energy, which may now be inserted into Eq. (D5). An integration by parts is useful for evaluating the integral on  $\lambda$ . One finds that

$$\begin{aligned} \Omega - \Omega_0 &= \frac{1}{N_c N_f} \frac{(m^* - m_0)^2}{4(N_c N_f + \frac{1}{2})G} - \frac{M_0^2}{4G} \\ &\quad - \frac{2}{\beta} \int \frac{d^3 p}{(2\pi)^3} \\ &\quad \times \log \frac{\cosh \tfrac{1}{2}\beta\omega_p^+(1) \cosh \tfrac{1}{2}\beta\omega_p^-(1)}{\cosh \tfrac{1}{2}\beta\omega_p^+(0) \cosh \tfrac{1}{2}\beta\omega_p^-(0)}, \end{aligned} \quad (\text{D12})$$

where  $\omega_p^\pm(\lambda) = E_p(\lambda) \pm [\mu + M_0(\lambda)]$ . With the interaction fully on,  $m^*(1) = m^*$  and  $m_0(1) = m_0$ , as determined by Eqs. (5.38) and (5.39); with the interaction switched fully off, one has for zero current quark mass, for example,  $m^*(0) = 0$  and  $M_0(0) = 0$ , so that  $\omega_p^\pm = p \pm \mu$ . Inserting this into (D12) and writing out the cosh function explicitly enable one to identify

$$\frac{\Omega_0}{N_c N_f} = -\frac{2}{\beta} \int \frac{d^3 p}{(2\pi)^3} \log[1 + e^{-\beta(p+\mu)}][1 + e^{-\beta(p-\mu)}] - 2 \int \frac{d^3 p}{(2\pi)^3} p \quad (\text{D13})$$

and to subtract this off to obtain the result quoted in Eq. (5.41).

## APPENDIX E: THE POLARIZATION PROPAGATOR AT FINITE TEMPERATURE

In this appendix we look at one example of the proper polarization, viz., that for the scalar mode. The Feynman rules for finite temperature<sup>5</sup> can be used to translate Fig. 16. One has

$$\Pi_s(\mathbf{q}, i\nu_n) = -\frac{1}{\beta} \sum_{\omega_1} \int \frac{d^3 p}{(2\pi)^3} \text{Tr} \mathcal{S}(\mathbf{q} + \mathbf{p}, \nu_n + \omega_1) \mathcal{S}(\mathbf{p}, \omega_1). \quad (\text{E1})$$

For simplicity, we shall use  $\mathcal{S}(\mathbf{p}, \omega_n)$  from Eq. (5.30), setting the chemical potential to zero. Then the spinor trace of the potential must be evaluated. One can immediately write

$$\begin{aligned} \text{tr} \mathcal{S}(\mathbf{p} + \mathbf{q}, \nu_n + \omega_1) \mathcal{S}(\mathbf{p}, \omega_1) = & \frac{1}{E_p E_q} \left[ \frac{1}{i(\nu_n + \omega_1) - E_{p+q}} \frac{1}{i\omega_1 - E_p} [E_p E_{p+q} + m^2 - \mathbf{p} \cdot (\mathbf{p} + \mathbf{q})] \right. \\ & + \frac{1}{i(\nu_n + \omega_1) - E_{p+q}} \frac{1}{i\omega_1 + E_p} [E_p E_{p+q} - m^2 + \mathbf{p} \cdot (\mathbf{p} + \mathbf{q})] \\ & + \frac{1}{i(\nu_n + \omega_1) + E_{p+q}} \frac{1}{i\omega_1 - E_p} [E_p E_{p+q} - m^2 + \mathbf{p} \cdot (\mathbf{p} + \mathbf{q})] \\ & \left. + \frac{1}{i(\nu_n + \omega_1) + E_{p+q}} \frac{1}{i\omega_1 + E_p} [E_p E_{p+q} + m^2 + \mathbf{p} \cdot (\mathbf{p} + \mathbf{q})] \right]. \quad (\text{E2}) \end{aligned}$$

Next, the frequency sums must be evaluated. This can be done either directly via contour integration, or by inserting a redundant factor  $\exp i\omega_1 \eta$  into each double sum and expressing it in partial fractions. One knows that

$$\frac{1}{\beta} \sum_n e^{i\omega_n \eta} \frac{1}{i\omega_n \mp e_p} = f(\pm e_p), \quad (\text{E3})$$

so that

$$\begin{aligned} \Pi_s(\mathbf{q}, i\nu_n) = & -N_c N_f \int \frac{d^3 p}{(2\pi)^3} \frac{1}{E_p E_{p+q}} \left[ [E_p E_{p+q} + m^2 - \mathbf{p} \cdot (\mathbf{p} + \mathbf{q})] \frac{f(E_p) - f(E_{p+q})}{i\nu_n - E_{p+q} - E_p} \right. \\ & + [E_p E_{p+q} - m^2 + \mathbf{p} \cdot (\mathbf{p} + \mathbf{q})] \frac{f(-E_p) - f(E_{p+q})}{i\nu_n - E_{p+q} - E_p} \\ & + [E_p E_{p+q} - m^2 + \mathbf{p} \cdot (\mathbf{p} + \mathbf{q})] \frac{f(E_p) - f(-E_{p+q})}{i\nu_n - E_{p+q} - E_p} \\ & \left. + [E_p E_{p+q} + m^2 - \mathbf{p} \cdot (\mathbf{p} + \mathbf{q})] \frac{f(-E_p) - f(-E_{p+q})}{i\nu_n + E_{p+q} - E_p} \right]. \quad (\text{E4}) \end{aligned}$$

One notes now that the change of variable  $\mathbf{p} \rightarrow -\mathbf{p}' - \mathbf{q}$  has the consequence that  $\mathbf{p} \cdot (\mathbf{p} + \mathbf{q}) \rightarrow \mathbf{p}' \cdot (\mathbf{p}' + \mathbf{q})$ . Also,  $E_{p+q} \rightarrow E_{p'}$ , and  $E_p \rightarrow E_{p'+q}$ . Applying this now to the second and last terms of Eq. (E4) leads to considerable simplification, and one finds

<sup>5</sup>We use the conventions of Mattuck (1976), which differ from those of Fetter and Walecka (1971) by a minus sign.

$$\begin{aligned} \Pi_s(\mathbf{q}, i\nu_n) = & -2N_c N_f \int \frac{d^3p}{(2\pi)^3} \frac{1}{E_p E_{p+q}} [E_p E_{p+q} + m^{*2} - \mathbf{p} \cdot (\mathbf{p} + \mathbf{q})] \frac{f(E_p) - f(E_{p+q})}{i\nu_n - E_{p+q} + E_p} \\ & + N_c N_f \int \frac{d^3p}{(2\pi)^3} \frac{1}{E_p E_{p+q}} [E_p E_{p+q} - m^{*2} + \mathbf{p} \cdot (\mathbf{p} + \mathbf{q})] \tanh \frac{1}{2} \beta E_p \left[ \frac{1}{i\nu_n + E_{p+q} + E_p} - \frac{1}{i\nu_n - E_{p+q} - E_p} \right], \end{aligned} \quad (\text{E5})$$

where the first term is the relativistic generalization of the nonrelativistic polarization propagator, while the second reflects the presence of the negative-energy sea. The analytic continuation of this equation

$$\Pi_s(\mathbf{q}, \omega) = \Pi_s(\mathbf{q}, i\nu_n) \big|_{i\nu_n \rightarrow \omega + i\eta}$$

is now required. The associated mass of the scalar meson is obtained, however, at  $\mathbf{q}=0$ . These results are listed as Eqs. (5.45) and (5.46) of the main text.

#### APPENDIX F: EIGENVALUES OF THE FIELD-STRENGTH TENSOR AND EVALUATION OF TRACES

Schwinger (1951) has shown that trace operations over both Lorentz and spinor indices on equations involving the field-strength tensor  $F^{\mu\nu}$  can be calculated from the eigenvalues of the tensor. This has been used in the previous section for the functions given in Eqs. (6.21), (6.22a), and (6.22b). In this section we shall briefly repeat Schwinger's arguments, firstly to show how these functions may be obtained, but more importantly, to extend the results to cover further trace operations that are required. The eigenvalue equation for  $F^{\mu\nu}$  is

$$F^{\mu\nu} \varphi_\nu(F) = F \varphi^\mu(F), \quad (\text{F1})$$

leading to the determinantal condition  $\det(F^{\mu\nu} - F g^{\mu\nu}) = 0$  for the eigenvalues. By recalling the identities (see, for example, Itzykson and Zuber, 1980)

$$F^{\mu\nu} \tilde{F}_{\nu\rho} = g^\mu_\rho \mathcal{G}$$

and

$$\tilde{F}_{\mu\lambda} \tilde{F}^{\lambda\nu} = F_{\mu\lambda} F^{\lambda\nu} + \frac{1}{2} g_\mu^\nu F_{\alpha\beta} F^{\alpha\beta}, \quad (\text{F2})$$

and applying these to the eigenvector  $\varphi$ , one may obtain a quartic for  $F$  in terms of the invariants  $\mathcal{F}$  and  $\mathcal{G}$ :

$$F^4 + 2\mathcal{F}F^2 - \mathcal{G}^2 = 0, \quad (\text{F3})$$

from which it follows that

$$F^2 = -\mathcal{F} \pm (\mathcal{F}^2 + \mathcal{G}^2)^{1/2}. \quad (\text{F4})$$

The four solutions can be written as  $\pm iF'$  and  $\pm F''$  where

$$\begin{aligned} iF' &= \frac{i}{\sqrt{2}} [(\mathcal{F} + i\mathcal{G})^{1/2} - (\mathcal{F} - i\mathcal{G})^{1/2}], \\ F'' &= \frac{1}{\sqrt{2}} [(\mathcal{F} + i\mathcal{G})^{1/2} + (\mathcal{F} - i\mathcal{G})^{1/2}]; \end{aligned} \quad (\text{F5})$$

i.e.,

$$F'' + iF' = \sqrt{2}(\mathcal{F} + i\mathcal{G})^{1/2},$$

provided that the square root is taken on the first sheet.  $F'$  and  $F''$  are both real and positive, which may be seen by writing

$$\mathcal{F} \pm i\mathcal{G} = |\mathcal{F} + i\mathcal{G}| \exp(\pm i\phi),$$

$$0 \leq \phi < 2\pi.$$

Then the eigenvalues are given as

$$\begin{aligned} F' &= \sqrt{2}(\mathcal{F}^2 + \mathcal{G}^2)^{1/2} \sin \phi / 2, \\ F'' &= \sqrt{2}(\mathcal{F}^2 + \mathcal{G}^2)^{1/2} \cos \phi / 2 \end{aligned} \quad (\text{F6})$$

and are shown in Fig. 30.

For a pure  $E$  field,  $\mathcal{G}=0$  and  $\mathcal{F} = -\frac{1}{2}E^2 < 0$ , so that  $\phi = \pi$  and  $F' = E$  while  $F'' = 0$ . For a pure  $B$  field, on the other hand,  $\mathcal{G}=0$  while  $\mathcal{F} = \frac{1}{2}B^2 > 0$ , so that  $\phi = 0$  and  $F' = 0$  and  $F'' = B$ .

The adjoint problem is defined by the eigenvalue equation

$$F^{\mu\nu} \phi_\nu(\tilde{F}) = \tilde{F} \phi^\mu(\tilde{F}), \quad (\text{F7})$$

where  $\phi^\mu(\tilde{F}) = \varphi(-F)$ , is antisymmetric. The completeness and orthogonality relations involve both  $\phi(F)$  and  $\varphi(F)$  and are given by

$$\begin{aligned} \sum_F \phi^\mu(F) \varphi^\mu(F) &= g^{\mu\nu}, \\ \sum_\mu \phi^\mu(F_1) \varphi_\mu(F_2) &= \delta_{F_1 F_2}, \end{aligned} \quad (\text{F8})$$

where  $F_1$  and  $F_2$  are any two eigenvalues. Now the tensor  $F^{\mu\nu}$  may be represented in terms of its eigenvectors  $\varphi^\mu(F)$  and the eigenvector  $\varphi^\nu(\tilde{F})$  of the adjoint problem,

$$F^{\mu\nu} = \sum_F \varphi^\mu(F) F \varphi^\nu(F). \quad (\text{F9})$$

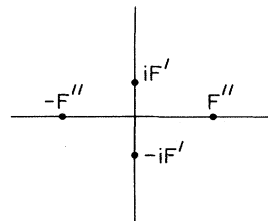


FIG. 30. Eigenvalues of the field-strength tensor  $F$ .



This display facilitates the calculation of the Lorentz trace of a function  $f$  of  $F^{\mu\nu}$ , which is in itself a matrix  $f^{\mu\nu}$ . Assuming that  $f^{\mu\nu}$  has a power-series representation in the operator  $\hat{F}=F^{\mu\nu}$ , one has

$$f^{\mu\nu}(\hat{F}) = \sum_F \varphi^\mu(f) f(F) \phi^\nu(F), \quad (\text{F10})$$

so that

$$\sum_\mu f^\mu_\mu = \sum_F f(F). \quad (\text{F11})$$

Thus, applying this to  $L(\tau)$  in Eq. (6.17), one has

$$L(\tau) = \ln[(q\tau F)^{-1} \sinh(q\tau F)] + \ln[(q\tau F'')^{-1} \sinh(q\tau F'')], \quad (\text{F12})$$

which leads directly to the result (6.21).

The spinor traces of equations involving the combinations  $\frac{1}{2}\sigma F = \frac{1}{2}\sigma_{\mu\nu}F^{\mu\nu}$  are more complicated. A direct evaluation of this combination gives

$$\frac{1}{2}\sigma F = \gamma^0 \gamma^5 (\boldsymbol{\gamma} \cdot \mathbf{B}) + i\gamma^0 (\boldsymbol{\gamma} \cdot \mathbf{E}), \quad (\text{F13})$$

from which it follows that

$$(\frac{1}{2}\sigma F)^2 = 2(\mathcal{F} - i\gamma^5 \mathcal{G}). \quad (\text{F14})$$

This  $4 \times 4$  matrix in spinor space is diagonalized by the unitary matrix

$$\begin{aligned} \exp(iq\tau\sigma F/2) &= 1 + iq\tau\sigma F/2 + \frac{1}{2!}(iq\tau)^2 \left[ \frac{\sigma F}{2} \right]^2 + \dots \\ &= \cosh[iq\tau(F'' - i\gamma^5 F')] + \left[ \frac{\sigma F}{2} \right] \frac{F'' + i\gamma_5 F'}{(F'')^2 + (F')^2} \sinh[iq\tau(F'' - i\gamma_5 F')]. \end{aligned} \quad (\text{F18})$$

Since  $(\gamma^5)^2 = 1$ , both hyperbolic functions can be written as a simple sum of products, e.g.,

$$\cosh[iq\tau(F'' - i\gamma^5 F')] = \cosh(q\tau F'') \cos(q\tau F') + i\gamma^5 \sinh(q\tau F'') \sin(q\tau F') \quad (\text{F19})$$

Thus, for example,

$$\begin{aligned} \text{tr} \exp(iq\tau\sigma F/2) &= 4 \cosh(q\tau F'') \cos(q\tau F'), \\ \text{tr} i\gamma^5 \exp(iq\tau\sigma F/2) &= -4 \sinh(q\tau F'') \cos(q\tau F'), \end{aligned} \quad (\text{F20})$$

since the traces of all other terms in (F19) vanish. This result was quoted in Eqs. (6.22a) and (6.22b). Finally, we comment that the traces that occur in the calculation of

$$U = (1 + \gamma^0 \gamma^5) / \sqrt{2}.$$

One has

$$U^\dagger (\frac{1}{2}\sigma F)^2 U = 2(\mathcal{F} + i\gamma^0 \mathcal{G}), \quad (\text{F15})$$

so that the eigenvalues of  $(\frac{1}{2}\sigma F)^2$  are  $2(\mathcal{F} + i\mathcal{G})$ , each value being doubly degenerate. Because of this degeneracy,  $U$  does not diagonalize  $\frac{1}{2}\sigma F$  simultaneously. In fact, the form

$$U^\dagger (\frac{1}{2}\sigma F) U = -(\boldsymbol{\Sigma} \cdot \mathbf{B}) + i\gamma^5 (\boldsymbol{\gamma} \cdot \mathbf{E}),$$

with  $\boldsymbol{\Sigma} = \gamma^5 \boldsymbol{\gamma}^0 \boldsymbol{\gamma}$ , is only block diagonal. However, the four eigenvalues of  $\frac{1}{2}\sigma F$  are given by

$$\sqrt{2}(\mathcal{F} + i\mathcal{G})^{1/2} = \pm(F'' \pm iF'), \quad (\text{F16})$$

in view of Eqs. (F5) and (F15). It is useful to observe that the square of this result is summarized by the statement

$$2(\mathcal{F} + i\gamma^0 \mathcal{G}) = (F'' + i\gamma^0 F')^2;$$

from this equation and from (F15) it follows that

$$\begin{aligned} (\frac{1}{2}\sigma F)^2 &= U(F'' + i\gamma^0 F')^2 U^\dagger \\ &= (F'' - i\gamma^5 F')^2. \end{aligned} \quad (\text{F17})$$

One can employ Eq. (F17) to express the spinor function  $e(-\tau) = \exp(iq\tau\sigma F/2)$  as

the meson modes, as described in the next section, are evaluated most easily by the method displayed here.

## APPENDIX G: THE POLARIZATION PROPAGATOR, INCLUDING A U(1) FIELD

We sketch the calculation of the polarization propagator  $\Pi_{\text{ps}}$  briefly. Inserting Eq. (6.19) into (6.31), one has

$$\begin{aligned} \frac{1}{i} \Pi_{\text{ps}}(k) &= -\frac{1}{(4\pi)^4} \int_{-\infty}^0 \frac{d\tau_1}{\tau_1^2} \int_{-\infty}^0 \frac{d\tau_2}{\tau_2^2} e^{im^2\tau_1 - L(\tau_1)} e^{im^2\tau_2 - L(\tau_2)} \\ &\quad \times \int d^4x e^{ikx + (i/4)xKx} N_c N_f \text{tr} \left[ \frac{1}{2} \gamma^\mu M_{\mu\nu}(\tau_1) x^\nu + m \right] e(-\tau_1) \left[ \frac{1}{2} \gamma^\mu M_{\mu\nu}(\tau_2) x^\nu + m \right] e(-\tau_2), \end{aligned} \quad (\text{G1})$$

where  $K_{12} = K_1 + K_2$  and

$$e(-\tau_1) = \exp(iq\sigma_{\mu\nu}F^{\mu\nu}\tau_1/2),$$

which commutes with  $\gamma_5$ . On making the change of variable  $\alpha_i = -\tau_i$ , and noting that  $L(-\alpha) = L(\alpha)$  and that  $e(\alpha)$  has an even number of Dirac matrices, one obtains

$$\frac{1}{i} \Pi_{\text{ps}}(k) = -\frac{1}{(4\pi)^4} \int_0^\infty \frac{d\alpha_1}{\alpha_1^2} \int_0^\infty \frac{d\alpha_2}{\alpha_2^2} e^{-im^2\alpha_1 - L(\alpha_1)} e^{-im^2\alpha_2 - L(\alpha_2)} \\ \times \int d^4x e^{ikx - \frac{1}{2}xKx} N_c N_f \left[ \frac{1}{4} (xM_1)_\mu (xM_2)_\nu \text{tr} \gamma^\mu e(\alpha_1) \gamma^\nu e(\alpha_2) + m^2 \text{tr} e(\alpha_1) e(\alpha_2) \right]. \quad (\text{G2})$$

The space-time integrals can be performed on making a shift of variable

$$y_\mu = x_\mu - 2(K_{12}^{-1})^\rho_\mu k_\rho.$$

One finds

$$\int d^4x \exp \left[ ikx - \frac{i}{4} x K_{12} x \right] = (4\pi)^2 i |J| \exp(ikK_{12}^{-1}k) \quad (\text{G3})$$

and

$$\int d^4x \exp \left[ ikx - \frac{i}{4} x K_{12} x \right] (xM_1)_\mu (xM_2)_\nu \\ = (4\pi)^2 i |J| \exp(ikK_{12}^{-1}k) (-2i [M_1^T K_{12}^{-1} M_2]_{\mu\nu} \\ + 4 [M_1^T K_{12}^{-1} k]_\mu [M_2^T K_{12}^{-1} k]_\nu), \quad (\text{G4})$$

where

$$|J| = \prod_{\mu=0}^3 (K_{12}^{-1/2})^\mu_\mu. \quad (\text{G5})$$

Using the results of the previous section, one may evaluate the constructs  $K_{\mu\nu}$ ,  $(K_{12}^{-1})_{\mu\nu}$ , and  $|J|$ . In general, one has

$$K_{\mu\nu}(\alpha) = [qF \coth qF\alpha]_{\mu\nu} = \sum_f \varphi_\mu(F) qF \coth(qF\alpha) \phi_\nu(F),$$

$$(K_{12})_{\mu\nu} = K(\alpha_1)_{\mu\nu} + K(\alpha_2)_{\mu\nu} \\ = \sum_F \varphi(F) \frac{qF \sinh qF(\alpha_1 + \alpha_2)}{\sinh(qF\alpha_1) \sinh(qF\alpha_2)} \phi_\nu(F), \quad (\text{G6})$$

$$(K_{12}^{-1})_{\mu\nu} = \sum_F \varphi_\mu(F) \frac{1}{qF} \frac{\sinh(qF\alpha_1) \sinh(qF\alpha_2)}{\sinh qF(\alpha_1 + \alpha_2)} \phi_\nu(F).$$

We specialize now to the case of a pure  $E$  field. Then the eigenvectors of  $F^{\mu\nu}$  are

$$\varphi_\mu(F) = [1, 0, 0, \mp 1]/\sqrt{2}$$

for  $F = \pm E$ , plus the orthogonalized pair  $[0, 1, 0, 0]$  and  $[0, 0, 1, 0]$  for the double root at zero. The corresponding adjoint vectors are

$$\phi_\mu(F) = [1, 0, 0, \pm 1]/\sqrt{2}$$

and  $[0, -1, 0, 0]$  and  $[0, 0, -1, 0]$ . One thus finds that

$$K_{00} = -K_{33} = qE \coth(qE\alpha), \quad -K_{11} = -K_{22} = \frac{1}{\alpha}, \quad (\text{G7})$$

so that

$$(K_{12})_{00} = -(K_{12})_{33} \\ = qE \frac{\sinh[qE(\alpha_1 + \alpha_2)]}{\sinh(qE\alpha_1) \sinh(qE\alpha_2)}, \quad (\text{G8}) \\ -(K_{12})_{11} = -(K_{12})_{22} = \frac{\alpha_1 + \alpha_2}{\alpha_1 \alpha_2}.$$

The matrix elements of  $K_{12}^{-1}$  are the inverse of this set. Now the Jacobian  $|J|$  can be explicitly evaluated,

$$|J| = \frac{1}{qE} \frac{\sinh(qE\alpha_1) \sinh(qE\alpha_2)}{\sinh qE(\alpha_1 + \alpha_2)} \frac{\alpha_1 \alpha_2}{\alpha_1 + \alpha_2}, \quad (\text{G9})$$

and the factor occurring in the exponential of Eqs. (C3) and (C4) is given as

$$kK_{12}^{-1}k = (k_0^2 - k_3^2) \frac{1}{qE} \frac{\sinh(qE\alpha_1) \sinh(qE\alpha_2)}{\sinh qE(\alpha_1 + \alpha_2)} \\ - k_1^2 \frac{\alpha_1 \alpha_2}{\alpha_1 + \alpha_2}, \quad (\text{G10})$$

with  $k_1^2 = k_1^2 + k_2^2$ . One requires the remaining traces

$$\text{tr} e(\alpha_1) e(\alpha_2) = 4 \cosh qE(\alpha_1 + \alpha_2) \quad (\text{G11})$$

and

$$\text{tr} \gamma^\mu e(\alpha_1) \gamma^\nu e(\alpha_2) = 4g^{\mu\nu} \cosh qE(\alpha_1 + \alpha_2) - 4(g^{\mu 3} g^{\nu 0} - g^{\mu 0} g^{\nu 3}) \sinh qE(\alpha_1 - \alpha_2) + 8(g^{\mu 3} g^{\nu 3} - g^{\mu 0} g^{\nu 0}) \sinh qE\alpha_1 \sinh qE\alpha_2, \quad (\text{G12})$$

in order to reassemble the equation for  $(1/i)\Pi_{\text{ps}}$ , Eq. (G2), as

$$\frac{1}{i}\Pi_{\text{ps}}(k) = -\frac{N_c N_f}{(4\pi)^2} \int_0^\infty d\alpha_1 \int_0^\infty d\alpha_2 e^{-im^2(\alpha_1+\alpha_2)} qE \coth qE(\alpha_1+\alpha_2) \frac{e^{ikK_{12}^{-1}k}}{\alpha_1+\alpha_2} \\ \times \left[ 4im^2 + \frac{4qE}{\sinh qE(\alpha_1+\alpha_2) \cosh qE(\alpha_1+\alpha_2)} + \frac{4}{\alpha_1+\alpha_2} \right. \\ \left. - 4ik_\perp^2 \frac{\alpha_1\alpha_2}{(\alpha_1+\alpha_2)^2} + 4i(k_0^2 - k_3^2) \frac{\sinh qE\alpha_1 \sinh qE\alpha_2}{\sinh qE(\alpha_1+\alpha_2) \cosh qE(\alpha_1+\alpha_2)} \right]. \quad (\text{G13})$$

One now proceeds in a standard fashion of inserting

$$\int_0^\infty d\lambda \delta(\lambda - \alpha_1 - \alpha_2) = 1$$

and rescaling  $\alpha_i \rightarrow \lambda \alpha_i$ , so that one may do one of the  $\alpha$  integrals. The resulting integral is then regulated via the Pauli-Villars procedure, as in Sec. VI.A.1. One then obtains the expression given in Eq. (6.38).

## REFERENCES

- Adami, C., and G. E. Brown, 1990, SUNY preprint NTG90-38.  
 Amendolia, S. R., *et al.*, 1984, Phys. Lett. B **146**, 116.  
 Amendolia, S. R., M. Arik, *et al.*, 1986, Nucl. Phys. B **277**, 168.  
 Amendolia, S. R., G. Batignani, *et al.*, 1986, Phys. Lett. B **178**, 435.  
 Antipov, Y. M., *et al.*, 1985, Z. Phys. C **26**, 496.  
 Asakawa, M., and K. Yazaki, 1989, Nucl. Phys. A **504**, 668.  
 Bardeen, W. A., C. T. Hill, and M. Lindner, 1990, Phys. Rev. D **41**, 1647.  
 Bernard, V., 1986, Phys. Rev. D **34**, 1601.  
 Bernard, V., 1987, Phys. Lett. **198**, 93.  
 Bernard, V., R. L. Jaffe, and U.-G. Meissner, 1988, Nucl. Phys. B **308**, 753.  
 Bernard, V., and U.-G. Meissner, 1988a, Phys. Rev. D **38**, 1551.  
 Bernard, V., and U.-G. Meissner, 1988b, Phys. Rev. Lett. **61**, 2296.  
 Bernard, V., and U.-G. Meissner, 1988c, Nucl. Phys. A **489**, 647.  
 Bernard, V., U.-G. Meissner, and I. Zahed, 1987a, Phys. Rev. D **36**, 819.  
 Bernard, V., U.-G. Meissner, and I. Zahed, 1987b, Phys. Rev. Lett. **59**, 966.  
 Bernard, V., and D. Vautherin, 1989, Phys. Rev. D **40**, 1615.  
 Blin, A. W., B. Hiller, and J. da Providência, 1990, Phys. Lett. B **241**, 1.  
 Blin, A. W., B. Hiller, and M. Schaden, 1988, Z. Phys. A **331**, 75.  
 Brodsky, S. J., and J. R. Primack, 1969, Ann. Phys. (N.Y.) **52**, 315.  
 Buchmüller, W., 1984, Lectures presented at the International School of Exotic Atoms, Erice.  
 Casher, A., H. Neuberger, and S. Nussinov, 1979, Phys. Rev. D **20**, 179.  
 Chakrabarti, A., and B. Hu, 1976, Phys. Rev. D **13**, 2347.  
 Cheng, T.-P., and L.-F. Li, 1984, *Gauge Theory of Elementary Particle Physics* (Clarendon, Oxford).  
 Christ, N. H., 1991, Nucl. Phys. A **527**, 539.  
 Clark, T. E., S. T. Love, and W. A. Bardeen, 1990, Phys. Lett. B **237**, 235.  
 Claudson, M., A. Yildiz, and P. H. Cox, 1980, Phys. Rev. D **22**, 2022.  
 Cox, P. H., and A. Yildiz, 1985, Phys. Rev. D **32**, 819.  
 da Providência, J., M. C. Ruivo, and C. A. de Sousa, 1987, Phys. Rev. D **36**, 1882.  
 Dolan, L., and R. Jackiw, 1974, Phys. Rev. D **9**, 3320.  
 Dumbrajs, O., 1983, Nucl. Phys. B **216**, 277.  
 Ebert, D., 1985, Z. Phys. **28**, 433.  
 Ebert, D., and H. Reinhardt, 1986, Nucl. Phys. B **271**, 188.  
 Ebert, D., and M. K. Volkov, 1983, Z. Phys. C **16**, 305.  
 Eguchi, T., 1976, Phys. Rev. D **14**, 2755.  
 Eguchi, T., and H. Sugawara, 1974, Phys. Rev. D **10**, 4257.  
 Ericson, T. E. O., and J. Hüfner, 1973, Nucl. Phys. B **57**, 604.  
 Fetter, A. L., and J. D. Walecka, 1971, *Quantum Theory of Many Particle Systems* (McGraw-Hill, New York).  
 Feynman, R., 1950, Phys. Rev. **80**, 440.  
 Finger, J. R., and J. E. Mandula, 1982, Nucl. Phys. B **199**, 168.  
 Gasser, J., 1981, Ann. Phys. (N.Y.) **136**, 62.  
 Gasser, J., and H. Leutwyler, 1982, Phys. Rep. **87**, 77.  
 Gasser, J., and H. Leutwyler, 1984, Ann. Phys. (N.Y.) **158**, 142.  
 Gasser, J., and H. Leutwyler, 1985, Nucl. Phys. B **250**, 465.  
 Gasser, J., and H. Leutwyler, 1987, Phys. Lett. B **184**, 83.  
 Gasser, J., H. Leutwyler, and M. E. Sainio, 1991, Phys. Lett. B **253**, 252.  
 Gatoff, G., A. K. Kerman, and T. Matsui, 1987, Phys. Rev. D **36**, 114.  
 Gell-Mann, M., R. Oakes, and B. Renner, 1968, Phys. Rev. **175**, 2195.  
 Gerber, P., and H. Leutwyler, 1989, Nucl. Phys. B **321**, 387.  
 Giacomo, A. D., M. Maggiore, and S. Olejnik, 1990, Nucl. Phys. B **347**, 441.  
 Gilman, F. J., and R. Kauffman, 1987, Phys. Rev. D **36**, 2761.  
 Ginzburg, V. L., and L. D. Landau, 1950, Zh. Eksp. Teor. Fiz. **20**, 1064. For an English translation, see *Men of Physics: L. D. Landau*, Vol. 1, p. 138 (Pergamon, Oxford, 1965).  
 Göckler, M., R. Horsley, and E. Laermann, 1990, Nucl. Phys. B **334**, 527.  
 Goldberger, M. L., and S. B. Treiman, 1958, Phys. Rev. **110**, 1178.  
 Goldstone, J., 1961, Nuovo Cimento **19**, 154.  
 Goldstone, J., A. Salam, and S. Weinberg, 1962, Phys. Rev. **127**, 965.  
 Gor'kov, L. P., 1959, Zh. Eksp. Teor. Fiz. **36**, 1918 [Sov. Phys. JETP **9**, 1364 (1959)].  
 Hansson, T. H., M. Prakash, and I. Zahed, 1990, Nucl. Phys. B **335**, 67.  
 Hatsuda, T., 1988, Phys. Lett. B **213**, 361.  
 Hatsuda, T., and T. Kunihiro, 1984, Phys. Lett. B **145**, 7.  
 Hatsuda, T., and T. Kunihiro, 1985a, Prog. Theor. Phys. **74**,

- 765.
- Hatsuda, T., and T. Kunihiro, 1985b, *Phys. Rev. Lett.* **55**, 158.
- Hatsuda, T., and T. Kunihiro, 1987a, *Phys. Lett. B* **185**, 304.
- Hatsuda, T., and T. Kunihiro, 1987b, *Phys. Lett. B* **198**, 126.
- Hosaka, A., 1990, *Phys. Lett. B* **244**, 363.
- Huang, K., 1982, *Quarks, Leptons and Gauge Fields* (World Scientific, Singapore).
- Itzykson, C., and J.-B. Zuber, 1980, *Quantum Field Theory* (McGraw-Hill, New York).
- Jaminon, M., G. Ripka, and P. Stassart, 1989, *Phys. Rev. Lett.* **B 227**, 191.
- Kawarabayashi, K., and M. Suzuki, 1966, *Phys. Rev. Lett.* **16**, 255.
- Kikkawa, K., 1976, *Prog. Theor. Phys.* **56**, 947.
- Klevansky, S. P., 1991, *Nuovo Cimento A* **104**, 1035.
- Klevansky, S. P., J. Jaenicke, and R. H. Lemmer, 1991, *Phys. Rev. D* **43**, 3040.
- Klevansky, S. P., and R. H. Lemmer, 1989, *Phys. Rev. D* **39**, 3478.
- Klevansky, S. P., and R. H. Lemmer, 1990, *Z. Phys. A* **336**, 223.
- Klimt, S., M. Lutz, and W. Weise, 1990, *Phys. Lett. B* **249**, 386.
- Klimt, S., M. Lutz, U. Vogl, and W. Weise, 1990, *Nucl. Phys. A* **516**, 429.
- Kocić, A., 1986, *Phys. Rev. D* **33**, 1785.
- Kogut, J. B., 1980, *Phys. Rep.* **67**, 67.
- Kogut, J. B., D. B. Sinclair, and K. C. Wang, 1991, *Phys. Lett. B* **263**, 101.
- Kogut, J. B., and L. Susskind, 1975, *Phys. Rev. D* **11**, 395.
- Kruglov, S. I., 1984, *Acta Phys. Pol. B* **15**, 725.
- Kruglov, S. I., 1988, *Sov. J. Phys.* **3**, 198.
- Kruglov, S. I., 1989a, *Acta Phys. Pol. B* **20**, 723.
- Kruglov, S. I., 1989b, *Acta Phys. Pol. B* **20**, 729.
- Kruglov, S. I., 1989c, *Sov. J. Phys.* **6**, 413.
- Kruglov, S. I., 1990, *Acta Phys. Pol. B* **21**, 985.
- Kunihiro, T., 1987, *Phys. Lett. B* **185**, 307.
- Kunihiro, T., 1988, *Prog. Theor. Phys.* **80**, 34.
- Kunihiro, T., 1989a, *Genshikaku Kenkyu Summer School, Iiama (Japan)* **33**, No. 5, 19.
- Kunihiro, T., 1989b, *Phys. Lett. B* **219**, 363.
- Kunihiro, T., 1991, *Nucl. Phys. B* **351**, 593.
- Kunihiro, T., and T. Hatsuda, 1988, *Phys. Lett. B* **206**, 385.
- Lee, T. D., 1981, *Particle Physics and Introduction to Field Theory* (Harwood, New York).
- LeYaouanc, A., *et al.*, 1988, *Phys. Rev. D* **39**, 924.
- Low, F., 1975, *Phys. Rev. D* **12**, 163.
- Lutz, M., and W. Weise, 1990, *Nucl. Phys. A* **518**, 156.
- Martin, C., and D. Vautherin, 1988, *Phys. Rev. D* **38**, 3593.
- Mattuck, R. D., 1976, *A Guide to Feynman Diagrams in the Many-body Problem* (McGraw-Hill, New York).
- Meissner, U.-G., 1988, *Phys. Rep.* **161**, 213.
- Meissner, Th., F. Grümmer, and K. Goeke, 1990, *Ann. Phys. (N.Y.)* **202**, 297.
- Meissner, Th., E. Ruiz-Arriola, F. Grümmer, and H. Mavromatis, 1988, *Phys. Lett. B* **214**, 312.
- Nambu, Y., and G. Jona-Lasinio, 1961a, *Phys. Rev.* **122**, 345.
- Nambu, Y., and G. Jona-Lasinio, 1961b, *Phys. Rev.* **124**, 246.
- Olsson, M. G., and C. J. Suchyta, III, 1987, *Phys. Rev. D* **36**, 1459.
- Pauli, W., and F. Villars, 1949, *Rev. Mod. Phys.* **21**, 434.
- Pham, X.-Y., 1990, *Phys. Lett. B* **241**, 111.
- Pokorski, S., 1989, *Gauge Field Theories*, Cambridge Monographs on Mathematical Physics (Cambridge University, New York), p. 329.
- Ramond, P., 1981, *Field Theory: A Modern Primer* (Benjamin, London/New York).
- Rebbi, C., 1986, *Phys. Rep.* **137**, 63.
- Redlich, K., and L. Turko, 1980, *Z. Phys. C* **5**, 201.
- Reinders, L., J. H. Rubinstein, and S. Yazaki, 1985, *Phys. Rep.* **127**, 2.
- Reinhardt, H., 1990, *Phys. Lett. B* **244**, 316.
- Reinhardt, H., 1991, *Phys. Lett. B* **257**, 375.
- Riazuddin, and Fayyazuddin, 1966, *Phys. Rev.* **147**, 1071.
- Rosenstein, B., B. J. Warr, and S. H. Park, 1991, *Phys. Rep.* **205**, 59.
- Ruiz Arriola, E., 1991, *Phys. Lett. B* **253**, 430.
- Ruiz Arriola, E., V. Christov, and K. Goeke, 1989, *Phys. Lett. B* **221**, 39.
- Salam, A., and J. Strathdee, 1975, *Nucl. Phys. B* **90**, 203.
- Schüren, C., E. Ruiz Arriola, and K. Goeke, 1991, *Bochum Preprint, RUB-TPII-07-91*.
- Schwinger, J., 1951, *Phys. Rev.* **82**, 644.
- Serot, B. D., and J. D. Walecka, 1986, *The Relativistic Nuclear Many-Body Problem*, Advances in Nuclear Physics, Vol. 16, edited by J. W. Negele and Erich Vogt (Plenum, New York/London).
- Skyrme, H., 1961, *Proc. R. Soc. London Ser. A* **260**, 127.
- Skyrme, H., 1962, *Nucl. Phys.* **31**, 556.
- Stephens, C. R., 1988, *Ann. Phys. (N.Y.)* **181**, 120.
- Suganuma, H., and T. Tatsumi, 1990, *Proceedings of the Workshop on High Density Nuclear Matter*, 18–21 September, KEK, Japan, edited by J. Chiba, KEK report, in press, KEK Preprint KUNS 1049.
- Suganuma, H., and T. Tatsumi, 1991, *Ann. Phys. (N.Y.)* **208**, 470.
- Suzuki, M., 1963, *Prog. Theor. Phys.* **30**, 138.
- Takizawa, M., K. Kubodera, and F. Myhrer, 1991, *Phys. Lett. B* **261**, 221.
- Takizawa, M., K. Tsushima, Y. Kohyama, and K. Kubodera, 1989, *Nucl. Phys. A* **507**, 611.
- Tarrach, R., 1979, *Z. Phys. C* **2**, 221.
- 't Hooft, G., 1973, *Nucl. Phys. B* **62**, 444.
- 't Hooft, G., 1974, *Nucl. Phys. B* **74**, 461.
- 't Hooft, G., 1976a, *Phys. Rev. Lett.* **37**, 8.
- 't Hooft, G., 1976b, *Phys. Rev. D* **14**, 3432.
- Turko, L., 1981, *Phys. Lett. B* **104**, 153.
- Vogl, U., M. Lutz, S. Klimt, and W. Weise, 1990, *Nucl. Phys. A* **516**, 469.
- Vogl, U., and W. Weise, 1991, *Prog. Part. Nucl. Phys.* **27**, 195.
- Volkov, M. K., 1984, *Ann. Phys. (N.Y.)* **157**, 282.
- Volkov, M. K., 1986, *Sov. J. Part. Nucl.* **17**, 186.
- Weinberg, S., 1967, *Phys. Rev. Lett.* **18**, 507.
- Wess, J., and B. Zumino, 1979, *Phys. Lett. B* **37**, 164.
- Witten, E., 1979, *Nucl. Phys. B* **160**, 57.
- Witten, E., 1983, *Nucl. Phys. B* **223**, 422, 433.
- Yildiz, A., and P. H. Cox, 1980, *Phys. Rev. D* **22**, 2022.